CONS/0008-3
NASA CR-135430

CERAMIC REGENERATOR SYSTEMS DEVELOPMENT PROGRAM

PROGRESS REPORT FOR PERIOD JAN. 1, 1978 TO MAR. 31, 1978

J. A. COOK, C. A. FUCINARI, J. N. LINGSCHEIT, C. J. RAHNKE, AND V. D. RAO

RESEARCH STAFF
FORD MOTOR CO.
DEARBORN, MICHIGAN 48121

(NASA-CR-135430) CERAMIC REGENERATOR SYSTEMS DEVELOPMENT PROGRAM Progress Report, 1 Jan. - 31 Mar. 1978 (Ford Motor Co.) 108 p HC A06/MF A01 CSCL 11C

N78-26997

Unclas
G3/85 23550

MAY 1978

Prepared for the
NATIONAL AERONAUTICS AND SPACE ADMINISTRATION
Lewis Research Center
Cleveland, Ohio 44135

Contract DEN 3-8

As a part of the

DEPARTMENT OF ENERGY
Division of Transportation Energy Conservation
Heat Engine Highway Vehicle Systems Program

1. Report No. NASA CR-135430	2. Government Accession No.	3. Recipient's Catalog No.
4. Title and Subtitle Ceramic Regenerator Systems Development Program Progress Report for Period Jan. 1, 1978 to Mar. 31, 1978		5. Report Date February 1978 6. Performing Organization Code
7. Author(s) J. A. Cook, C. A. Fucinari, J. N. Lingscheit, C. J. Rahnke, and V. D. Rao		8. Performing Organization Report No. 10. Work Unit No.
9. Performing Organization Name and Address Research Staff Ford Motor Co. Dearborn, Michigan 48121		11. Contract or Grant No. Den 3-8
12. Sponsoring Agency Name and Address Department of Energy Division of Transportation Energy Conservation Washington, D.C. 20545		13. Type of Report and Period Covered Contractor Report 14. Sponsoring Agency Report No. CONS/0008-3

15. Supplementary Notes Interim Report. Prepared under Interagency Agreement EC-77-A-31-1040

Project Manager, Thomas J. Miller, Transportation Propulsion Division, NASA Lewis Research Center, Cleveland, Ohio 44135

16. Abstract

The primary objective of the DOE/NASA Ceramic Regenerator Design and Reliability Program is to develop ceramic regenerator cores that can be used in passenger car gas turbine engines, Stirling engines, and industrial/truck gas turbine engines.

The major cause of failure of early gas turbine regenerators was found to be chemical attack of the ceramic material. Improved materials and design concepts aimed at reducing or eliminating chemical attack were placed on durability test in Ford 707 industrial gas turbine engines late in 1974.

This report describes the results of 4805 hours of turbine engine durability testing accumulated during the period from January 1, 1978 to March 31, 1978. Two materials, aluminum silicate and magnesum aluminum silicate, continue to show promise toward achieving the durability objectives of this program. A regenerator core made from aluminum silicate shows minimal evidence of chemical attack damage after 7804 hours of engine test at 800°C (1472°F) and another shows little distress after 4983 hours at 982°C (1800°F).

The results obtained during this period in ceramic material screening tests, aerothermodynamic performance tests, stress analysis, cost studies, and material specifications are also included in this report.

17. Key Words (Suggested by Author(s))	18. Distribution Statement
Heat Exchangers Ceramic Regenerator Systems Ceramic Materials Heat Exchanger Manufacturing	Unclassified — unlimited STAR Category 85 DOE Category UC-96

19. Security Classif. (of this report)	20. Security Classif. (of this page)	21. No. of Pages	22. Price*
Unclassified	Unclassified	99	—

*For sale by the National Technical Information Service, Springfield, Virginia 22161

TABLE OF CONTENTS

TABLE OF CONTENTS

LIST OF ILLUSTRATIONS

LIST OF ILLUSTRATIONS

LIST OF ILLUSTRATIONS

LIST OF ILLUSTRATIONS

LIST OF TABLES

SUMMARY

Since the NASA/Ford Ceramic Regenerator Program is organized by tasks, the results obtained during the January 1, 1978 to March 31, 1979 period will also be summarized by Task.

Task I — Core Durability Testing at 800°C. Approximately 4128 hours of engine durability test (8256 core hours) at 800°C (1472°F) were completed from January 1, 1978 to March 31, 1978 on cores made from chemically-resistant materials and mounted with a rim support and drive system.

Turbine engine durability tests on aluminum silicate regenerator cores show that this material is relatively impervious to chemical attack. Eleven cores of this material have each accumulated over 4000 hours of engine test at 800°C (1472°F), and one core has attained 7804 hours of engine test with a minimal amount of chemical attack damage.

A high thermal expansion MAS core has accumulated 5381 hours at 800°C (1472°F). A MAS core made from a more advanced material having lower thermal expansion characteristics and greater strength has been placed on durability test and accumulated 475 hours during this report period.

One thin-wall AS core has now accumulated 6388 hours of engine test.

Separations in the elastomer-matrix bond region have occurred on all thin-wall cores bonded using the conventional technique. Utilization of a high-compliance elastomer system shows promise of solving this problem. Three cores of this configuration are now on test, with one having accumulated 4272 hours.

The cement holding the hub inserts in place failed in five out of the nineteen AS cores that have undergone engine test. A hub configuration which utilizes a solid ceramic ring around the hub insert is now on test, and one unit has accumulated 4300 hours.

The spring-roller ball bearings in the mounting system in one engine have been replaced by solid graphite bearings. Over 600 hours have been accumulated on these bearings with little or no wear.

Task II — Core Durability Testing at 1000°C (1832°C). A total of 1354 core-hours at 1000°C (1832°F) were accumulated during this period.

About 4983 hours of engine test at an average regenerator inlet temperature of 982°C (1800°F) have been accumulated on a thick-wall aluminum silicate core, and 2680 hours at this temperature have been accumulated on a thin-wall AS core. Neither core shows any signs of thermal or chemical attack damage after this exposure.

Task III — Material Screening Tests. A majority of the materials scheduled for laboratory testing under hot face and cold face conditions have progressed to completion, and the resulting data have been reported. The final chemical analyses for the first set of four matrix inserts exposed to engine accelerated corrosion testing have been completed and reported. These two, successive tests have generated supportive data, although the laboratory test appears to be more severe than the engine accelerated chemical attack test.

Task IV — Aerothermodynamic Performance. With the two additional extruded square matrices tested during this report period, a total of twenty-nine matrix fin configurations have been evaluated at the present time. Seventeen rectangular, eight

sinusoidal, two isosceles triangular, and two hexagonal configurations comprise the present matrix sample size.

Due to the significant reduction of the wall material thickness (.173 mm or .0068 in.) for the extruded square matrix 28, it exhibits superior heat transfer and pressure drop characteristics compared to equivalent geometry matrices previously evaluated.

Task V — Design Studies of Advanced Regenerator Systems. The radial and tangential modulii of elasticity of the Supplier A thin-wall sinusoidal fin AS matrix, and the radial and tangential flexure strength and modulii of the Supplier I extruded isosceles triangular fin matrix and the Supplier D embossed rectangular fin MAS-2 matrix have been evaluated using Weibull statistics.

Two compliant elastomer schemes have been evaluated. The interrupted elastomer scheme which has operated successfully in the engine has been shown to provide a 90% increase in compliance compared to the standard configuration.

Task VI — Ceramic Thermal Stability Tests. As the thermal stability testing of ceramic materials progresses, several trends are becoming evident. The MAS materials are more stable than the AS and LAS materials, at elevated temperatures under corrosive conditions. The leached LAS material iterations tested as of this writing are not servicable at 1100°C (2012°F) and 1200°C (2192°F).

Task VII — Manufacturing Cost Studies. A list of analysis models has been completed and a task prioritization agreed upon by Manufacturing Development Department cost analysts. Work is underway on configuration 1:a regenerator core for an automotive gas turbine engine.

Task VIII — Core Material and Design Specifications. An updated regenerator core material and design specification for 800°C (1472°F) has been completed as part of this contract task. The iteration of this document for 1000°C (1832°F) regenerator operation is dependent upon an ongoing test program which features both laboratory and engine evaluation of proposed regenerator materials and configurations.

Task IX — Program Management. As early as possible in the second quarter of 1978, two 800°C (1472°F) engines will be converted to 1000°C (1832°F) engines. In addition, the program completion date will be extended 6 months. Both NASA and Ford have agreed to these changes, which will be done at no additional cost to NASA, will result in four times more hours being accumulated at 1000°C (1832°F) under the revised program.

Task X — Reporting Requirements. The subjects and timing of the three "Topical Reports" have been determined by NASA and Ford personnel. The first report "Evaluation of Regenerator System Performance" will be published in the next quarter.

INTRODUCTION

Since 1965, Ford Motor Company has been engaged in developing a ceramic regenerator system for use in gas turbine engines. Over 100,000 hours of engine operating experience have been accumulated on a sample of approximately 1,000 regenerator cores fabricated of lithium aluminum silicate (LAS) and produced by two suppliers.

Because of unexpected failures of the LAS regenerator, in 1973 Ford started a series of controlled durability tests using the 707 turbine engine. When these tests were terminated in August 1973, 11 core failures had occurred out of a sample of 30 cores on test. It was determined that the failures were primarily caused by a severe chemical attack on the LAS material used. These test data showed that these regenerators had a B_{10} life of 600 hours and an average life of 1600 hours.

Late in 1973, an engineering research program was initiated to solve the regenerator core failure problem. The primary objective of this program is to develop ceramic regenerator cores that can be used in passenger car gas turbine engines, Stirling engines, industrial/truck gas turbine engines and other industrial waste heat recovery systems. Specific durability objectives are defined as achieving a B_{10} life of 10,000 hours on a truck/industrial gas turbine engine duty cycle at a regenerator inlet temperature of 800°C (1472°F).

In late 1973 Ford funded several companies to develop new ceramic regenerator materials. By 1974, new materials, including aluminum silicate (AS) and a magnesium aluminum silicate (MAS) were screened in laboratory and engine tests and found to have acceptable resistance to chemical attack. Regenerator cores made from new materials were placed on durability test late in 1974 and early in 1975.

The Ford 707 industrial turbine is being used as the test bed to evaluate these new regenerator materials and concepts. Since 1974, over 80,000 engine test hours (160,000 core hours) have been accumulated on regenerator systems. Core durability testing will continue in 1979 in an effort to demonstrate the B_{10} life of 10,000 hours required for an industrial gas turbine engine regenerator.

Late in 1974, the Alternate Automotive Power Systems Division of the Environmental Protection Agency joined with Ford Motor Company in an "Automotive Gas Turbine Ceramic Regenerator Design and Reliability Program." In early 1975, th's program was transferred to the newly-formed Energy Research and Development Administration (ERDA), and since 1976 this program has been under the direction of the National Aeronautics and Space Administration (NASA). A description of the work conducted in these programs is contained in References 1, 2, 3, and 4.

The present DOE/NASA cost-sharing program with Ford Motor Company continues the ceramic regenerator design and development work that was started under the original EPA/FORD contract. This latest program is subdivided into ten major tasks. These tasks are:

- Task I — Core Durability Testing at 800°C (1472°F)
- Task II — Core Durability Testing at 1000°C (1832°F)
- Task III — Material Screening Tests
- Task IV — Aero-Thermodynamic Performance
- Task V — Design Studies of Advanced Regenerator Systems
- Task VI — Ceramic Thermal Stability Tests
- Task VII — Manufacturing Cost Studies
- Task VIII — Core Material and Design Specifications
- Task IX — Program Management
- Task X — Reporting Requirements

The technical progress in each of these tasks for the period from January 1, 1978 to March 31, 1978 is recorded in the following sections of this report.

DISCUSSION OF RESULTS

TASK I. CORE DURABILITY TESTING AT 800°C (1472°F)

I.A. INTRODUCTION

Reference 1 describes the engine test results obtained by Ford Motor Company on lithium aluminum silicate ceramic regenerators used in the 707 turbine engine up to the end of 1973. These regenerator cores were mounted at the hub and driven through ceramic pins cemented into the rim. These data showed that chemical attack was the major cause of failure, and that this type of regenerator core configuration would have a B_{10} life of 600 hours and a B_{50} life of 1600 hours. A B_{10} life of 600 hours was obtained from a Weibull Analysis of the failures in this sample, and means that 10% of the regenerators of this configuration will fail in less than 600 hours of engine test. A B_{50} life of 1600 hours means that 50% of the regenerators will fail in less than 1600 hours of engine exposure.

Reference 1 also contains the engine test results that were obtained in 1974 and the first six months of 1975. Reference 2 describes the engine test results obtained during the last half of 1975 and the first three quarters of 1976. By this time, AS and MAS regenerators had been successfully fabricated, and showed promise in both accelerated and long-term engine durability tests. Reference 3 contains the test results obtained in the last quarter of 1976 and the first three quarters of 1977. Reference 4 describes the tests conducted in the last quarter of 1977.

This report describes the results of the additional engine tests that were conducted on these same concepts from January 1, 1978 to March 31, 1978. During this period, 4,128 engine test hours (8256 core hours) were accumulated at 800°C (1472°F), exceeding the program objective of 4000 engine hours for this period. The total accumulation of engine test hours since the start of the test program on January 1, 1974 increased to 80,000 hours (160,000 core hours).

I.B. STATUS

I.B.1 Durability Record of Aluminum Silicate Regenerators

To date 19 different aluminum silicate (AS) regenerators, fabricated by Supplier A, have been engine tested in the Ford 707 turbine. While all these cores are constructed from the same material, they can be broken down into two classifications depending upon their wall thickness. The original aluminum silicate configuration has an average matrix wall thickness of 0.11 mm (.0043 in.). In 1976, a high-performance, thin-wall configuration with a wall thickness of 0.07 mm (.0026 in.) was started on durability test.

Ten thick-wall AS cores are being tested at 800°C (1472°F) under identical operating conditions and these cores make up the control sample on which durability projections will be based. The durability status of these cores is shown in Figure I.B.1.1. All cores have acquired at least 985 hours of engine durability. About 52,000 core hours of engine test have been accumulated on this aluminum silicate sample with the highest hour core having attained 7804 hours. At least two failures are required before a Weibull Failure Analysis can be undertaken. There have been no failures of cores made from this material so a failure analysis cannot be started. A reliability projection, however, can now be made if the shape of the Weibull failure curve is estimated. Using Weibull theory and a sample consisting of the seven, highest-hour AS cores, together with an estimated failure curve slope, a B_{10} life of 5000 hours can be projected with 59% confidence. With the same theory, a B_{10} life of 3500 hours can be projected for AS material with almost 100% confidence. A B_{10} life of 3500 hours might be acceptable for an automotive application.

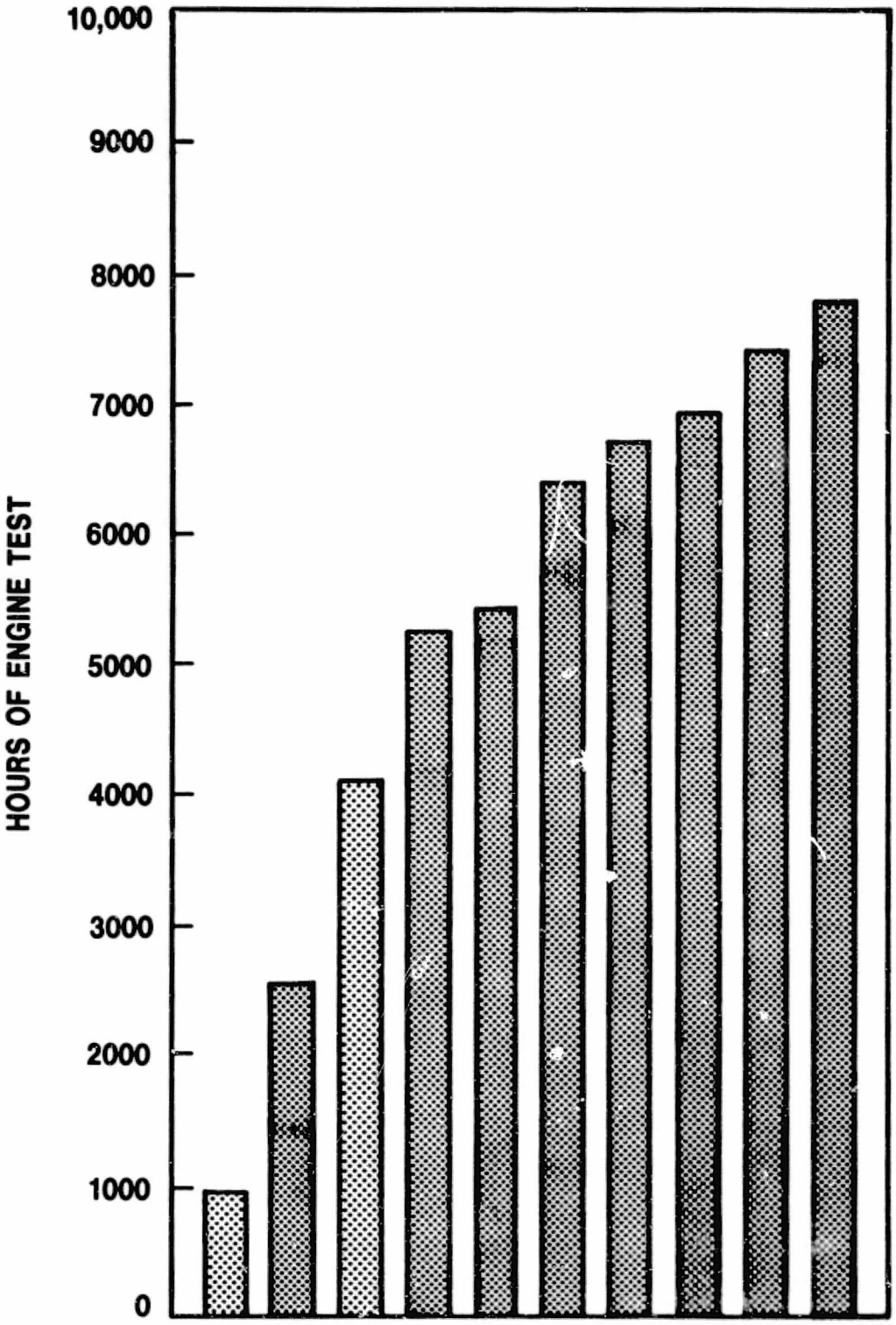

Figure I. B. 1. 1 Durability Record of Thick-Wail AS Regenerators Operating at 800°C (1472°F).

Seven thin-wall AS cores have also been engine tested at 800°C (1472°F) as shown in Figure I.B.1.2 and one core has accumulated over 6388 hours.

The running history of all of Supplier A's AS cores that have been engine tested are shown in Figure I.B.1.3. This figure also includes the two cores tested at 1000°C (1832°F) and described in Section II.B. Almost 71,000 hours of engine test have been accumulated on this material. None of these cores show any serious signs of thermal distress or chemical attack damage. To date, a total of eleven AS cores have each accumulated over 4,000 hours and six cores have each accumulated over 6,000 hours of engine test without visual distress.

It is planned to continue testing AS regenerators for the remainder of 1978 and the first half of 1979 to acquire additional long-term durability data.

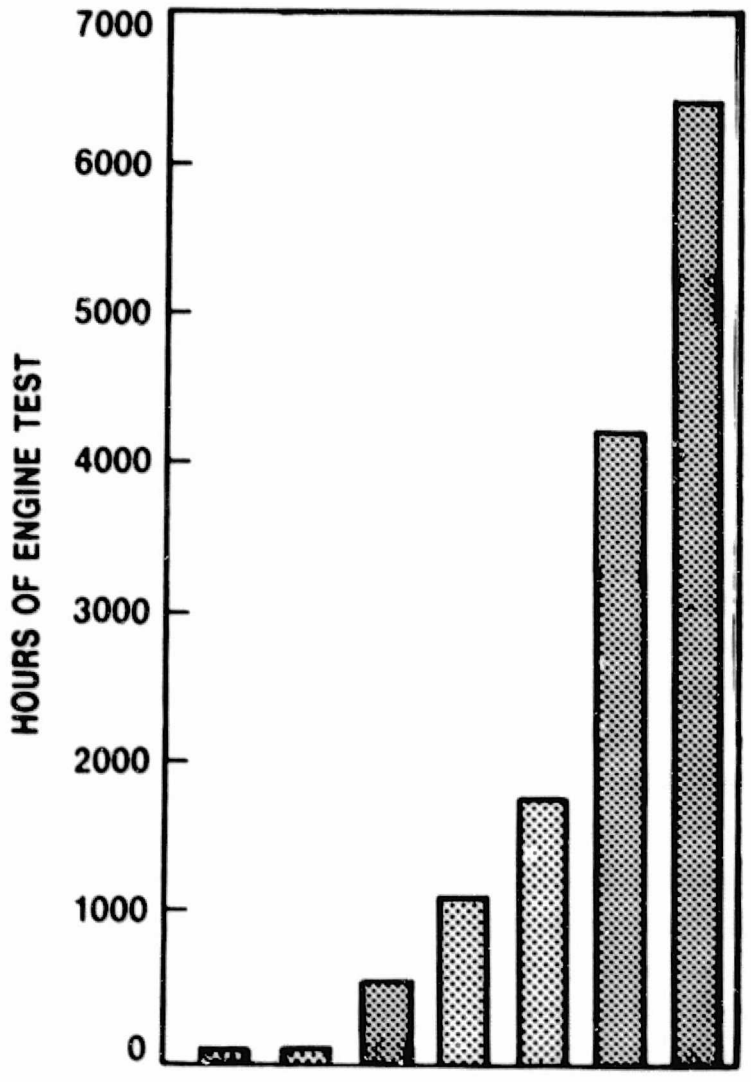

Figure I.B.1.2 Durability Record of Thin-Wall AS Regenerators Operating at 800°C (1472°F).

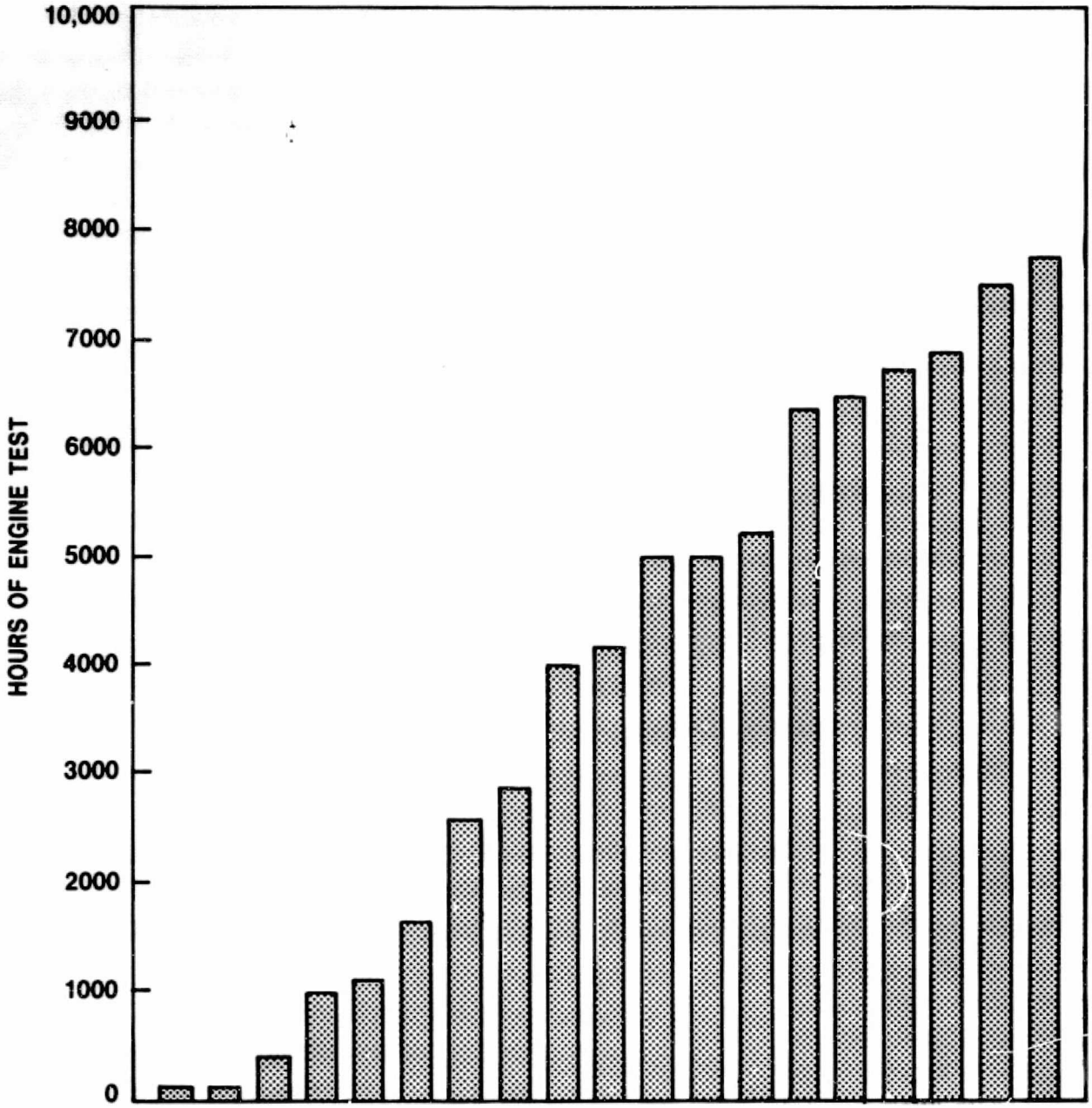

Figure I. B. 1.3 Durability Record of All AS Regenerators Tested in the Ford 707 Turbine Engine.

I. B. 2. Durability Record of Magnesium Aluminum Silicate Regenerators

Engine tests of two early MAS regenerators fabricated by Supplier D are described in Reference 1. The testing of both of these cores was terminated when the cement holding the hubs or center sections in place failed and caused damage in this region. Subsequently, an improved procedure for bonding the center insert to the rest of the matrix was developed and used on a third core provided by Supplier D. This core was evaluated in both the accelerated chemical attack engine test and long-term engine durability tests (Reference 2 and 3). The cement holding the center insert in place has failed, but the core has now accumulated 5381 total hours of engine test (Reference 4).

Thermal stress cracks developed in the third core after 200 hours of engine operation, but remained stable throughout the rest of the test. An analysis conducted on this MAS material showed that at the operating temperature of 800°C (1472°F) the rim thermal stress safety factor could be substantially below unity. The material in the rim area therefore, would be expected to fail and develop thermal cracks (Reference 4).

In late 1977, Supplier D successfully fabricated several cores made from a new MAS material which is stronger and has a lower thermal expansion coefficient than the material used in the original three cores. Three of these second-generation MAS cores have been placed on engine test, with a maximum time of 475 hours accumulated on one core. A summary of the operating experience on first and second generation MAS cores is shown in Figure I.B.2.1.

The new MAS cores have a 10 cm (4 inch) diameter hub insert that is smaller than that of the original MAS core which had a 23 cm (9 inch) diameter insert. This should decrease the likelihood of problems in the hub area.

The stress relieving slots in the new MAS cores extend all the way to the cold face and the ring gear is bonded to the cores with a greater compressive preload. Both of these changes were incorporated to increase the rim thermal-stress safety factor and are analyzed in detail in Section V.B.3. of Reference 4.

It is planned to continue testing the new MAS regenerator made from the advanced material in the 800°C (1472°C) engine operation. If schedules permit, this type of material and stress-relieving technique will also be evaluated in 1000°C (1832°F) engine tests.

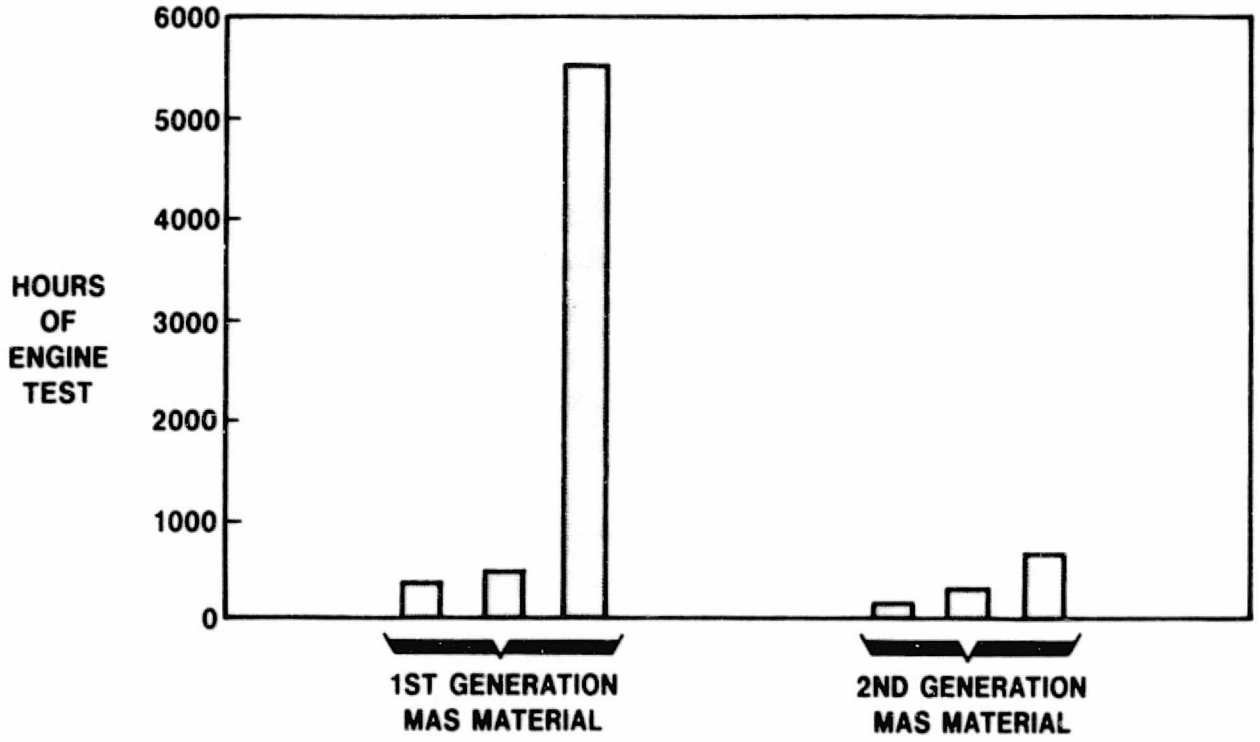

Figure I. B. 2. 1 Durability Record of First and Second Generation MAS Regenerators.

I.B.3. Hub Cement Failures

As reported in References 2 and 3, the cement holding the hub insert in place failed in five different AS cores out of 19 that have been engine tested in the 707 turbine. These cores, which were both thick and thin-wall, had accumulated between 68 and 4750 hours at the time of failure. In each case, the failure was attributed to improper composition or improper processing of the cement itself.

Several different concepts aimed at correcting this problem have been engine tested (Reference 3) and the most successful configuration is shown in Figure I.B.3.1. In this arrangement, the hub is cemented into a thin, 6.4 mm (.25 in) wide, solid ceramic ring and this sub-assembly is then cemented into the matrix. The ceramic ring allows better control of temperature during the firing of the cement, and it also provides a better match of the thermal expansion characteristics of the insert-matrix bond area to the rest of the matrix.

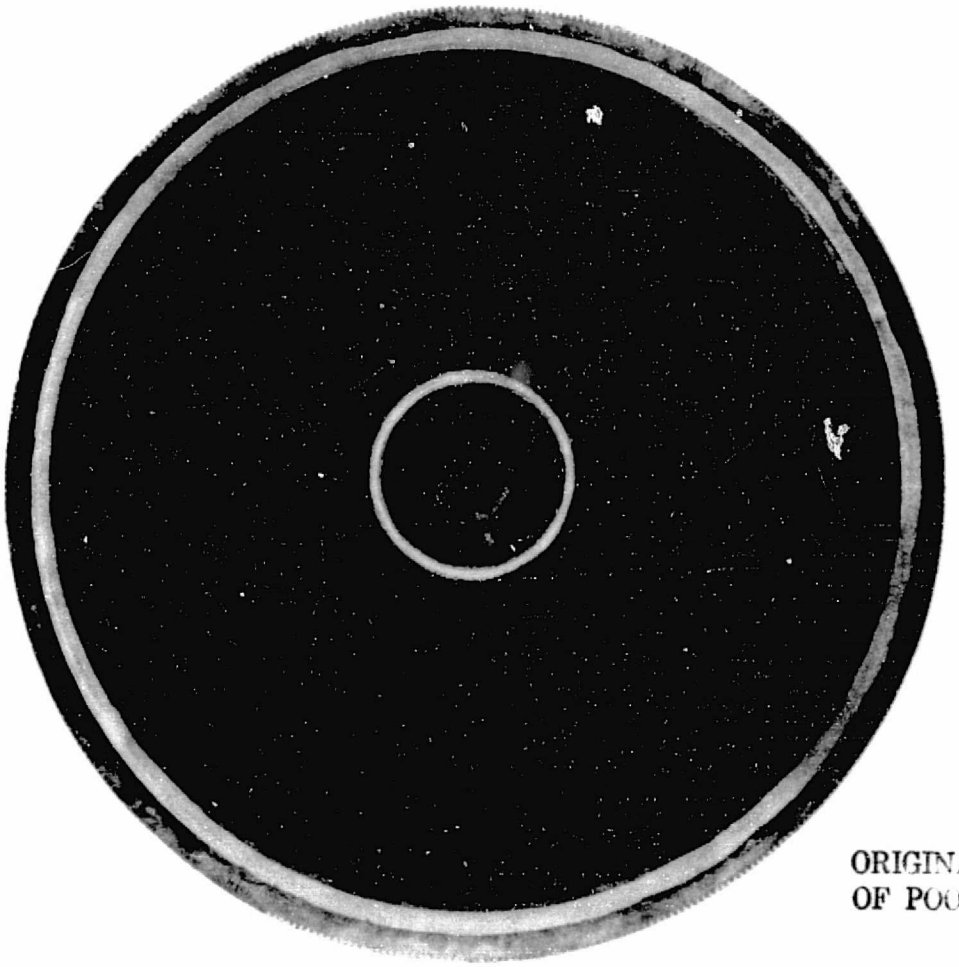

Figure I. B. 3. 1 Thick-Wall, AS Core Containing Solid Ceramic Ring Around Hub Insert.

All currently active AS cores that have undergone hub failures have been repaired to this configuration, and all new cores received from Supplier A have been built with this design. As a result, six cores with this new hub configuration have been on durability test since late 1976, and their durability record is shown in Figure I.B.3.2. One of these cores has accumulated over 4300 hours. One low-hour failure occurred during 1977, and after extensive investigations the cause of this failure is still unexplained.

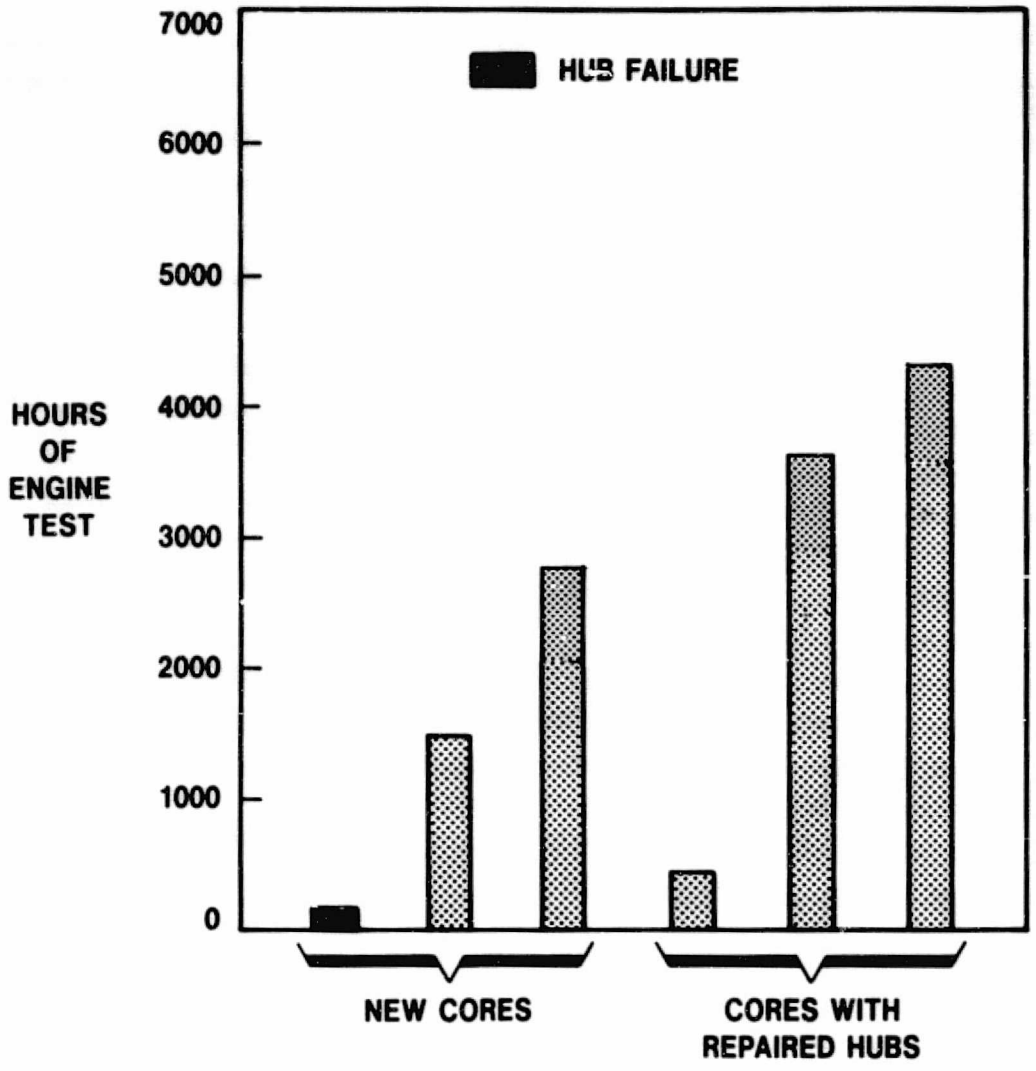

Figure I. B. 3.2 Durability Record of Cores with Solid Ceramic Ring Around Hub Insert.

These hub failures are still not considered to be a serious, fundamental problem. Hubs utilizing a solid ceramic ring around the hub insert have been fabricated into several AS cores, and their durability record appears better than the original hub configuration. More engine test hours are needed to determine the durability life of this concept.

I.B.4 Matrix — Elastomer Bond Separation

Reasonably good durability has been obtained with the elastomer bonded ring gear on the thick-wall AS cores. The results obtained with the same elastomeric drive on the thin-wall AS core have not been as successful. Since the thin-wall matrix has a thinner cross section, it is weaker and has less capability for carrying thermal and mechanical loads. Every thin-wall AS core, bonded with the same procedure used with the thick-wall cores, has had a separation in the elastomer-matrix bond area. The operating history is shown in Figure I.B.4.1. Experimental and analytical evidence presented in Reference 4 shows that the eventual solution to this problem is the development of a high-compliance, elastomer system in which the modulus of the elastomer is reduced at least 70%. This conclusion is supported by engine operating experience, also presented in Figure I.B.4.1, which shows that a 50% reduction in modulus is inadequate and failures will occur with this arrangement.

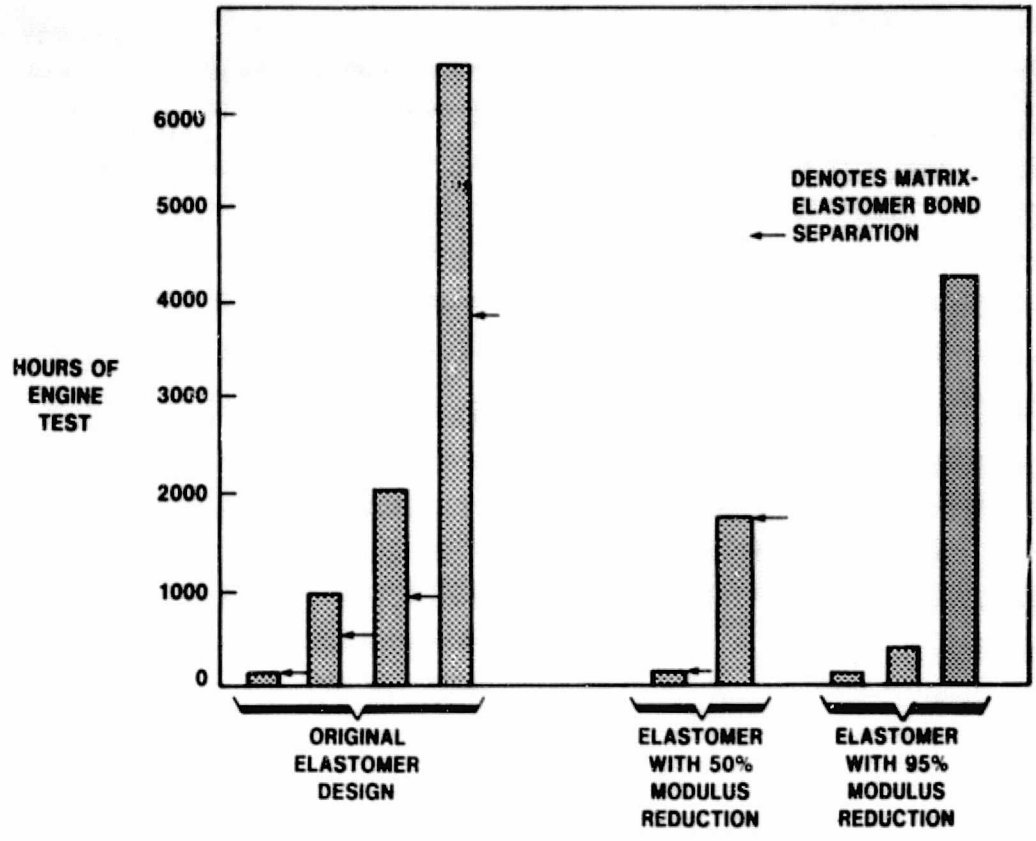

Figure I. B. 4. 1 Durability Record of Thin-Wall, AS Regenerators Utilizing Different Elastomer Bonding Approaches.

Three regenerator assemblies are now on test in which the modulus of the elastomer has been reduced by 90-95%. One of these assemblies has now accumulated 4,272 hours of engine test (Figure I.B.4.1.). These regenerator assemblies incorporate slots in the elastomer (Figure I.B.4.2.) to reduce the modulus.

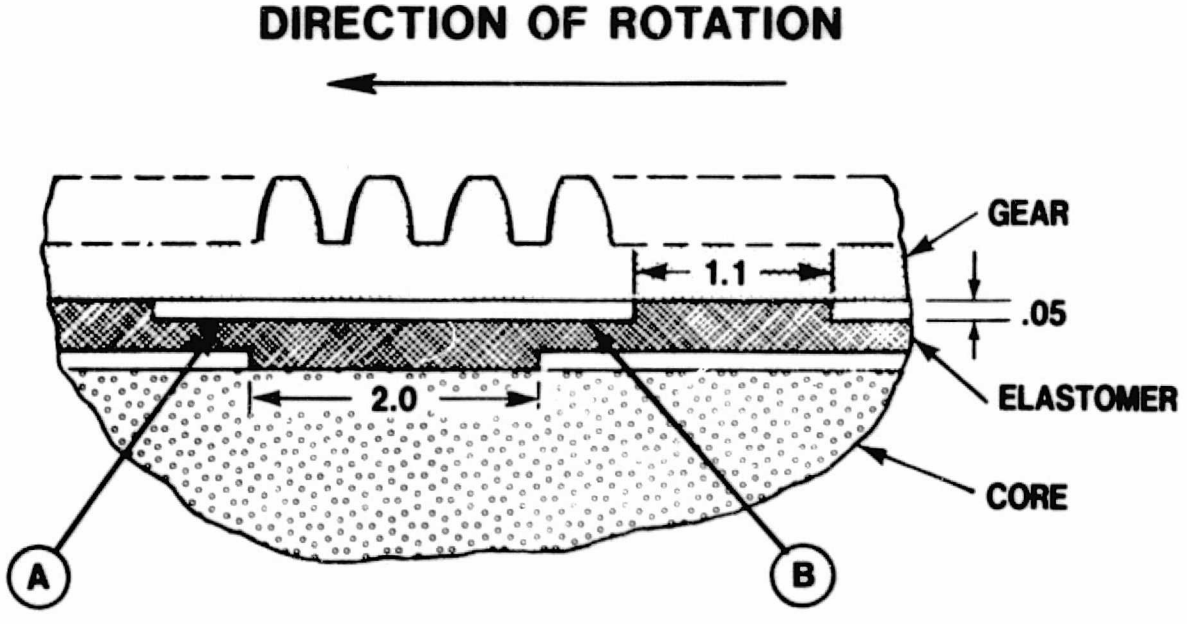

Figure I. B. 4. 2 High Compliance Elastomer Design.

Although the elastomer matrix bond area is still intact, a failure of the elastomer itself has occurred in the high-hour assembly. If the gear shown in the lower half of Figure I.B.4.2 moves from right to left, the drive torque will be transmitted as a tensile load through that portion of the elastomer marked "A" and as a compressive load through that portion marked "B." All of the tensile load carrying members, "A," have failed in the long-life assembly, and for the last 800 hours the drive torque has been transmitted by the compressive load members only. The cause of these elastomer failures is being investigated, but apparently they do not disturb the functional behavior of this concept.

It is planned to continue testing this slotted design through the remainder of the program, and all thick and thin-wall cores will be elastomerically bonded in the future with this configuration. The data accumulated to date suggest that this approach may result in the successful elastomeric bonding of the ring gear to thin-wall AS cores.

I.B.5 Drive and Support System

In 1974, the design and development of a rim-mount system was initiated to replace the hub-mounting system then in use in the Ford 707 turbine. The ring gear, which is attached to the rim with an elastomer, is supported at three points (Figure I.B.5.1). In addition to eliminating the need to develop solid ceramic hubs of AS and MAS materials, the elastomeric, rim-support system has stress reduction and cost advantages when compared to the earlier spring clip, hub-support system.

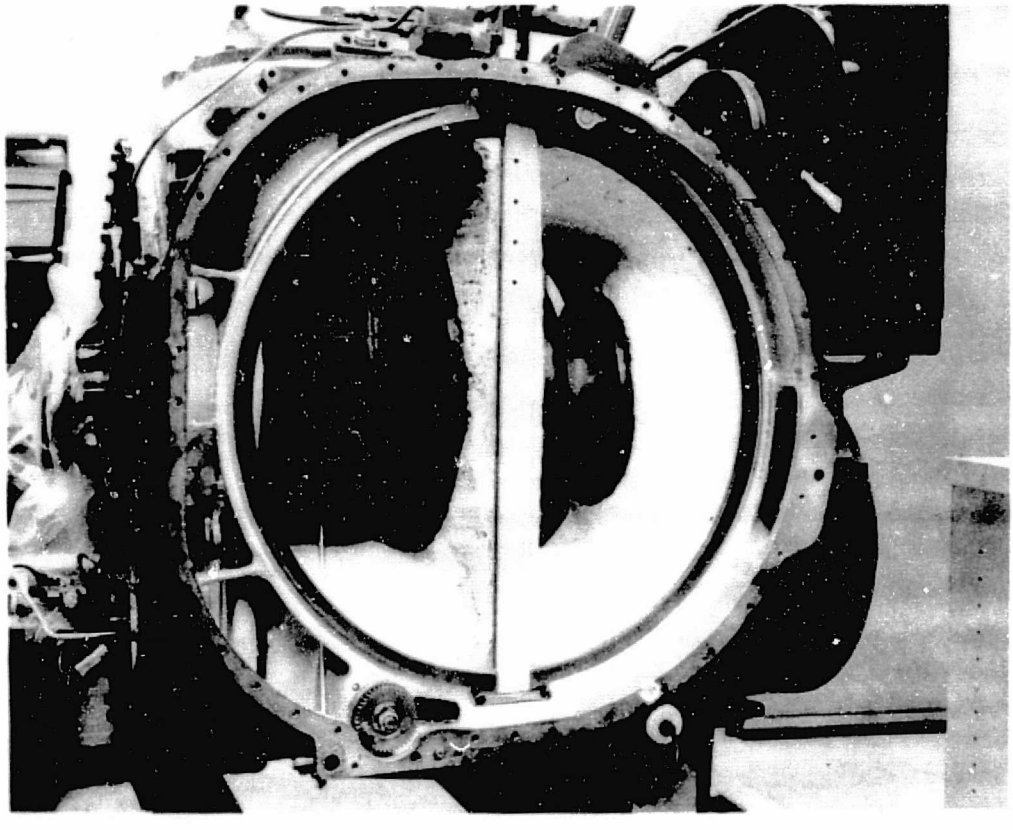

Figure I. B. 5. 1 Photograph of Ford 707 Turbine Engine Housing Showing Modifications Required to Incorporate the Present Rim-Support System.

Except at the pinion location, the roller assemblies contain an outer race support ring (Figure I.B.5.2) for the ball bearing. This provides additional rigidity, reduced bearing speeds, and lower contact stresses in the bearing.

Since the primary objective for operating these engines is to accumulate durability time on candidate regenerator materials and designs, the bearings are inspected every 350 to 400 hours in an effort directed at alleviating any difficulties in the drive system before damaging a high-hour regenerator matrix. As a precautionary measure, the bearings are re-greased after each inspection.

In order to eliminate the current necessity to lubricate these bearings, an experimental design concept was initiated during this report period. The new design replaces the ball bearing with a solid graphite bearing as shown on Figure I.B.5.3. This design concept was placed on test in one engine at the spring roller location, since it is lightly loaded compared to the fixed roller location. After 600 hours of engine test, the graphite bearing show no signs of distress with negligible wear.

Due to the encouraging results of this initial evaluation, additional graphite spring rollers will be placed on test during the next report period. In addition, a graphite design concept for the fixed roller location has been initiated.

At the present time, ten engines have been on test with the current three-point support system. No major difficulties have been encountered after 315, 1270, 1560, 1710, 2195, 2315, 3035, 3285, 5430 and 6865 hours for a total of 27,970 operating hours.

Figure I. B. 5. 2 Photograph Showing Ball Bearing, Outer Race Support Ring, and Snap Ring.

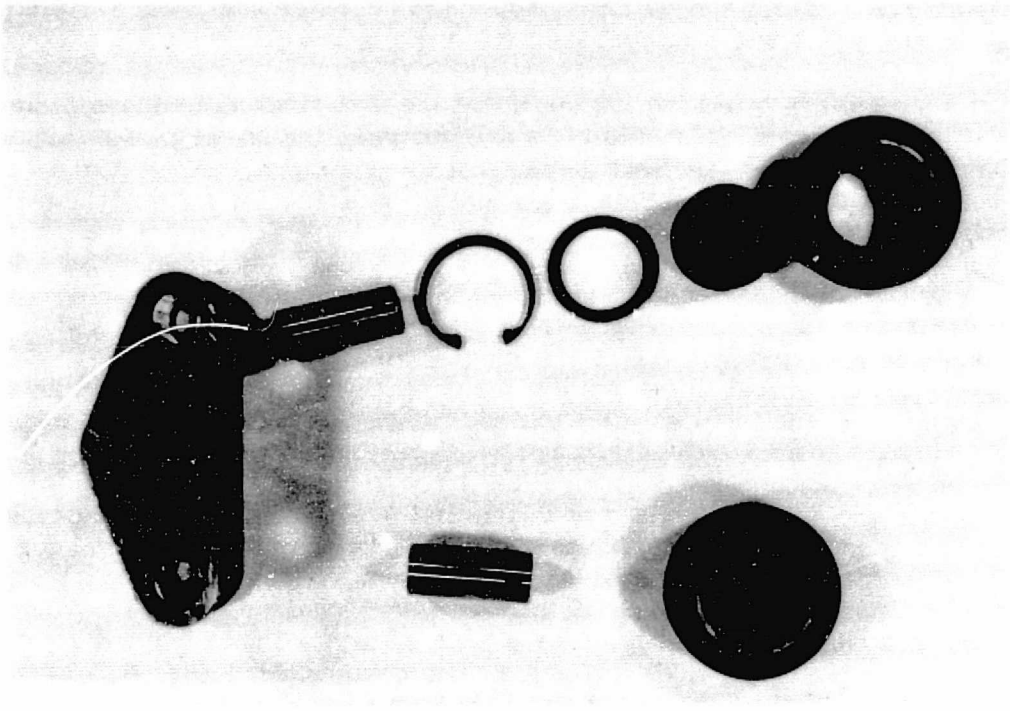

Figure I. B. 5.3 Photograph Showing Graphite Bearing, Outer Race Support Ring, Shaft, Snap Ring, and Yoke.

I. C. PROBLEM AREAS

Two problem areas exist and they are: failures of the cement bonding the hub insert to the matrix and separation at the elastomer-matrix interface in the thin-wall AS regenerator. The first problem is discussed in Section I.B.3 and the second is discussed in Section I.B.4. Corrective action consists of a ceramic ring for the first problem and high-compliance elastomer design for the second problem. Hardware incorporating these changes has now been started on engine test.

I. D. FUTURE PLANS

During the next quarter, the amount of engine testing at 800°C (1472°F) will be reduced, and more emphasis will be placed on engine tests at 1000°C (1832°F). This program change is discussed in detail in Section IX.B. of this report. Only the key, high-hour cores will continue on test in the two engines that will be committed to 800°C (1472°F) operation.

I. E. TASK SUMMARY

Approximately 4128 hours of engine durability test (8256 core hours) at 800°C (1472°F) were completed from January 1, 1978 to March 31, 1978 on cores made from chemically-resistant materials and mounted with a rim support and drive system.

Turbine engine durability tests on aluminum silicate regenerator cores show that this material is relatively impervious to chemical attack. Eleven cores of this material have each accumulated over 4000 hours of engine test at 800°C (1472°F), and

one core has attained 7804 hours of engine test with a minimal amount of chemical attack damage.

A high thermal expansion MAS core has accumulated 5381 hours at 800°C (1472°F). A MAS core made from a more advanced material having lower thermal expansion characteristics and greater strength has been placed on durability test and accumulated 475 hours during this report period.

One of Supplier A's thin-wall AS cores has now accumulated 6388 hours of engine test. Elastomeric bonding of the ring gear to this material requires additional development, since separations in the elastomer-matrix bond region have occurred on all thin-wall cores bonded using the conventional technique. Utilization of a high-compliance elastomer system shows promise of solving this problem. Three cores of this configuration are now on test, with one having accumulated 4272 hours.

The cement holding the hub inserts in place failed in five out of the eighteen AS cores that have undergone engine test. A hub configuration which utilizes a solid ceramic ring around the hub insert is now on test. One unexplained failure, has occurred in the six cores of this design that are now on test. Maximum operating time on this configuration is 4300 hours.

The spring-roller ball bearings in the mounting system in one engine have been replaced by solid graphite bearings. Over 600 hours have been accumulated on these bearings with little or no wear.

TASK II CORE DURABILITY TESTING AT 1000°C (1832°F)

II.A. INTRODUCTION

Since the fourth quarter of 1975, a special 707 turbine engine has been operated at elevated regenerator inlet temperatures. Throughout the test the engine has been operated at an average regenerator inlet temperature of 982°C (1800°F) with excursions of 30°C (52°F) above and below this value being permitted. These regenerator inlet temperatures are obtained by operating the engine at 1065-1080°C (1950-1975°F) turbine inlet temperatures at 60 to 65% gasifier spool speed and low power turbine speeds.

The objective of Task II of the DOE/NASA Ceramic Regenerator Program was to accumulate 1000 core-hours during the first quarter of 1978 at an inlet temperature of 1000°C (1832°F). A total of 1354 core-hours at this temperature were accumulated during this period.

II.B. STATUS

An AS thick-wall core is installed on one side of the high temperature engine and an AS thin-wall core is on the other side. The thick-wall AS core has been in place since the start of this test, and the thin-wall AS core was installed in 1976 when a core of an alternate material failed due to stresses induced by thermal gradients and chemical attack damage.

The thermal stress safety factor for aluminum silicate at these temperatures was determined in Reference 2. This material has a thermal stress safety factor of about 7.5 at 1000°C (1840°F). Providing the material is thermally stable, the aluminum silicate regenerator should have no problems with thermal stresses at this temperature. To date, the thick-wall AS core has accumulated 4983 hours at an average inlet temperature of 982°C (1800°F), and it shows no evidence of thermal or chemical distress.

The present Task II status is summarized in Table II.B.1 and shows that the thin-wall core has now accumulated 2680 hours at an average inlet temperature of 982°C (1800°F). A failure at the elastomer bond-matrix interface occurred in this thin-wall core after 271 hours. The failure is typical of thin-wall AS cores bonded with the original process. The core has been rebonded and returned to test. This failure mode and the corrective action are described in Section I.B.4.

II.C. PROBLEM AREAS

There are no problem areas associated with this task.

II.D. FUTURE PLANS

Testing of the thick and thin-wall AS cores described above will continue at 1000°C (1832°F). In addition, two more engines will be converted to 1000°C (1832°F) operation in the next quarter. This program change is described in more detail in Section IX.B. of this report. Additional thin-wall AS cores and MAS cores, if available, will be placed on durability test in these two additional engines.

II.E. TASK SUMMARY

About 4983 hours of engine test at an average regenerator inlet temperature of 982°C (1800°F) have been accumulated on a thick-wall aluminum silicate core, and 2680 hours at this temperature have been accumulated on a thin-wall AS core. Neither core shows any signs of thermal or chemical attack damage after this exposure.

MATERIAL	HOURS	SAFETY FACTOR	STATUS
AS THICK WALL	4983	7.5:1	NO DISTRESS
AS THIN WALL	2680	7.5:1	ELASTOMER-MATRIX BOND FAILURE

Table II. B. 1 Summary of Current Engine Tests at 982°C (1800°F).

TASK III MATERIAL SCREENING TESTS

III.A. INTRODUCTION

The material screening tests, a progressive series of three tests, carried out on laboratory samples, engine core inserts, and full-sized cores, are designed to systematically evaluate potential ceramic regenerator core materials. Materials successfully passing these tests should serve well as gas turbine regenerators at 800°C (1472°F).

Many of the data of this task and of Task VI, "Thermal Stability Tests of Ceramics," are reported graphically. The same graphing legend is used in both of these sections and is shown on each figure.

III.B. STATUS

III.B.1 Laboratory Tests

In this portion of the material screening tests, candidate materials are evaluated under laboratory conditions designed to simulate regenerator cold face and hot face chemical attack. Nine experimental materials (5-MAS, 2-leached LAS, 1-LAS, and 1-LAS/MAS) in addition to the 9455 LAS standard have been introduced into this testing program. Recently, three additional MAS materials were acquired, and these materials are presently being ground, cleaned and measured prior to their evaluation by this testing scheme.

During the past reporting period, three experimental materials have completed the cold face testing program. This completes the original group selected for testing, and the data are summarized in Figure III.B.1.1. By far the majority of the materials are quite stable under the cold face test conditions. One MAS, that of Supplier J, exhibits a consistent growth trend; while the LAS material of Supplier B experiences a small, but consistent contraction. Several data points are superimposed, and these points are indicated by arrows connecting the symbols with their proper position.

Figures III.B.1.2 through III.B.1.11 are the respective thermal expansion behaviors of the nine experimental materials and the 9455 LAS standard before and after cold face testing. A comparison of these figures, in light of the cold face test data of Figure III.B.1.1, points out the effect of the sulfuric acid exposure which may be encountered under some gas turbine regenerator cold face conditions. Note the difference in scales among the various figures.

The 9455 LAS standard, which exhibits quite a bit of growth under the cold face test conditions (Figure III.B.1.1) has undergone some pronounced changes in thermal expansion behavior (Figure III.B.1.2). Obviously, the material has undergone a physical (and most likely chemical) change. Figure III.B.1.5 depicts the thermal expansion depression experienced by the LAS/MAS material of Supplier K. The basic thermal expansion behavior has not been changed by the cold face test exposure, and the test data of Figure III.B.1.1 indicate the good stability, under cold face conditions, of this material. Of interest is the opposite behavior of the two LAS materials tested under cold face conditions: the 9455 standard and the experimental material of Supplier B. The standard expanded, while the other contracted (Figure III.B.1.1). Comparing Figures III.B.1.2 and III.B.1.7, one observes quite different thermal expansion changes; in one case (the standard) the thermal expansion is severely depressed by the proton-for-lithium ion exchange promoted by the cold face test conditions. The experimental LAS has experienced just the opposite effect; the post-test thermal expansion behavior is significantly higher. The final LAS-based materials tested were two leached LAS compositions: one from Supplier A and another from

Supplier B. Again, a comparison between their respective thermal expansion data plots (Figures III.B.1.3 and III.B.1.9) with respect to the cold face test data (Figure III.B.1.1) demonstrates the inter-consistency of the data. A small amount of cold face test growth was experienced by the leached LAS of Supplier A, and the attendant depression of the thermal expansion curve suggests further leaching. This trend is suggestive of the changes experienced by the 9455 LAS standard, although the leached LAS of Supplier A is less affected and retains the character of the original thermal expansion. In contrast, the thermal expansion of the leached LAS material of Supplier B is elevated after cold face testing (Figure III.B.1.9). This material suffered little measurable change during the course of the cold face laboratory test.

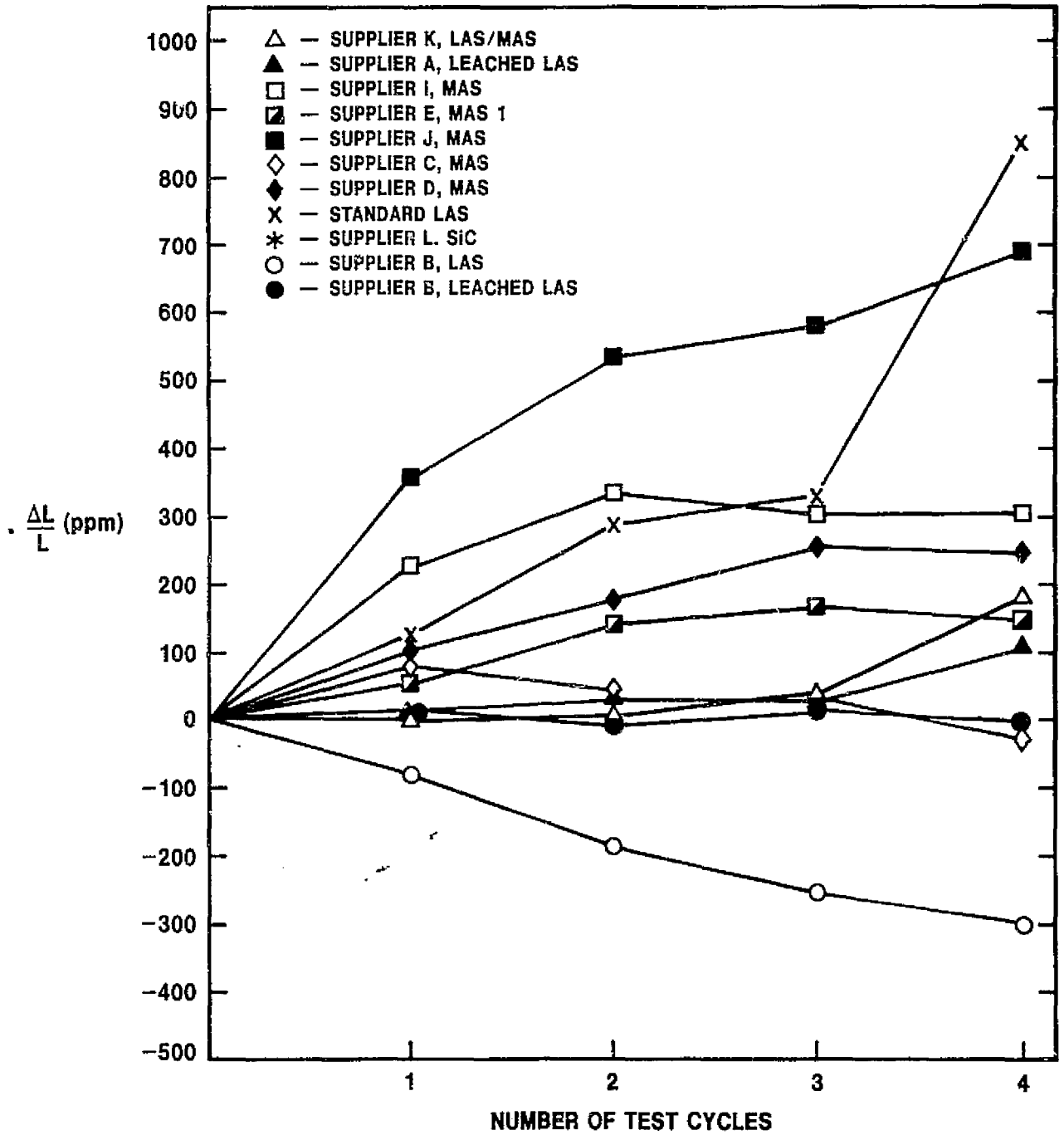

Figure III. B. 1. 1 Physical Stability of Various Materials Under Cold Face Test Conditions.

The MAS materials tested under cold face conditions also were examined for changes in thermal expansion behavior. Figures III.B.1.4, III.B.1.6, III.B.1.8, III.B.1.10, and III.B.1.11 compare measured thermal expansions of these materials before and after cold face testing. Again, the reader is cautioned to note the difference in graph scales when comparing one figure to another. An immediate observation of interest is the small amount of change in thermal expansion experienced by these materials which, for the majority, have demonstrated good resistance to the cold face test conditions. An interesting exercise is the ordering of the materials in the direction of increasing growth under cold face test conditions. This leads to the observation that the MAS materials exhibiting the greatest stability under cold face test conditions, Supplier C (Figure III.B.1.10) and Supplier E (Figure III.B.1.4), have a higher thermal expansion after testing. The remaining three MAS materials; those of Supplier D (Figure III.B.1.6), Supplier I (Figure III.B.1.8), and Supplier J (Figure III.B.1.11) experienced more growth under the cold face test conditions, and these materials were left with a lower thermal expansion behavior after testing. One might speculate that a stress corrosion mechanism may be operative in the extension of existing cracks in these materials, thereby effecting a microcrack-like effect and lowering the thermal expansion. Clearly, the less affected materials are influenced quite differently by the same test conditions. No mechanism to explain the attendant increase of the thermal expansion of these MAS specimens is offered, as the reader is certainly as capable of speculation as is the author. The effect has been observed and recorded and, perhaps combined with subsequent data and analyzed sufficiently, will one day be understood.

In complementary fashion, testing to evaluate regenerator materials under hot face conditions have been carried to completion on the same 9 materials plus the 9455 LAS standard. The data compiled to date are presented in Figure III.B.1.12. All but one material, the LAS/MAS of Supplier K, show improved resistance to sodium attack at 800°C (1472°F) compared to the 9455 LAS standard. The LAS material of Supplier B exhibits good stability under these test conditions, experiencing a growth intermediate between that of the most resistant MAS materials and the remainder of the test group. The two leached LAS materials behave alike. The group of MAS materials exhibit a range of stability; this variance in behavior has been previously observed and attributed to the individuality of each material in terms of composition and processing. Most of the materials experience an immediate and significant reaction to the elevated sodium treatment, followed by subsequent periods of virtual stability. In some cases there are small amounts of growth, and some of the materials experience a consistent, though diminished, growth after the initial treatment period. The final data reflect a growth in every material; and longer time data, such as that generated in the Thermal Stability Tests of Ceramics (Section VI), may be more informative. It would appear that the initial sodium intrusion into these materials may form a boundary zone through which further penetration is slowed. The diffusion of sodium from this boundary zone into adjacent, pristine material would then become the rate-controlling step. The progress of this diffusion, causing modification of the sodium ion concentration and the establishment of a gradient in the near-surface zone of exchange, could reactivate a subsequent utilization of surface sodium.

Figures III.B.1.13 through III.B.1.22 display the thermal expansion behavior of the nine experimental materials and the 9455 LAS standard before and after hot face testing. A comparison of these figures, using the hot face test data of Figure III.B.1.12 as a reference, provides an insight into the changes experienced by these materials during their exposure to the laboratory test conditions designed to simulate the hot face of a gas turbine regenerator.

Materials containing an LAS phase are the 9455 standard (Figure III.B.1.13), the LAS/MAS material of Supplier K (Figure III.B.1.16), and the material of Supplier B (Figure III.B.1.18). The 9455 standard experienced a mild elevation in thermal

expansion behavior, but the basic character of the material response to temperature change was unmodified. Although the LAS of Supplier B exhibited better stability under hot face test conditions, the thermal expansion change attending the testing was much more drastic. The nature of the thermal expansion has changed. Originally mildly contractive, this material has become slightly expansive after exposure to sodium at 800°C (1472°F) for 500 hours. The LAS/MAS material from Supplier K experienced a great change in thermal expansion behavior and is reflective of the lack of resistance to sodium which was evidenced during hot face testing.

The two leached LAS materials demonstrated comparable stability under hot face test conditions; however, the change in thermal expansion behavior after hot face

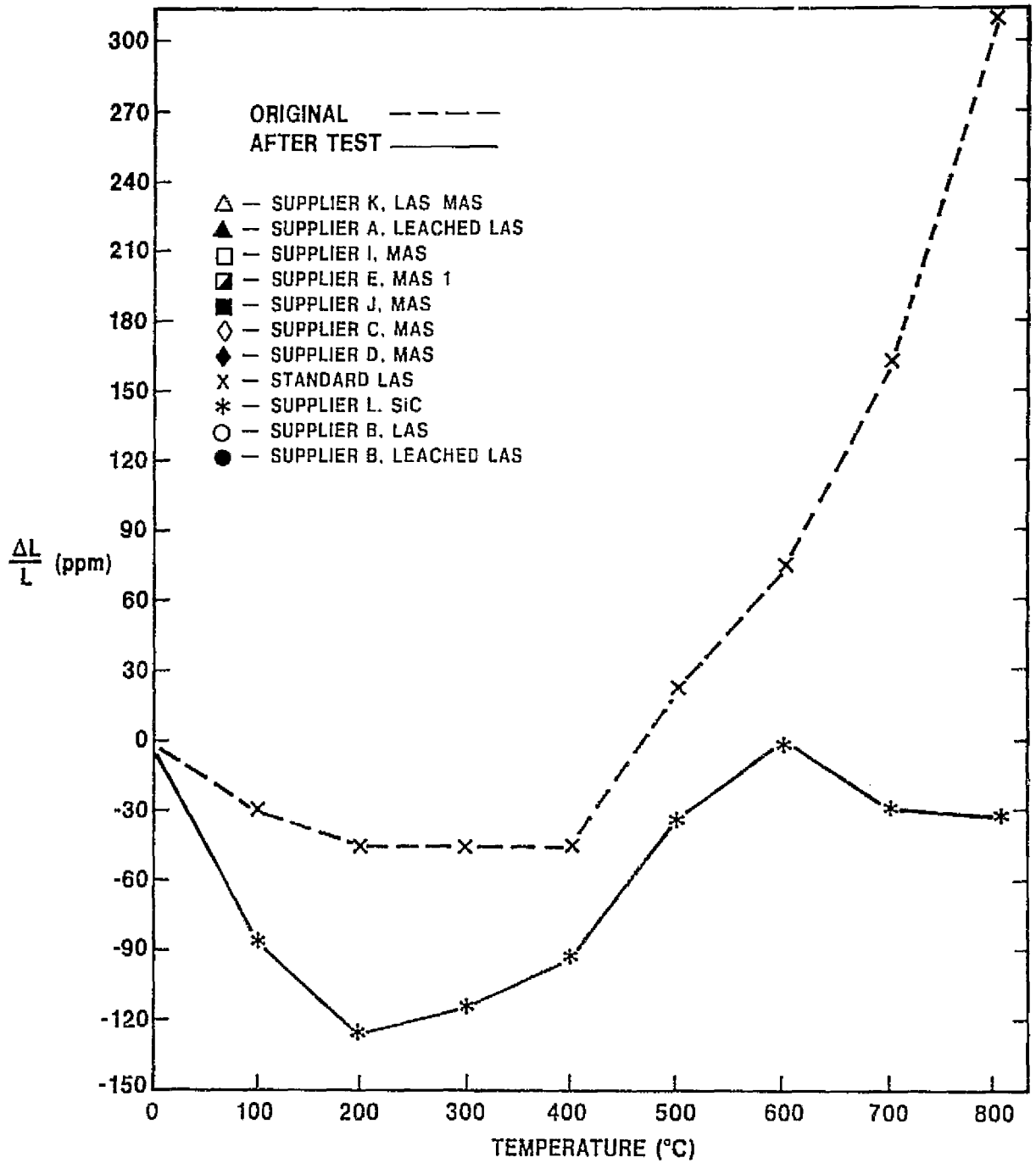

Figure III. B. 1. 2 9455 LAS Standard; Thermal Expansion Before and After Cold Face Testing.

testing was quite different for the respective materials. After testing, the leached LAS of Supplier A has become more strongly contractive with increasing temperature (Figure III.B.1.14). The leached LAS of Supplier B has become slightly expansive after testing (Figure III.B.1.20). This effect is rather dramatic, as the original expansion behavior, as measured dilatometrically, was rather contractive.

The MAS materials compared under hot face test conditions experienced a range of elongation varying from nil to 450 ppm after 504 test hours. An interesting trend emerges if one ranks the materials in order of increasing elongation (Suppliers: E,

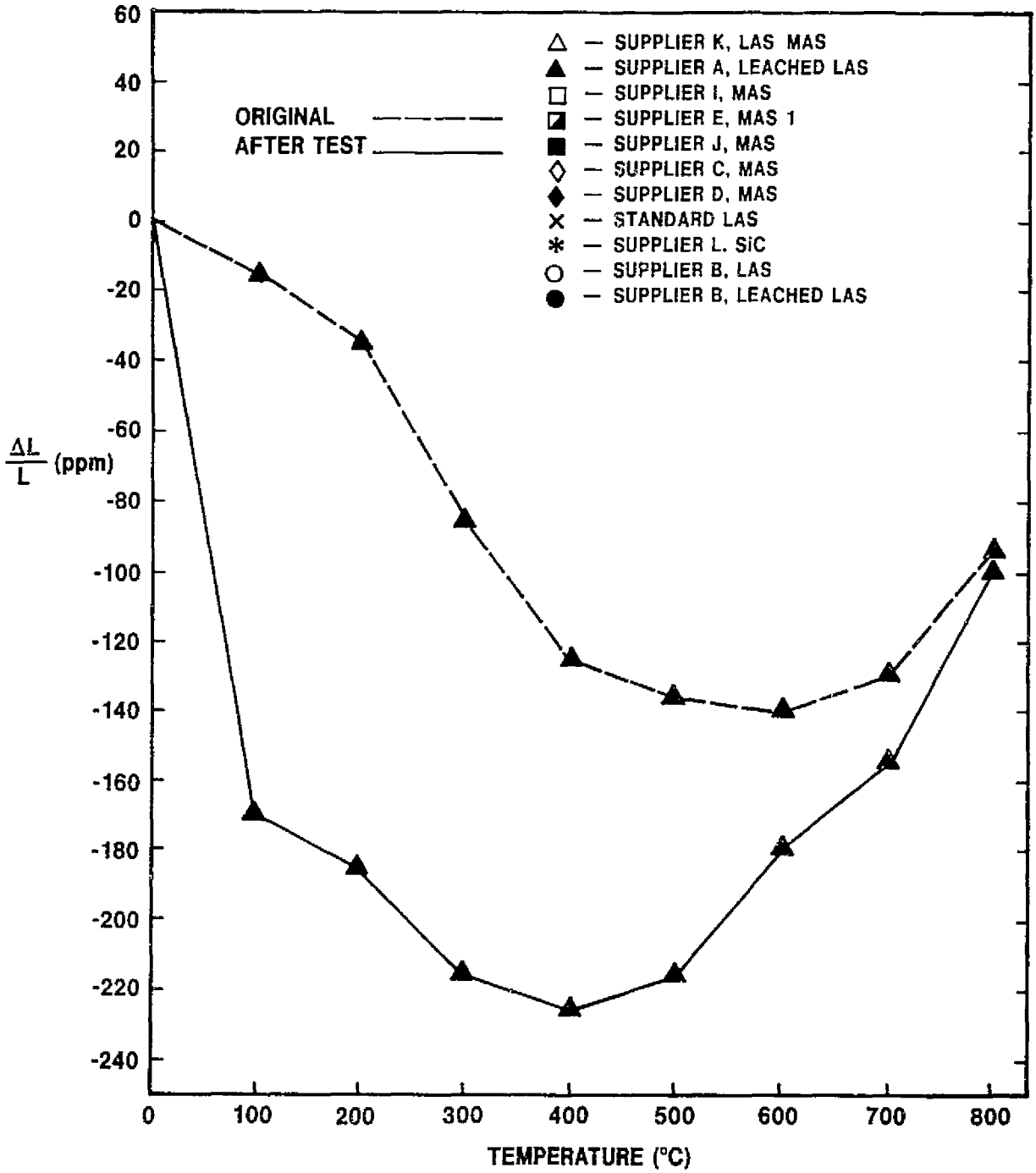

Figure III. B. 1. 3 Supplier A Leached LAS; Thermal Expansion Before and After Cold Face Testing.

C, I, J and D). Their respective thermal expansion plots before and after hot face testing (Figures: III.B.1.15, III.B.1.21, III.B.1.19, III.B.1.22, and III.B.1.17). The first two materials, which experienced virtually no physical change as a result of the hot face testing, have undergone negligible change in thermal expansion behavior. The remaining three materials, each suffering more hot face test growth than the last, also exhibit a correspondingly greater perturbation in their thermal expansion behaviors. The more resistant MAS materials experience a small decrease in thermal expansion after hot face testing, while the less resistant MAS materials experience an increase. This, again, is suggestive of a microcracking type of damage phenom-

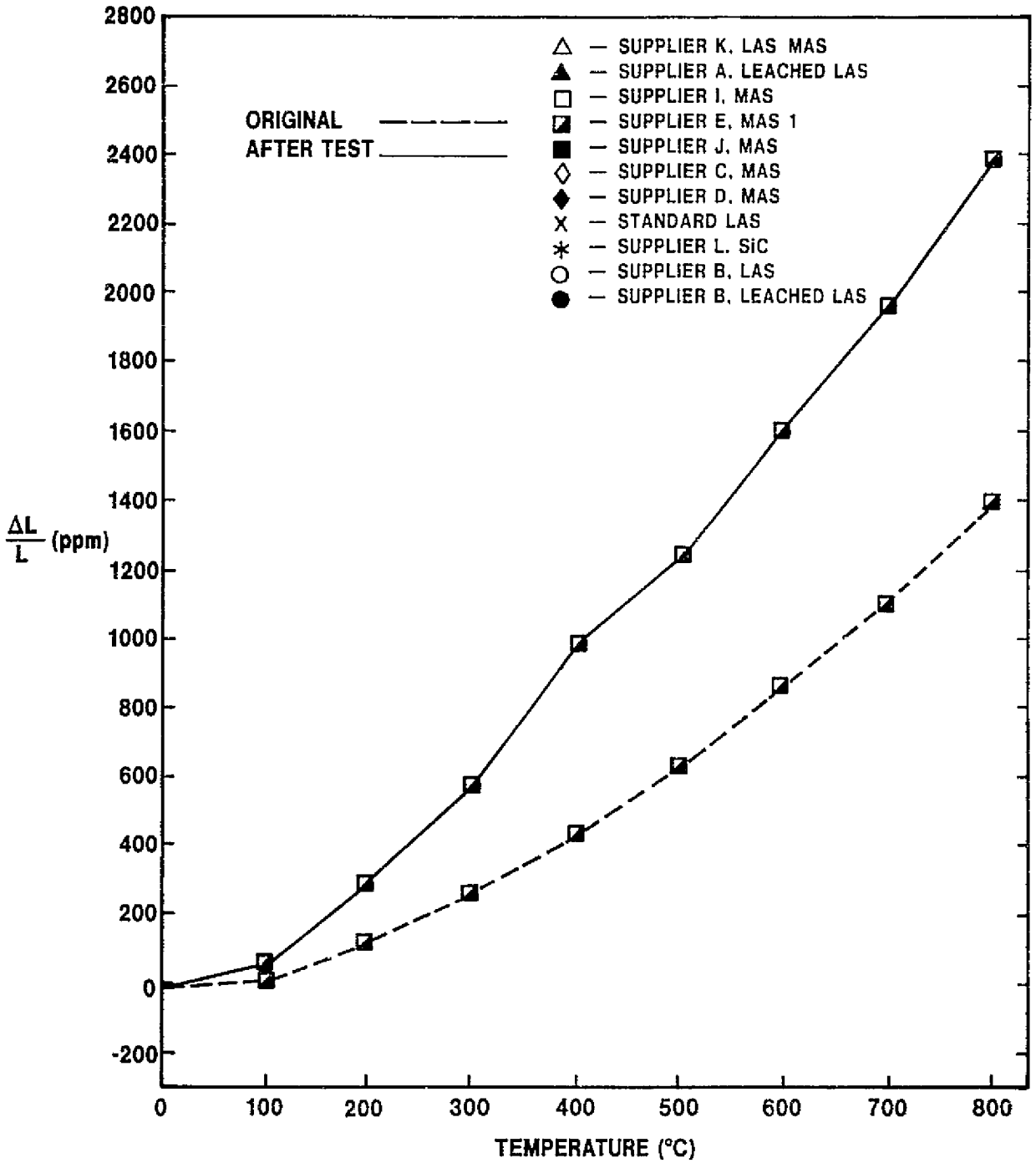

Figure III. B. 1. 4 Supplier E MAS; Thermal Expansion Before and After Cold Face Testing.

enon. Of interest is the observation that, for each respective MAS material, the change in thermal expansion after hot face testing is of opposite direction to that change following the cold face testing. These observations point out a consistency of material response to the test schemes; and, statistically, lend additional credence to the test data.

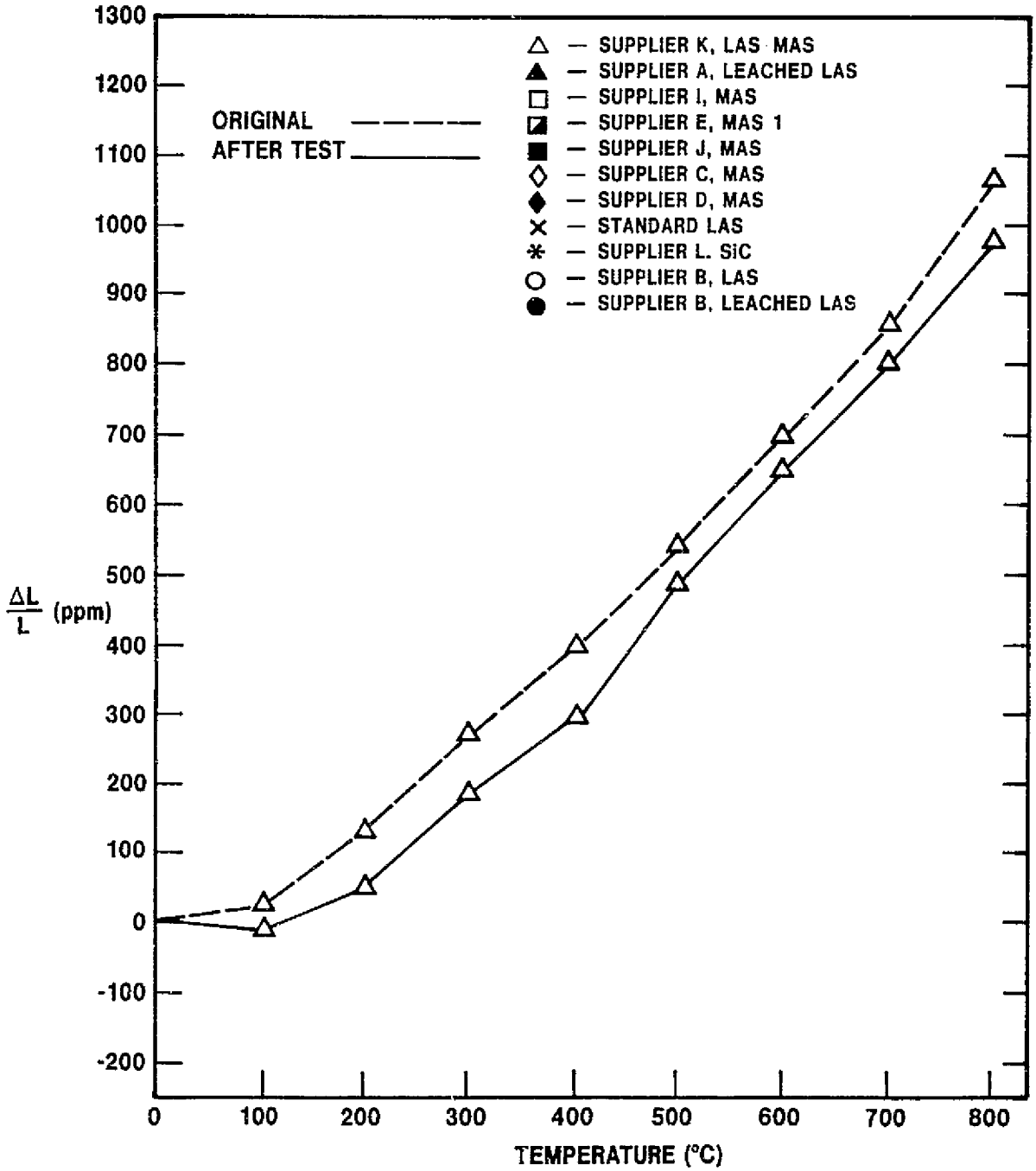

Figure III. B. 1. 5 Supplier K LAS/MAS; Thermal Expansion Before and After Cold Face Testing.

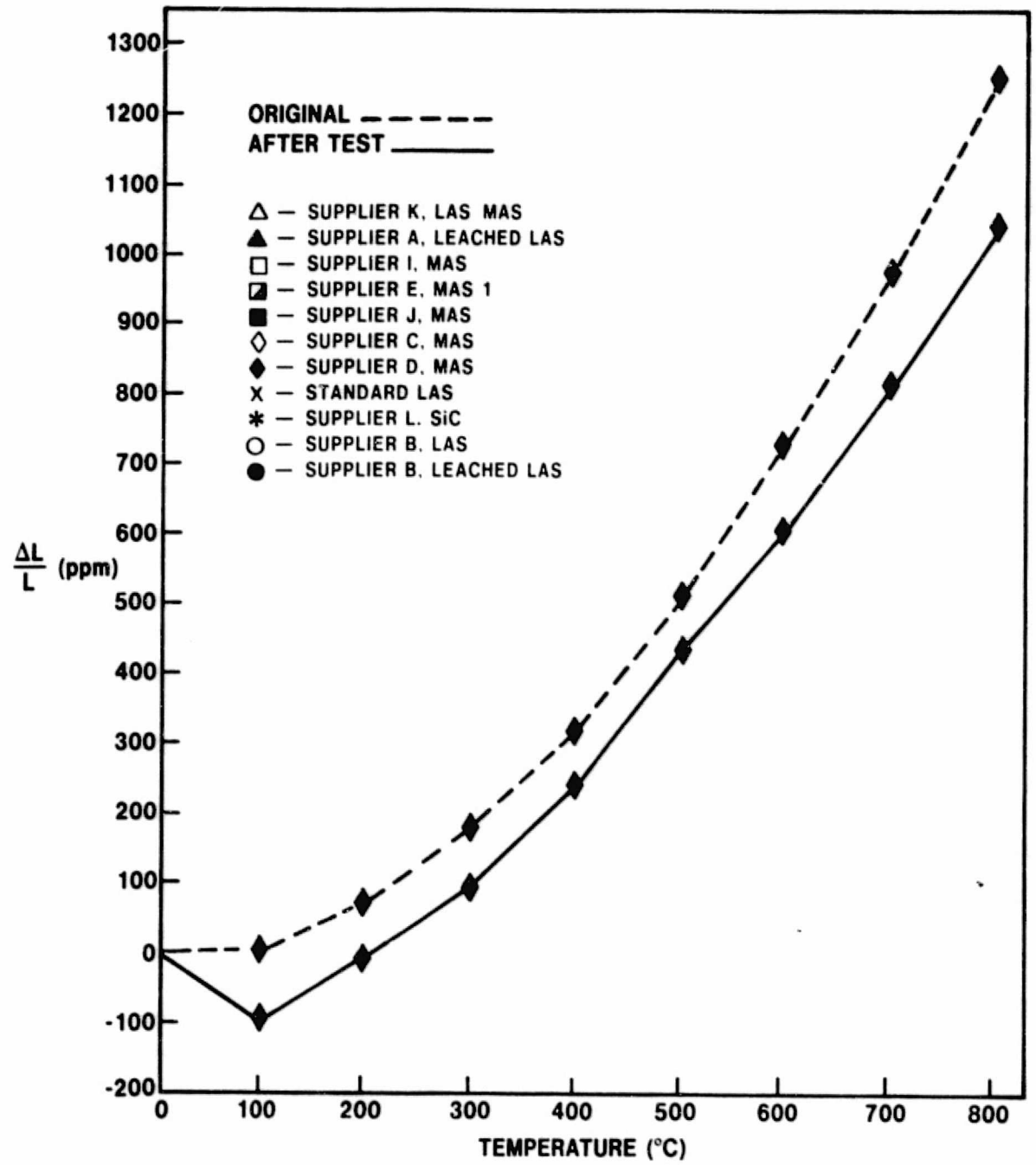

Figure III. B. 1. 6 Supplier D MAS; Thermal Expansion Before and After Cold Face Testing.

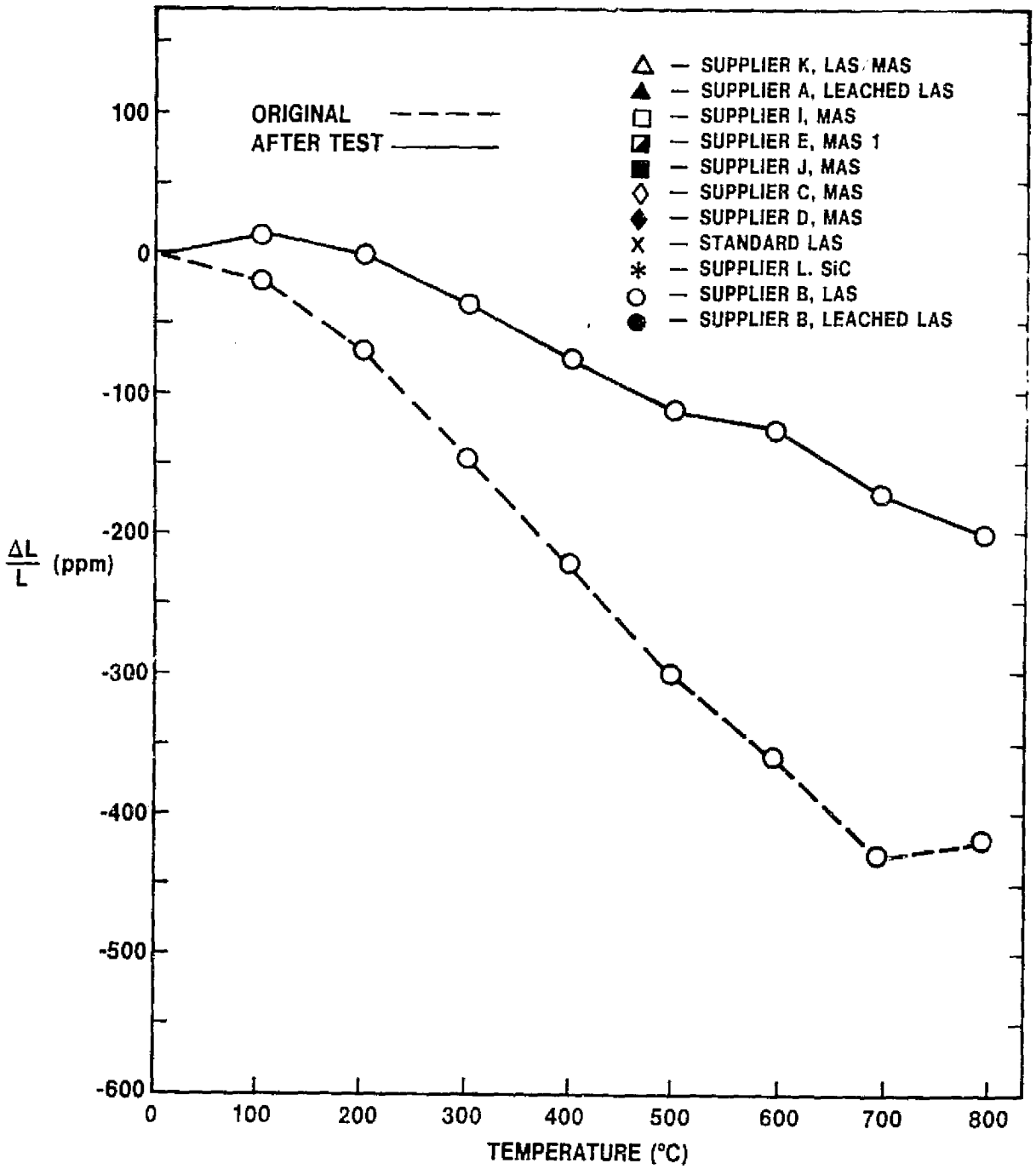

Figure III. B. 1. 7 Supplier B LAS; Thermal Expansion Before and After Cold Face Testing.

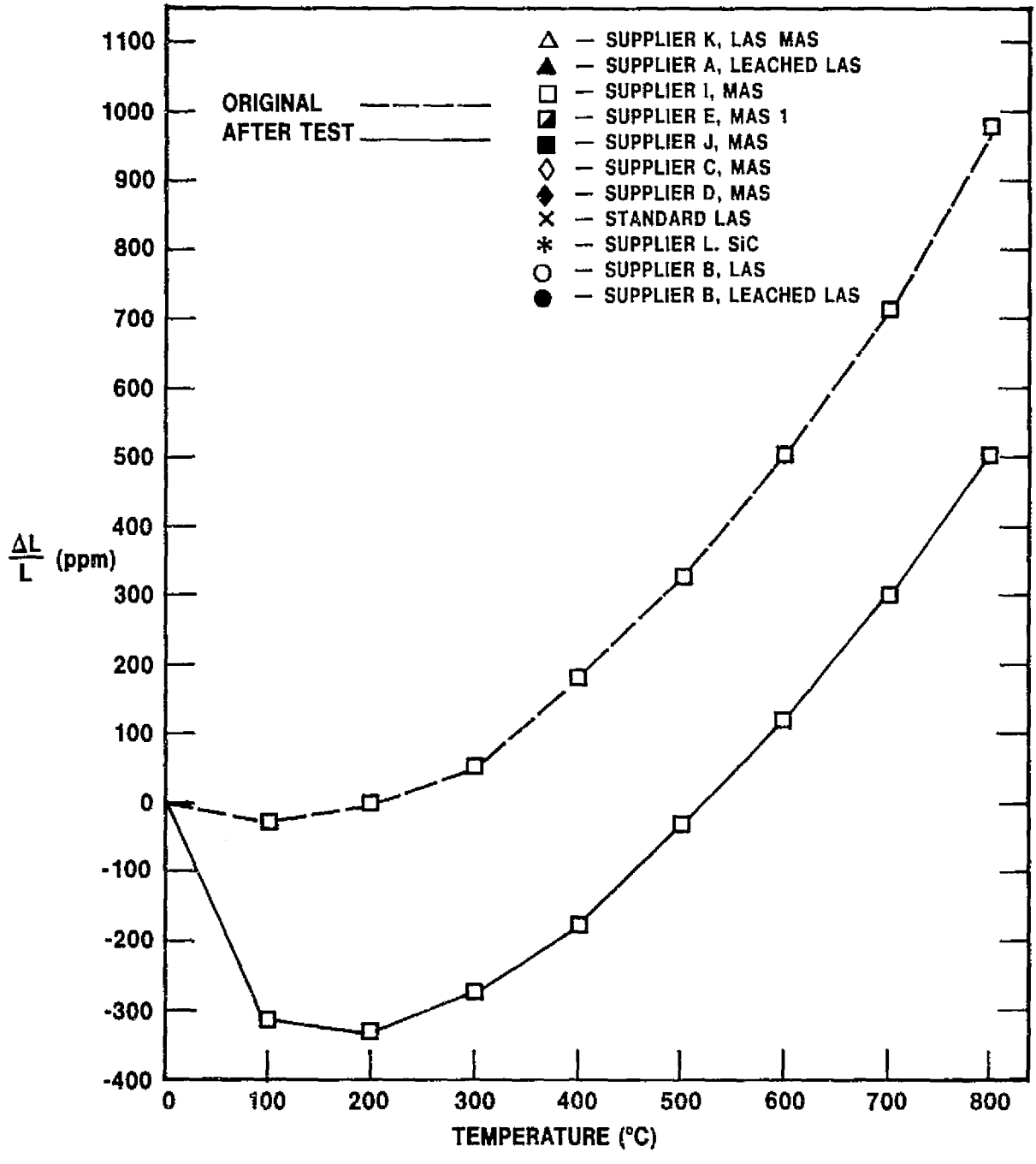

Figure III. B. 1. 8 Supplier I MAS; Thermal Expansion Before and After Cold Face Testing.

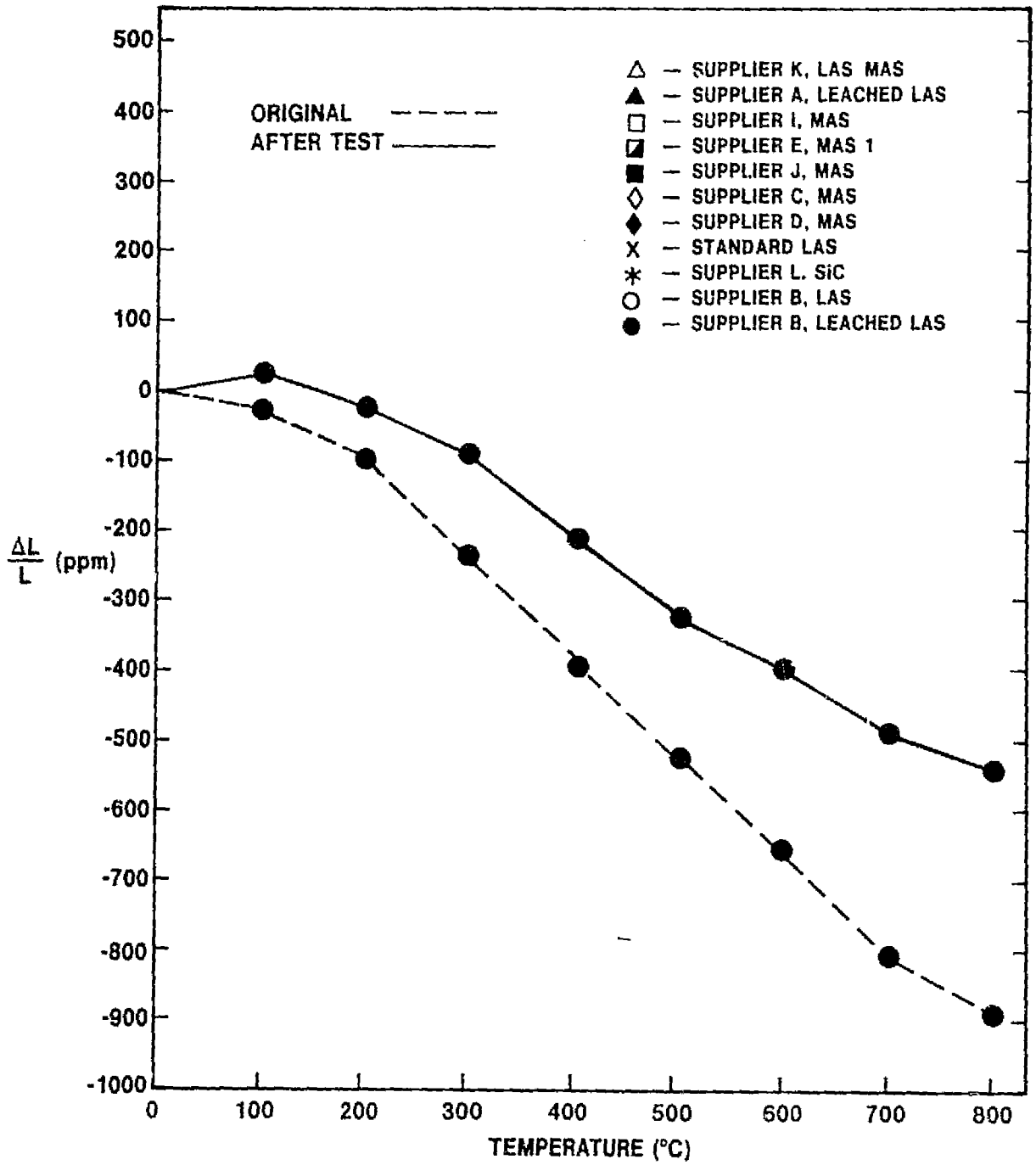

Figure III. B. 1. 9 Supplier B Leached LAS; Thermal Expansion Before and After Cold Face Testing.

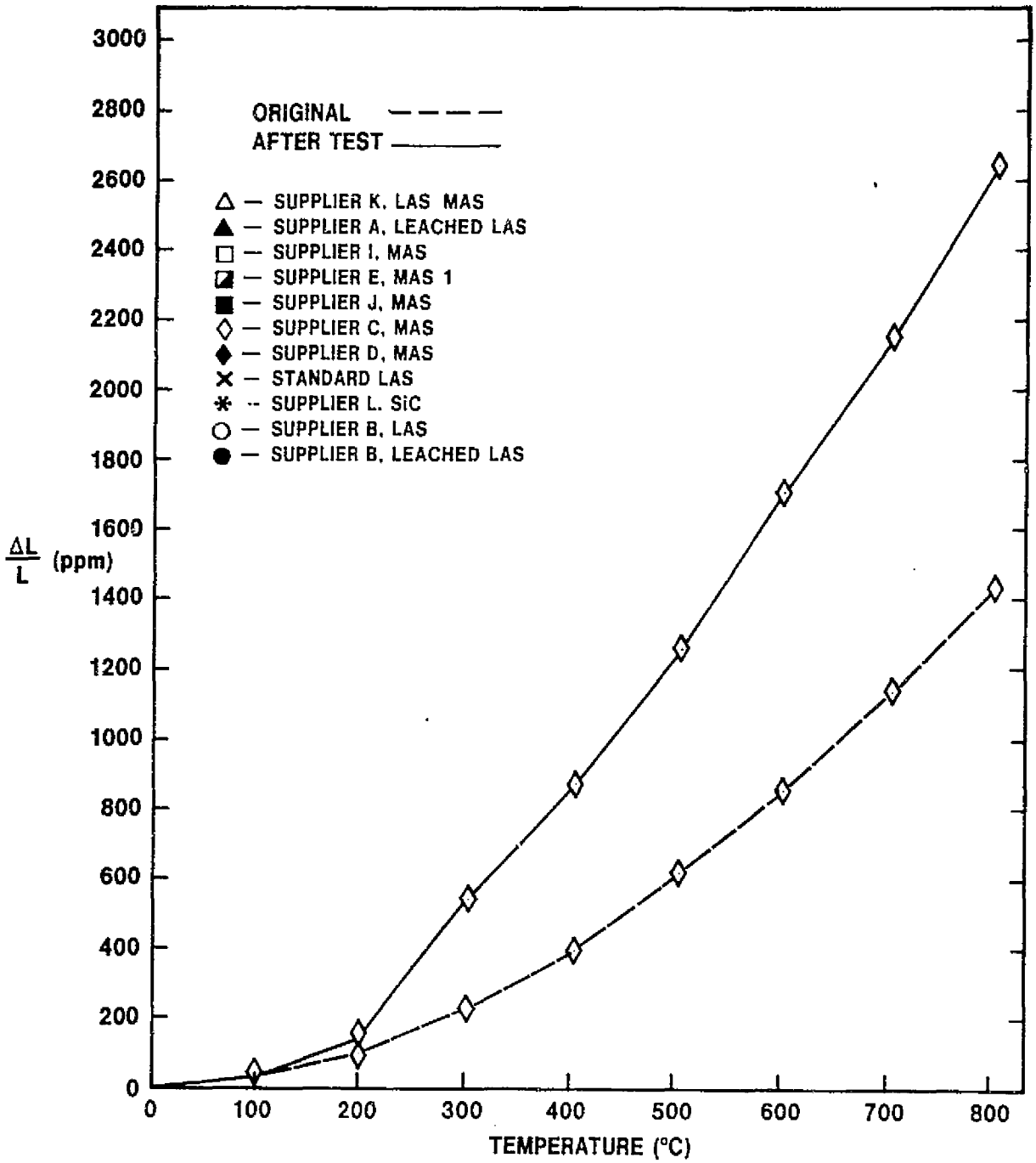

Figure III. B. 1. 10 Supplier C MAS; Thermal Expansion Before and After Cold Face Testing.

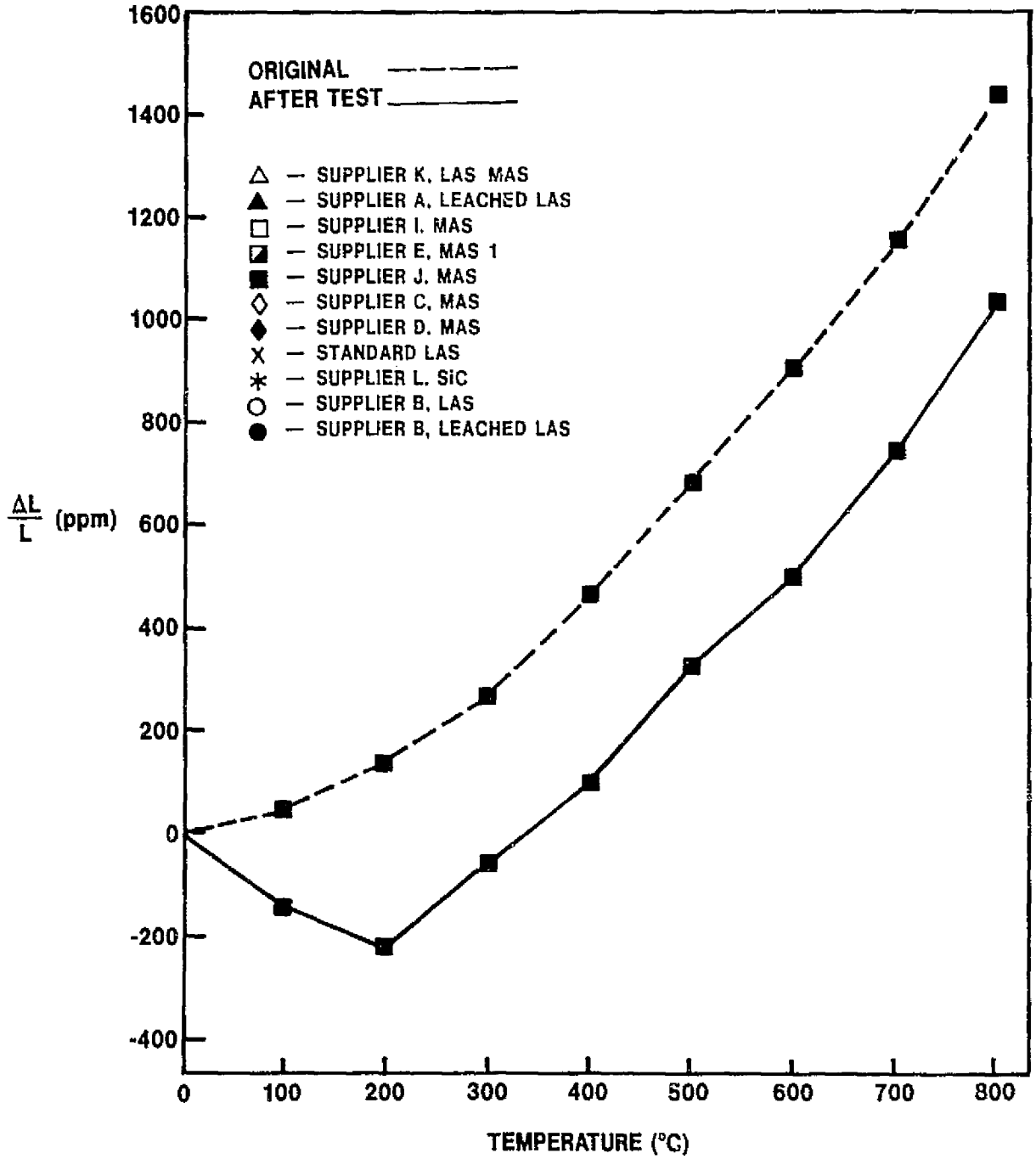

Figure III. B. 1. 11 Supplier J MAS; Thermal Expansion Before and After Cold Face Testing.

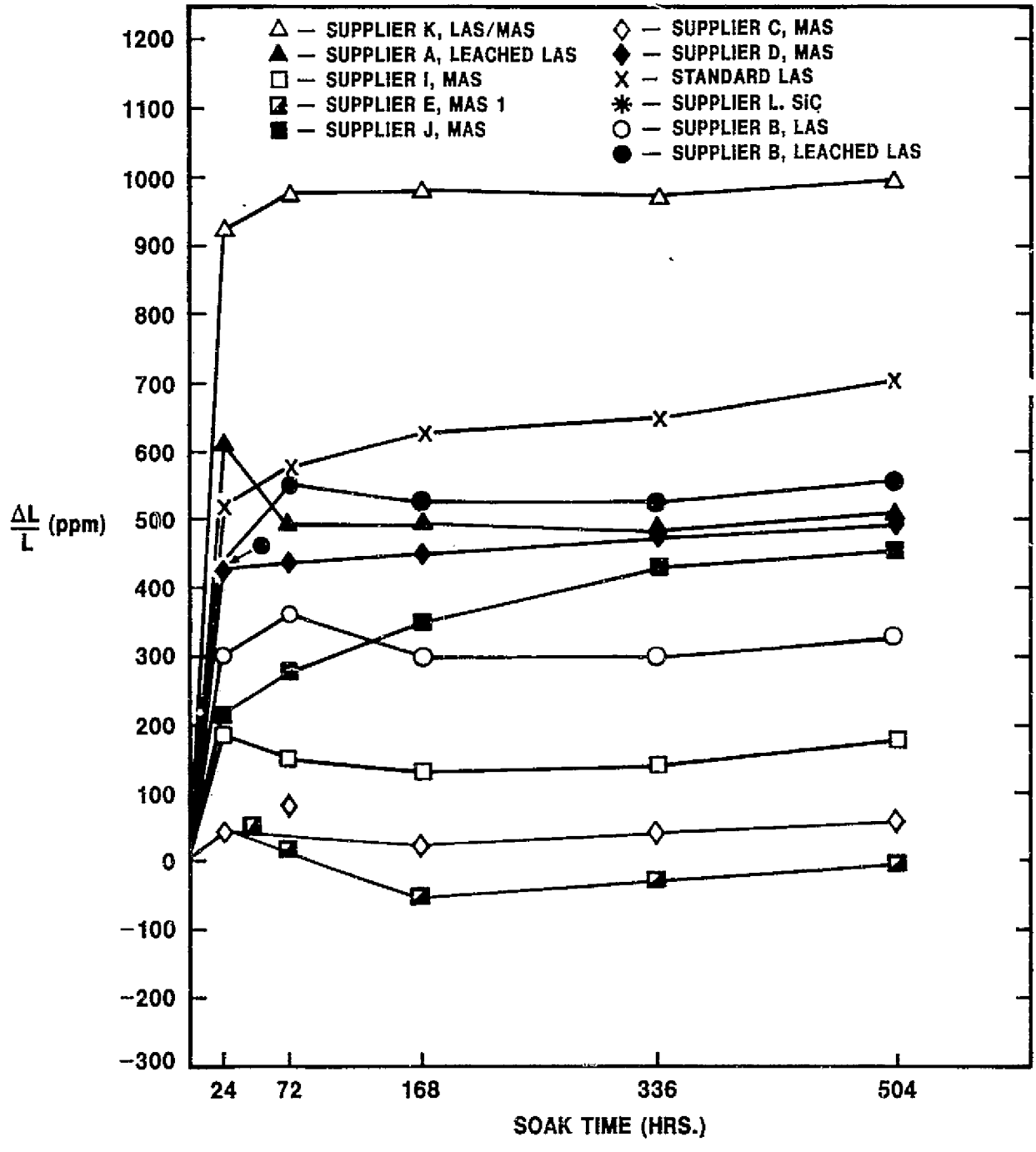

Figure III. B. 1. 12 Physical Stability of Various Materials Under Hot Face Test Conditions.

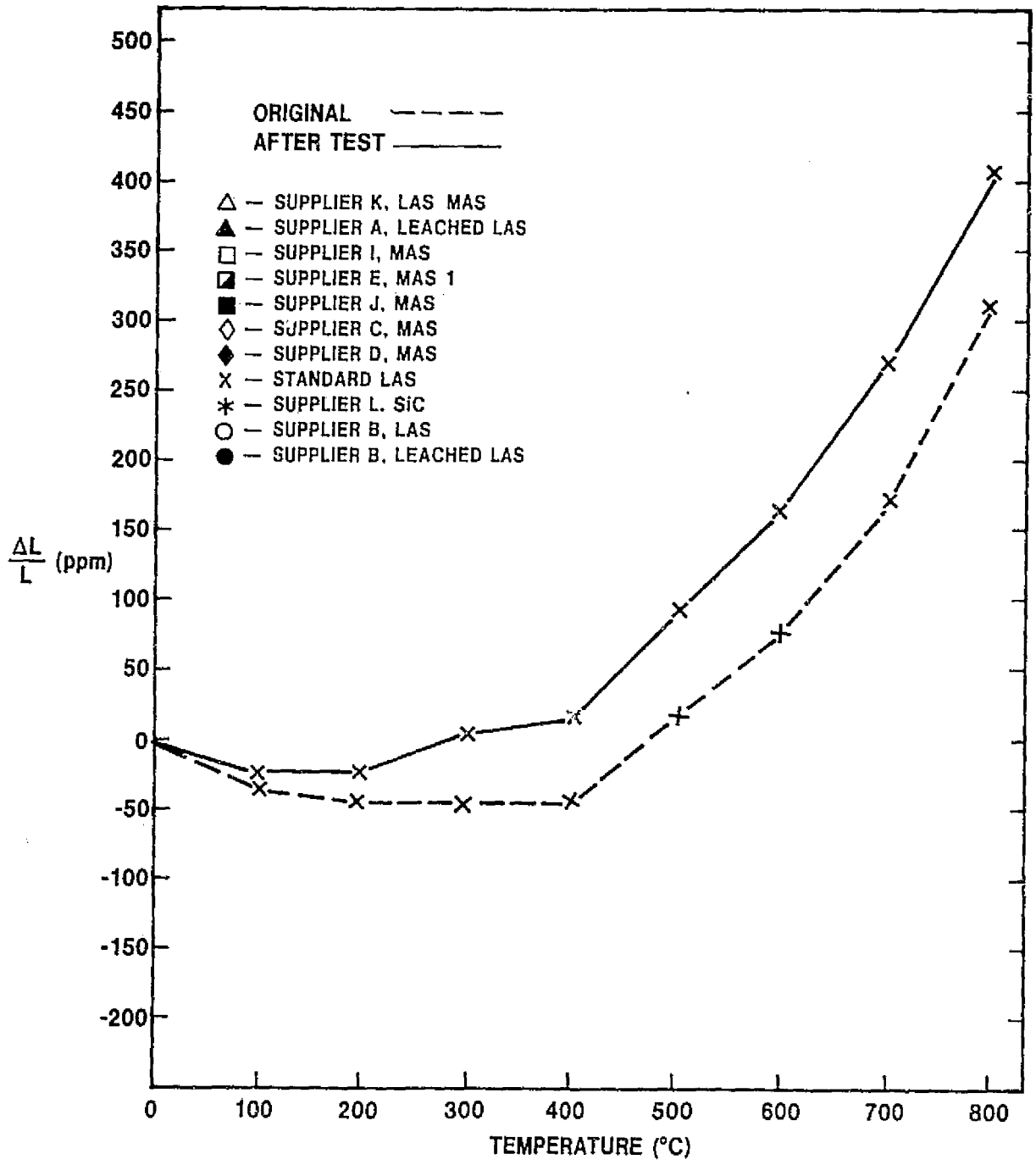

Figure III. B. 1. 13 9455 LAS Standard; Thermal Expansion Before and After Hot Face Testing.

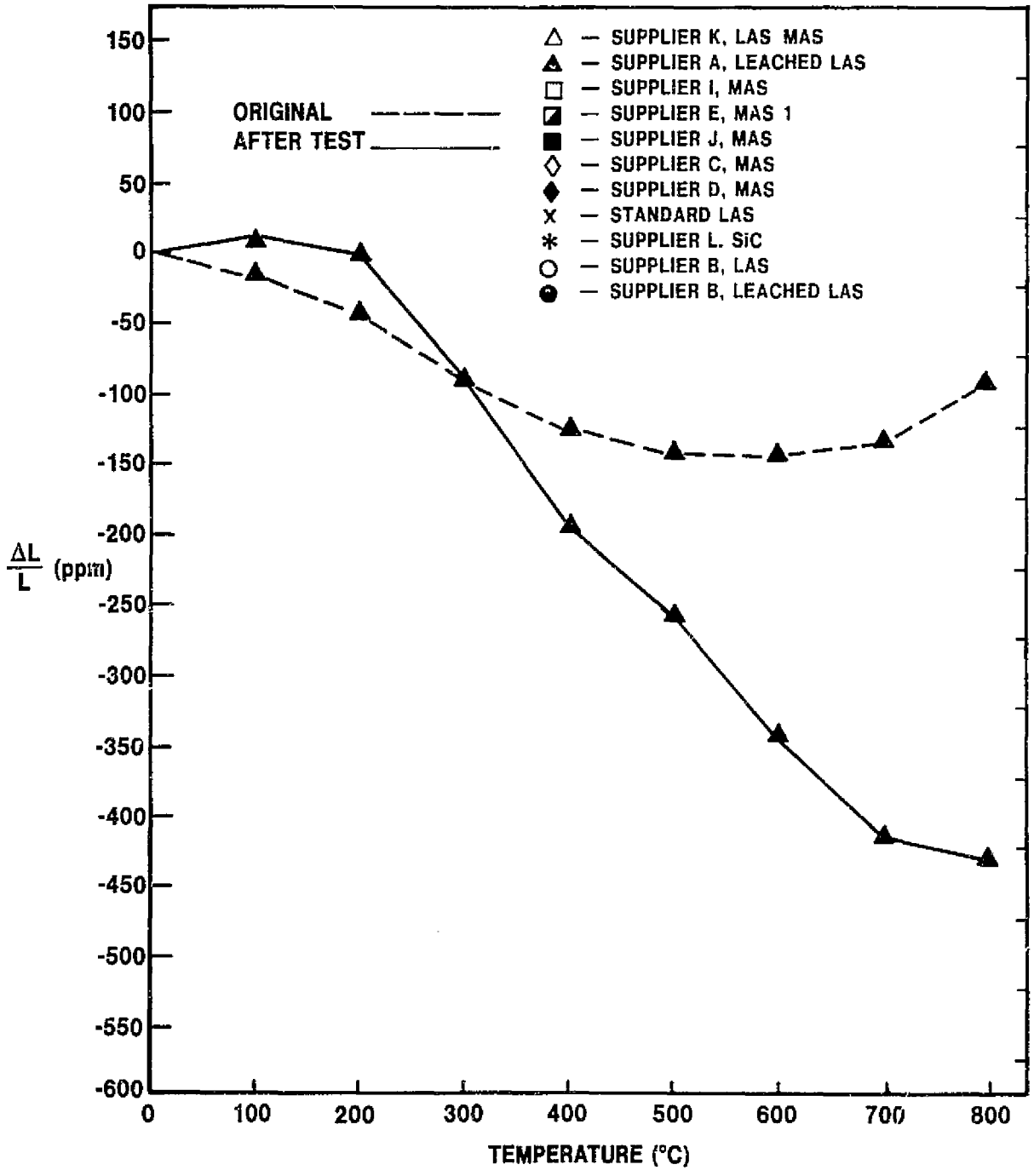

Figure III. B. 1. 14 Supplier A Leached LAS; Thermal Expansion Before and After Hot Face Testing.

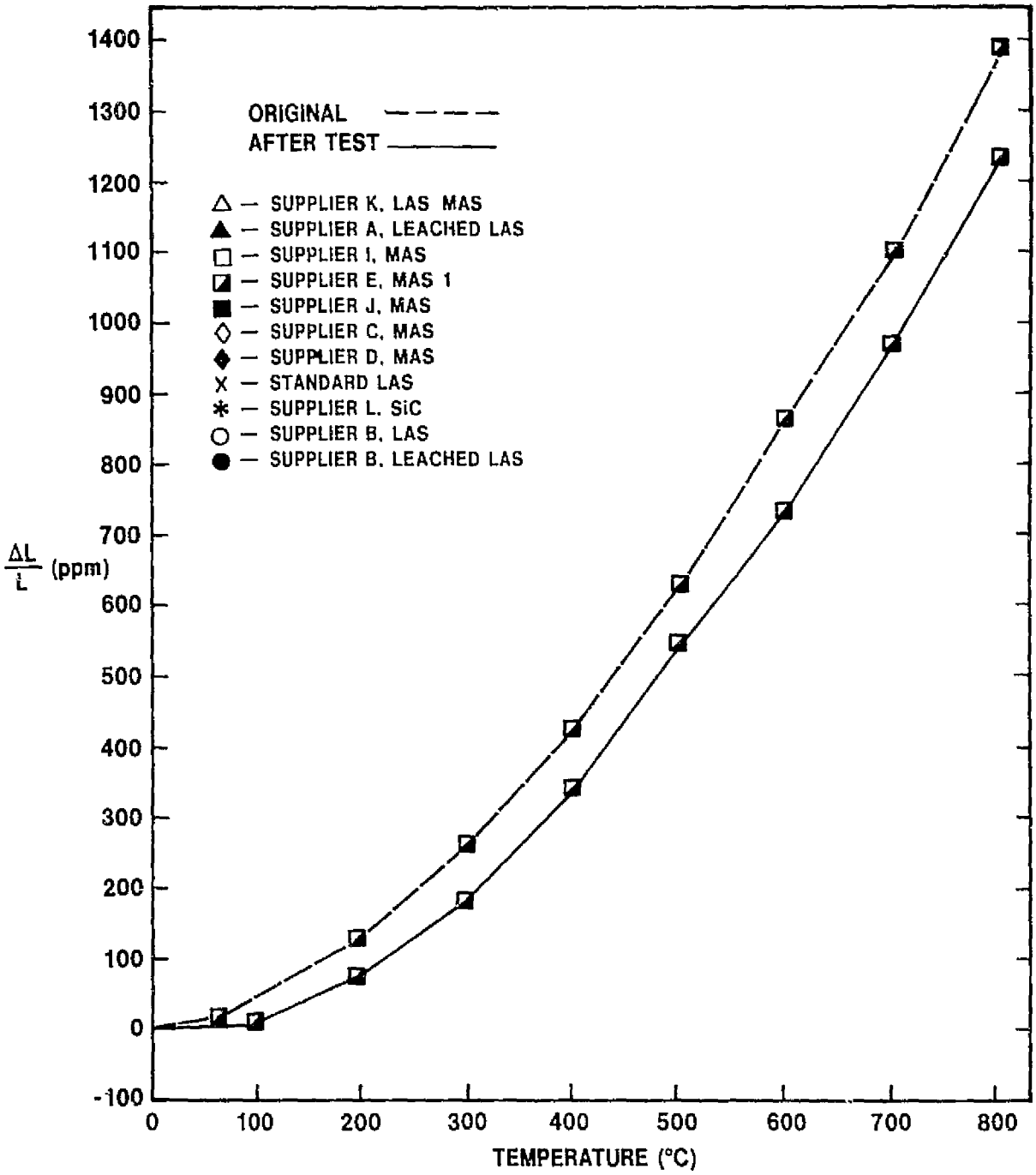

Figure III. B. 1. 15 Supplier E MAS; Thermal Expansion Before and After Hot Face Testing.

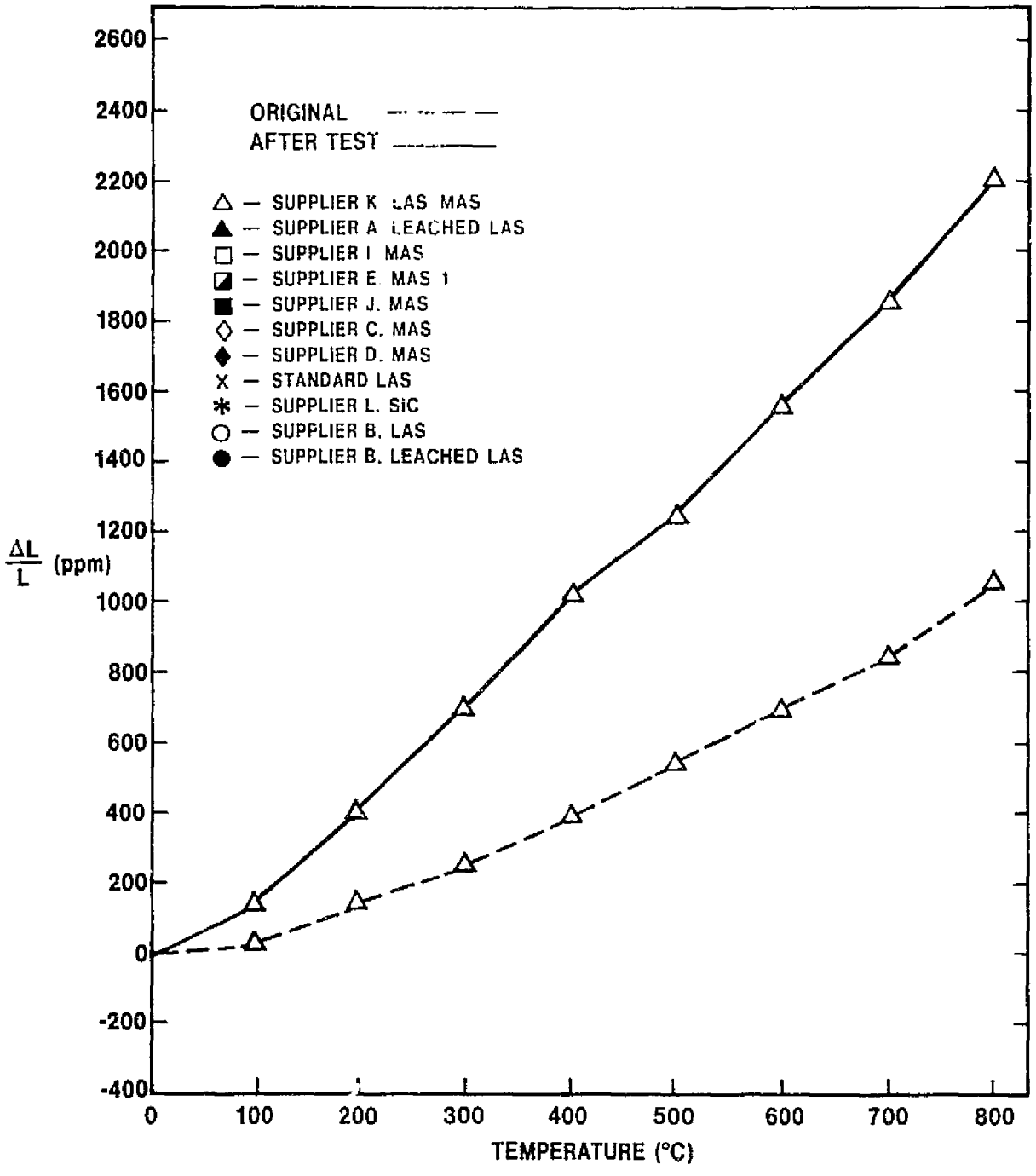

Figure III. B. 1. 16 Supplier K LAS/MAS; Thermal Expansion Before and After Hot Face Testing.

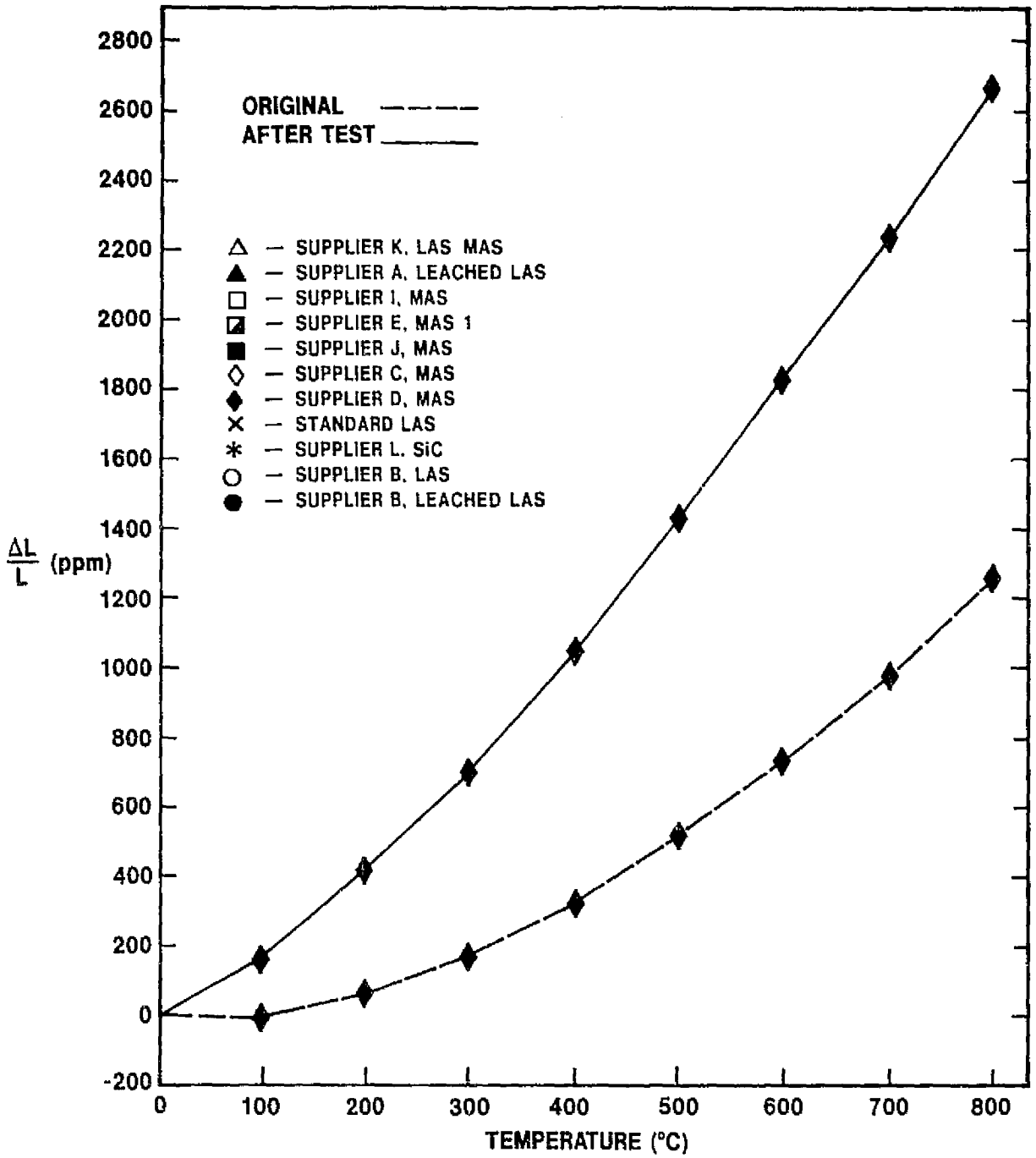

Figure III. B. 1. 17 Supplier D MAS; Thermal Expansion Before and After Hot Face Testing.

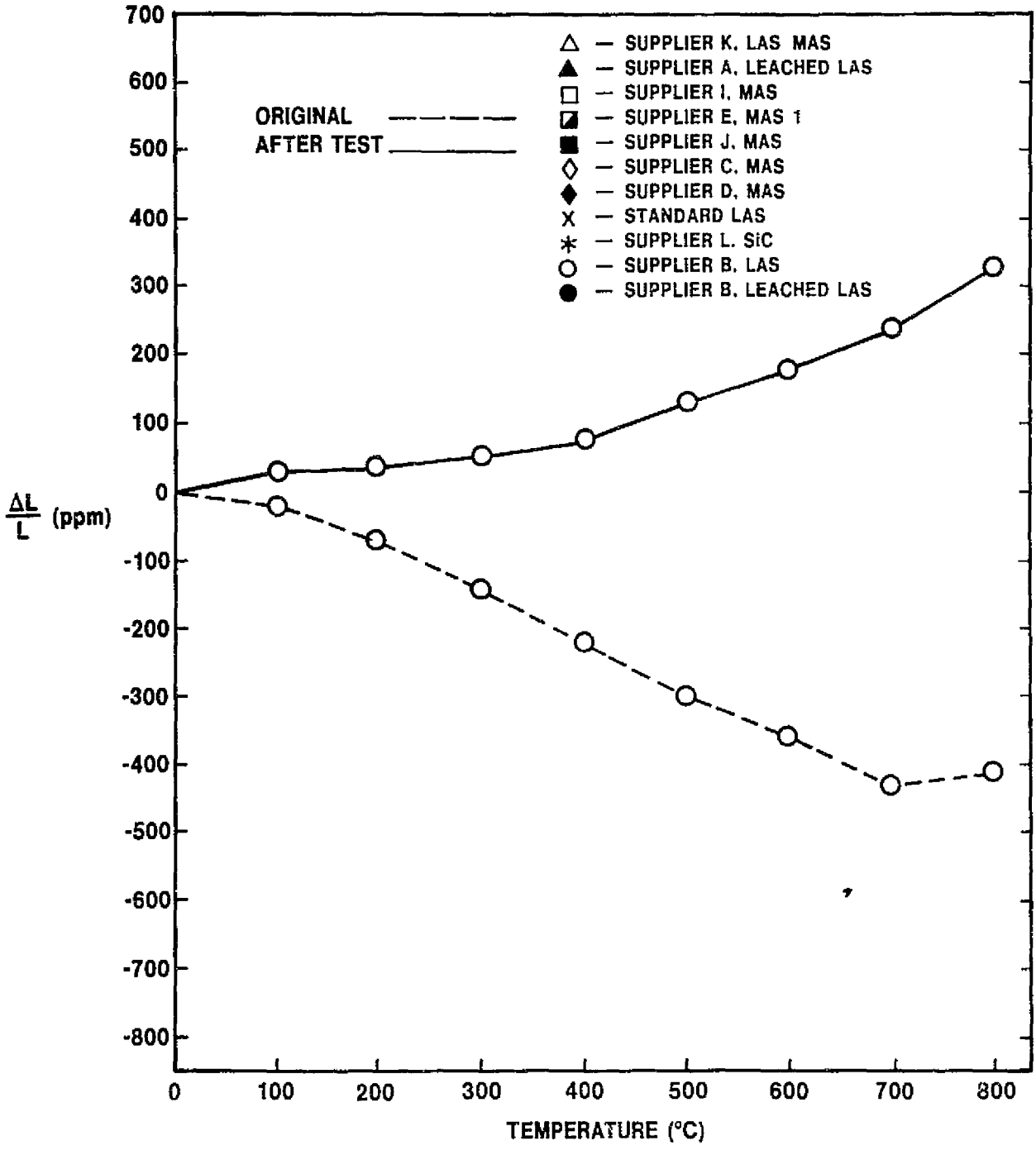

Figure III. B. 1. 18 Supplier B LAS; Thermal Expansion Before and After Hot Face Testing.

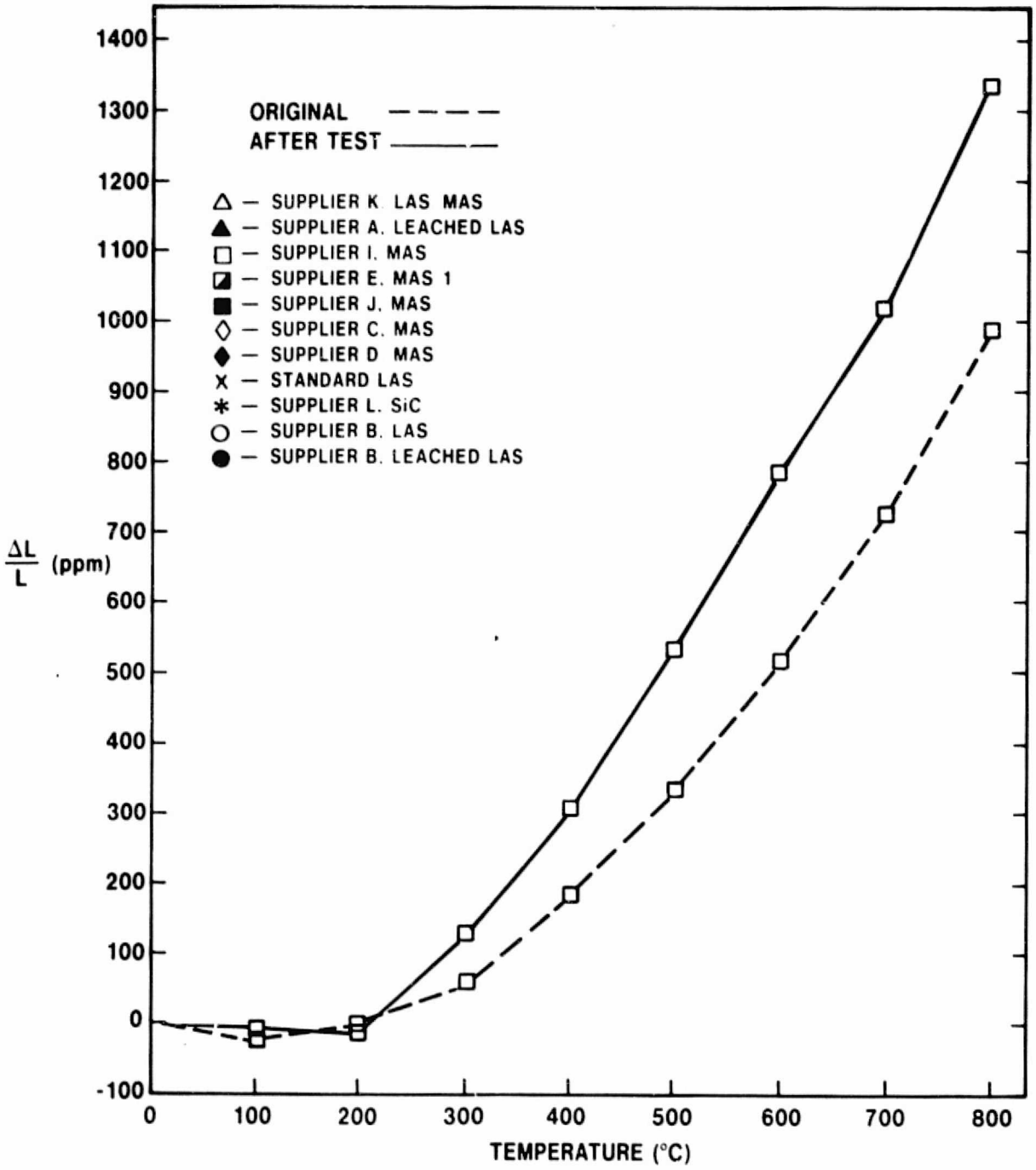

Figure III. B. 1. 19 Supplier I MAS; Thermal Expansion Before and After Hot Face Testing.

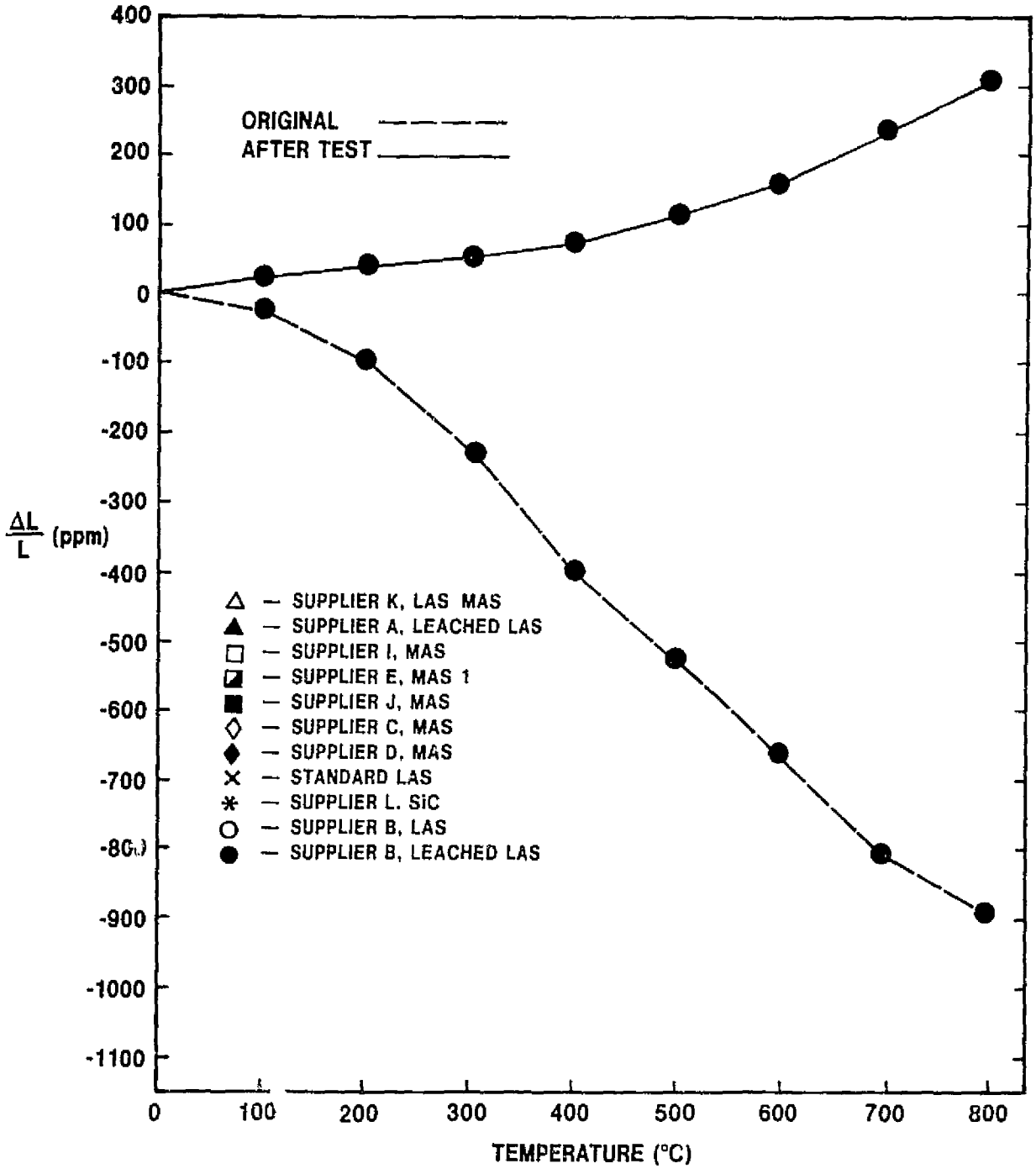

Figure III. B. 1.20 Supplier B Leached LAS; Thermal Expansion Before and After Hot Face Testing.

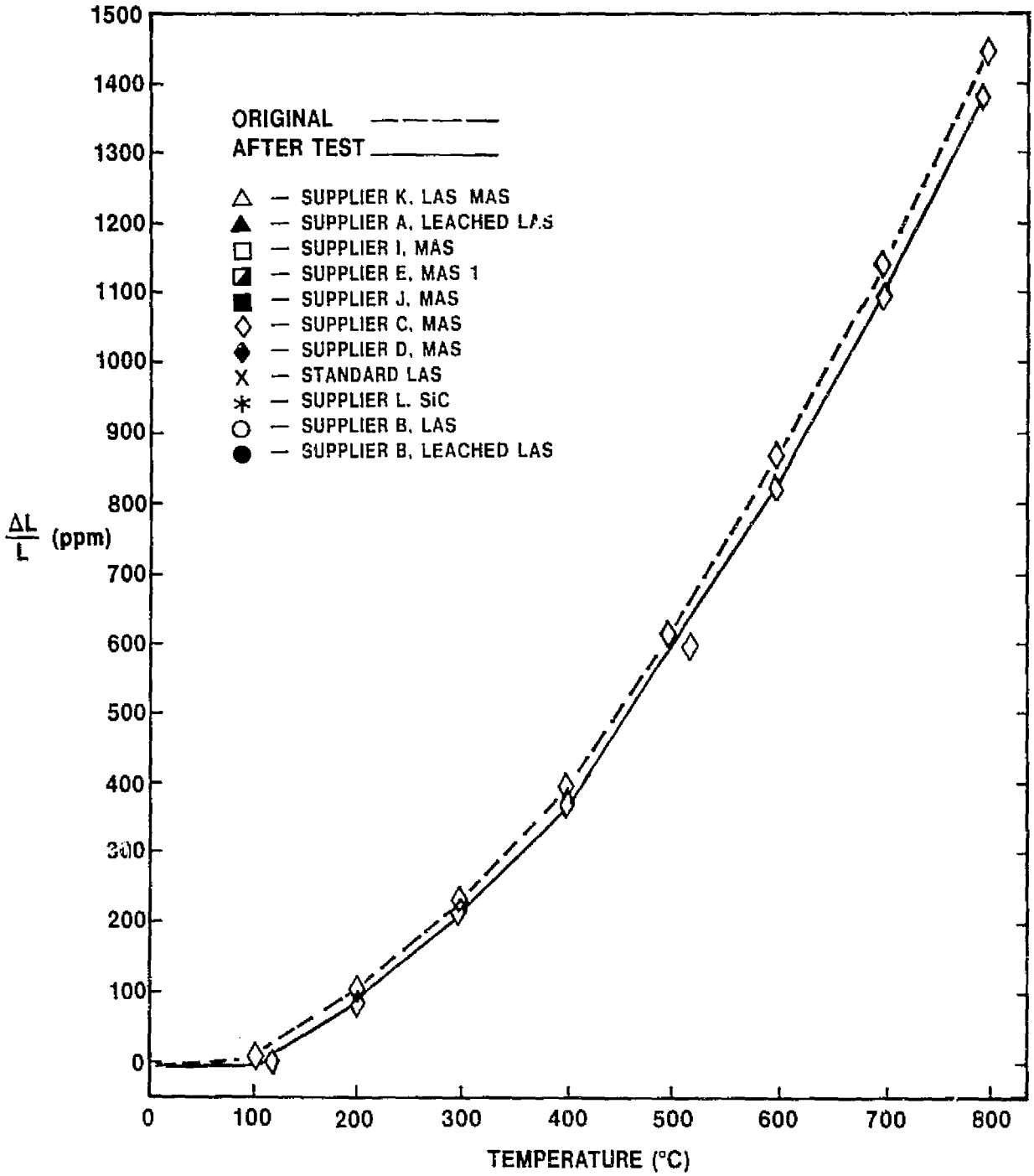

Figure III. B. 1. 21 Supplier C MAS; Thermal Expansion Before and After Hot Face Testing.

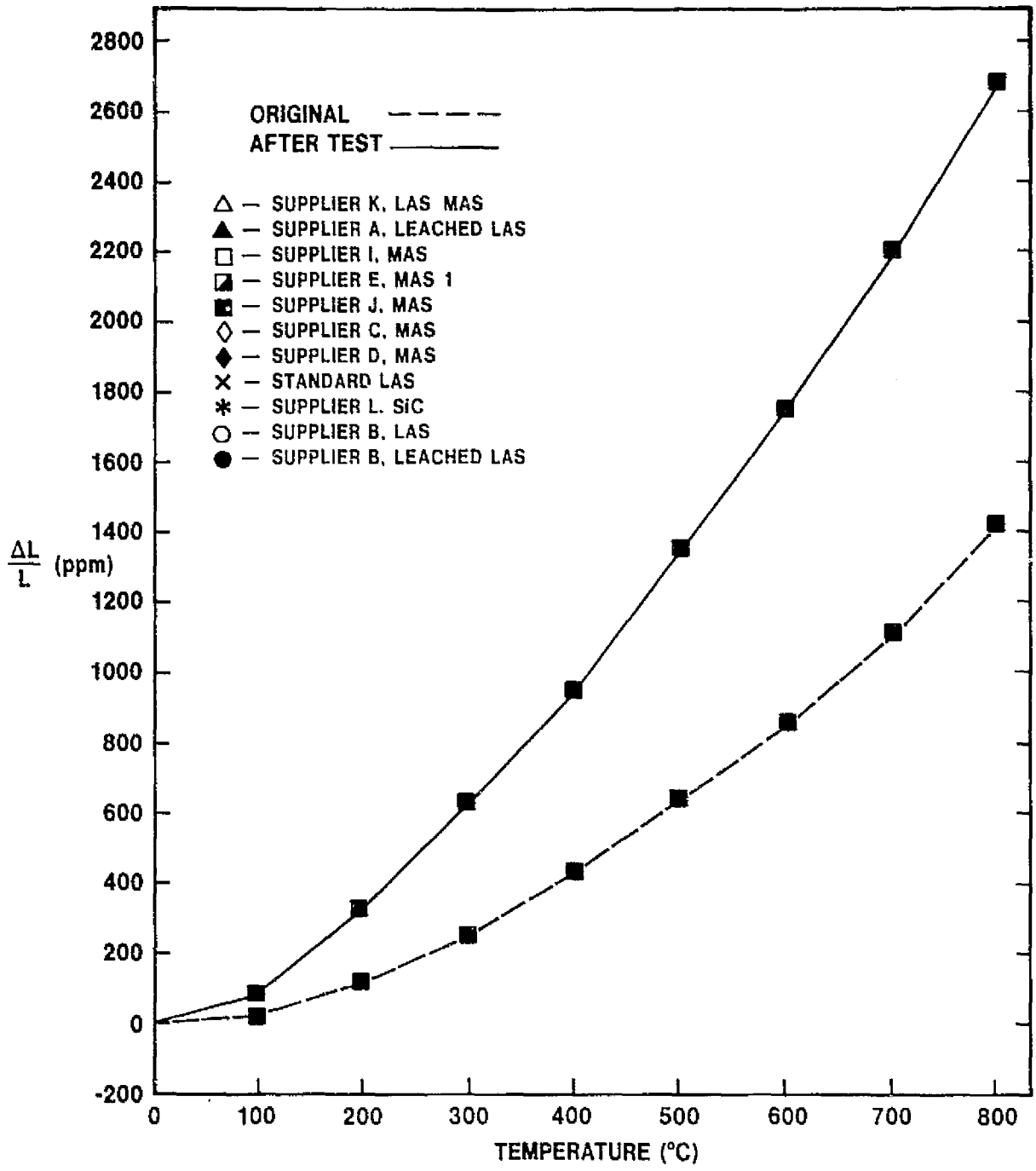

Figure III. B. 1. 22 Supplier J MAS; Thermal Expansion Before and After Hot Face Testing.

III.B.2 Accelerated Corrosion Testing — Matrix Inserts

Accelerated corrosion testing of the first set of matrix inserts (Supplier K-LAS/MAS, Supplier I-MAS, Supplier E-MAS, and Supplier J-MAS) was completed last reporting period. The sampling procedure was described and the 25-hour and 39-hour interval chemical test data were included in the report of the prior quarter of work (Reference 4).

During this reporting period, chemical analyses have been completed for the sampling intervals of 80 and 120 hours, which completes the accelerated corrosion testing of this first group of matrix inserts. These data are presented in Tables III.B.2.1 and III.B.2.2. These chemical analysis data corroborate the hot and cold face data in that the MAS materials seem quite stable in this sodium engine environment (test details may be found in Reference 3), while the LAS/MAS of Supplier K experiences a continual uptake of sodium during the course of the test. Similar to the hot face data, this sodium uptake is rather rapid initially, progresses quite slowly during the middle portion of the test, and finally increases in rate at longer times. There appears to be a complementary decrease in magnesium content of this material with time; however, the magnesium data for the MAS materials would suggest that the observed changes are within analytical precision.

These data should not be interpreted to mean that the MAS materials are unaffected by the accelerated corrosion testing. The magnitude of the changes experienced by the MAS materials is, however, quite less than that experienced by the LAS/MAS

Sample	Position	Solution	$\%Na_2O$	$\%Li_2O$	$\%M_gO$
Supplier K	Cold face	Water	0.74	0.10	0.03
LAS/MAS	Cold face	Acid	0.40	2.11	4.33
Supplier K	Hot face	Water	3.03	0.06	0.06
LAS/MAS	Hot face	Acid	1.66	2.43	5.89
Supplier I	Cold face	Water	4.48		0.02
MAS	Cold face	Acid	0.16		14.99
Supplier I	Hot face	Water	5.23		0.08
MAS	Hot face	Acid	1.20		12.94
Supplier E	Cold face	Water	0.85		0.01
MAS	Cold face	Acid	0.04		15.95
Supplier E	Hot face	Water	2.61		0.02
MAS	Hot face	Acid	0.34		15.55
Supplier J	Cold face	Water	1.32		0.07
MAS	Cold face	Acid	0.04		14.64
Supplier J	Hot face	Water	1.48		0.04
MAS	Hot face	Acid	0.52		12.89

N.D. = Not Detected

Blanks = No Analysis

Table III.B.2.1 Chemical Analysis After 80 Hours Exposure

material. This conclusion is demonstrated by the changes in thermal expansion experienced by these four materials after 120 hours of accelerated corrosion testing as matrix inserts. These data are presented in Figures III.B.2.1 through III.B.2.4. The MAS materials of Suppliers E and J (Figures III.B.2.3 and III.B.2.4, respectively) have experienced very little change in thermal expansion behavior, both from the point of view of the nature of the expansion curves and the magnitude of the change. Each is slightly depressed. The response of the MAS of Supplier E is similar (but smaller in magnitude) to the results of the hot face testing. Material of Supplier I experiences less change than it did under the conditions of the hot face test. The MAS of Supplier I (Figure III.B.2.2) experiences a similar change in thermal expansion behavior (through 600°C) as that resulting from the hot face test. Again, the magnitude of the change after accelerated corrosion testing as matrix inserts is less. The LAS/MAS material of Supplier K (Figure III.B.2.1) experiences a larger change in thermal expansion (note scale differences among figures) than did the MAS materials tested concurrently (although not significantly greater than that MAS of Supplier I). The change in thermal expansion is, like that experienced by the MAS materials, of the same character but smaller in magnitude than the thermal expansion changes observed after the same materials completed the hot face portion of the materials screening tests. In summary, these accelerated corrosion test data of matrix inserts support the conclusions based on the laboratory testing section of this series of materials screening tests. However, these data, when compared to the hot face test data would suggest that the hot face corrosion test is more demanding of the materials than is the accelerated corrosion testing, via the salt ingestion gas turbine engine, of matrix inserts.

Sample	Position	Solution	$\%Na_2O$	$\%Li_2O$	$\%M_gO$
Supplier K	Cold face	Water	0.85	0.18	0.03
LAS/MAS	Cold face	Acid	0.36	2.52	4.53
Supplier K	Hot face	Water	1.62	0.04	0.08
LAS/MAS	Hot face	Acid	2.05	2.59	4.73
Supplier I	Cold face	Water	3.73		0.02
MAS	Cold face	Acid	0.20		9.46
Supplier I	Hot face	Water	3.10		0.06
MAS	Hot face	Acid	0.82		9.07
Supplier E	Cold face	Water	1.04		0.01
MAS	Cold face	Acid	0.34		11.58
Supplier E	Hot face	Water	3.28		0.04
MAS	Hot face	Acid	0.50		11.06
Supplier J	Cold face	Water	2.05		0.09
MAS	Cold face	Acid	0.04		13.71
Supplier J	Hot face	Water	3.29		0.11
MAS	Hot face	Acid	0.58		14.17

N.D. = Not Detected

Blanks = No Analysis

Table III.B.2.2 Chemical Analysis After 120 Hours Exposure

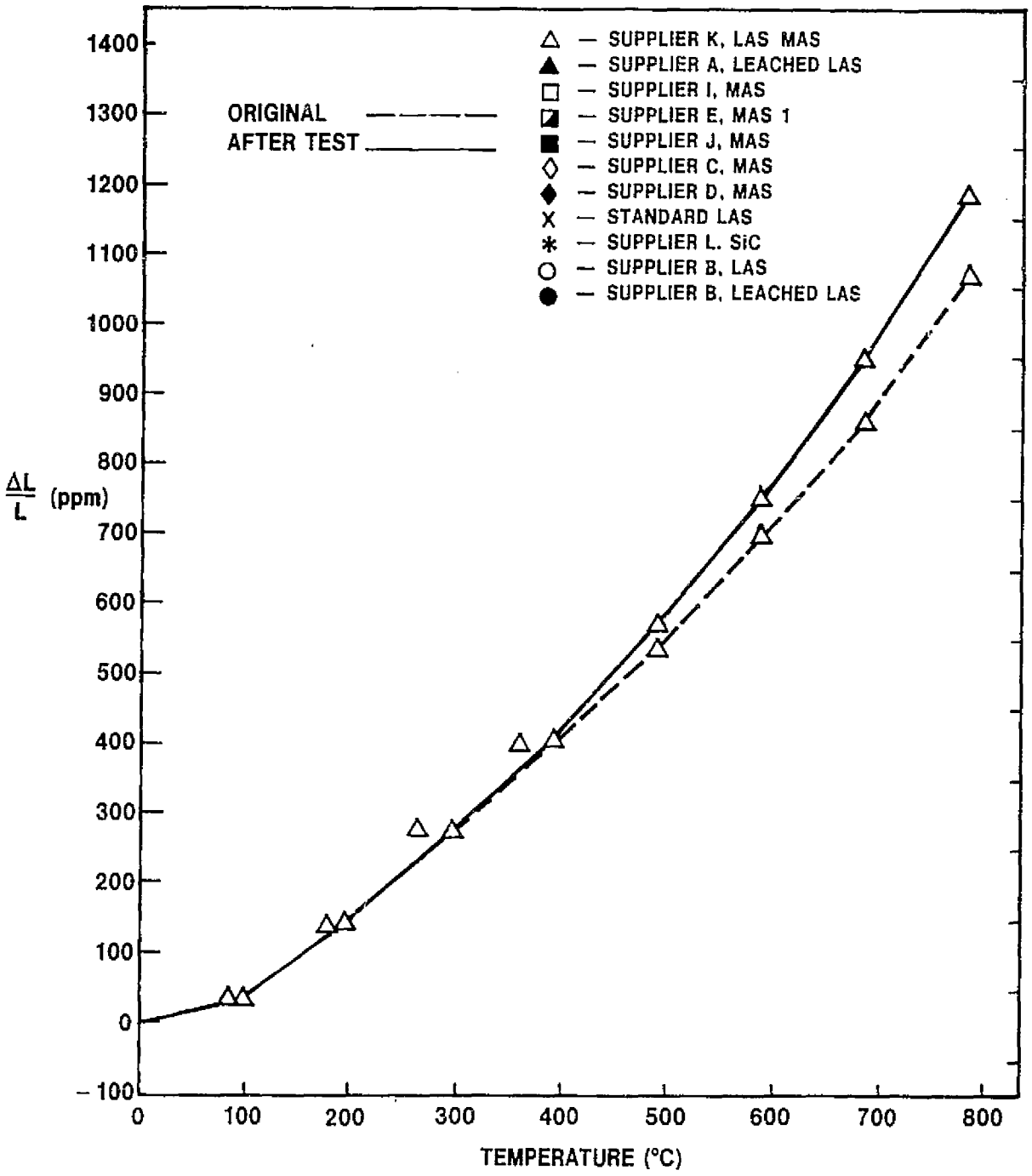

Figure III. B. 2. 1 Supplier K LAS/MAS; Thermal Expansion Before and After 120 Hours of Accelerated Corrosion Testing as a Matrix Insert.

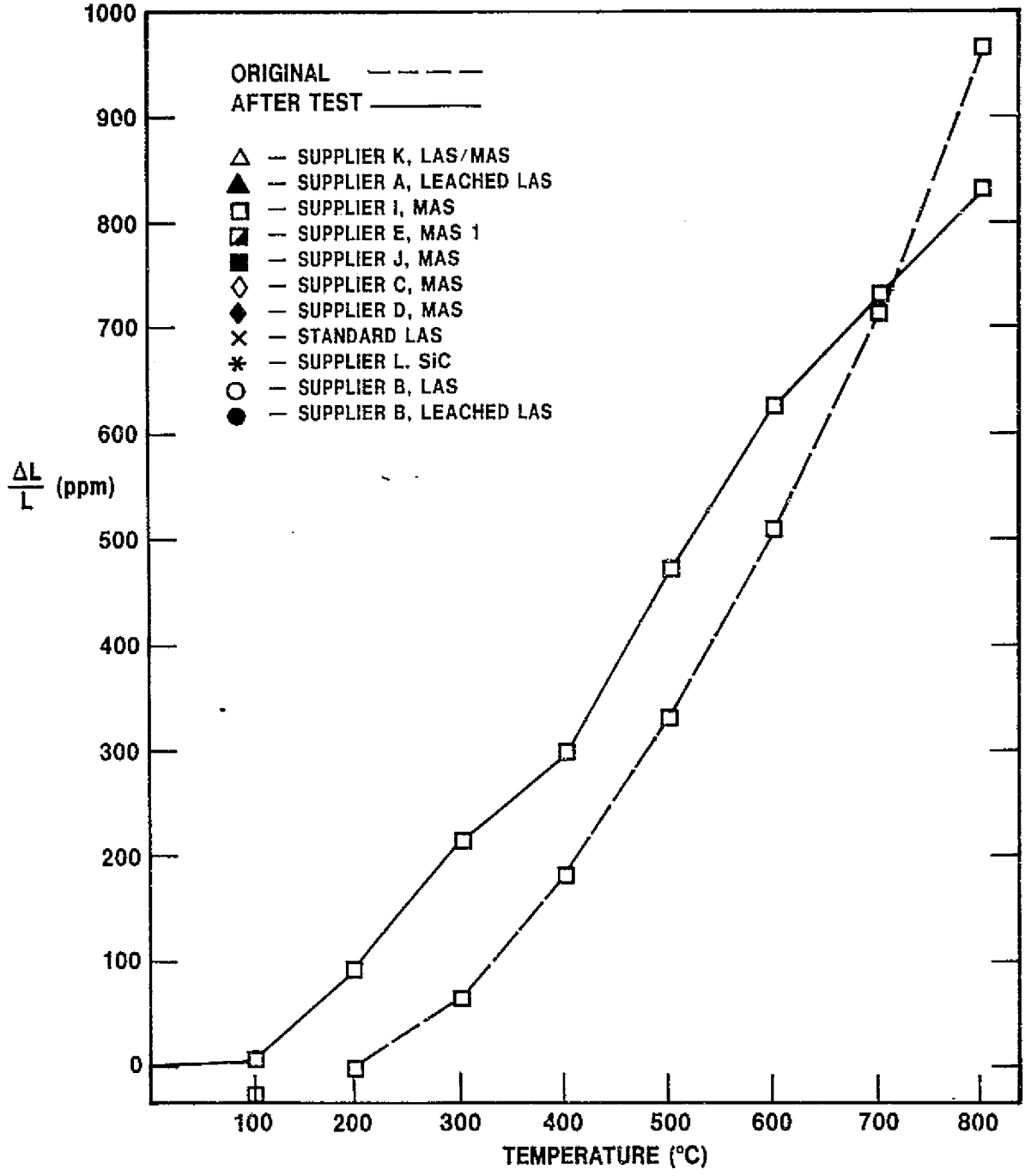

Figure III. B. 2. 2 Supplier I MAS; Thermal Expansion Before and After 120 Hours of Accelerated Corrosion Testing as a Matrix Insert.

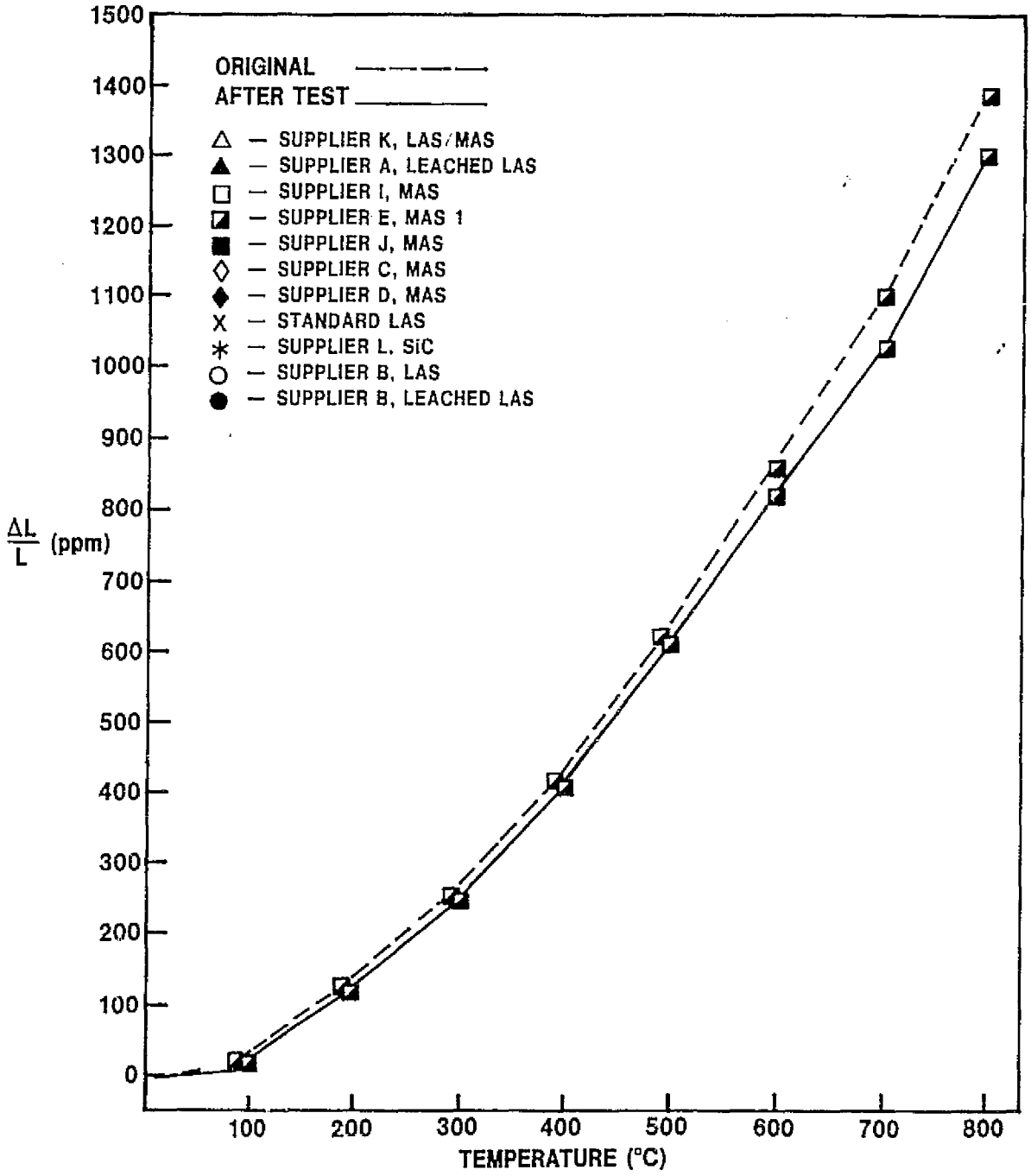

Figure III. B. 2. 3 Supplier E MAS; Thermal Expansion Before and After 120 Hours of Accelerated Corrosion Testing as a Matrix Insert.

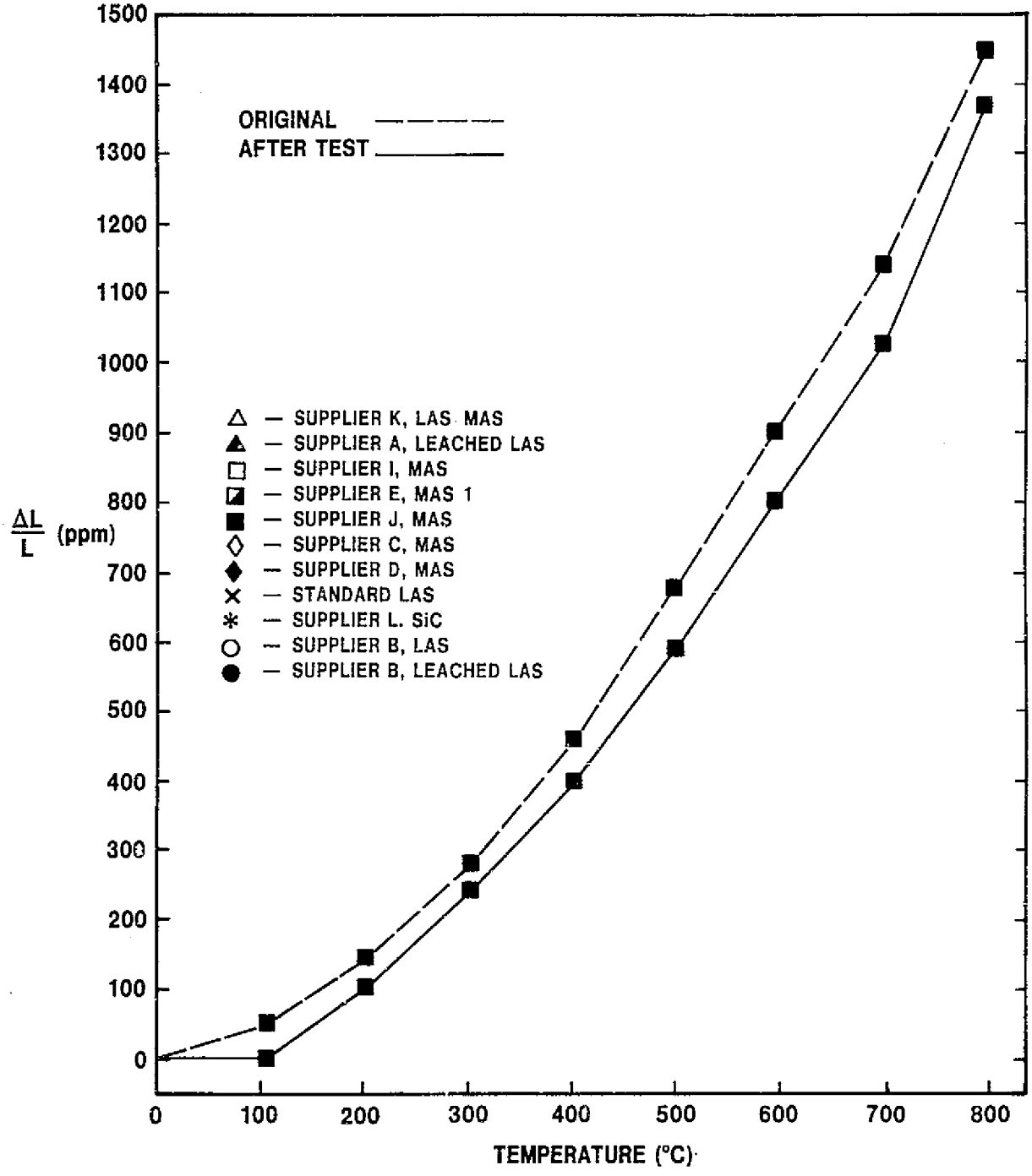

Figure III. B. 2. 4 Supplier J MAS; Thermal Expansion Before and After 120 Hours of Accelerated Corrosion Testing as a Matrix Insert.

III.B.3 Accelerated Corrosion Testing — Full Size Cores

Two full-size cores have been procured to begin this phase of the materials screening tests. The first core, Supplier D-MAS, has been prepared for engine service and is presently being run under non-accelerated test conditions for preliminary evaluation. The second core, Supplier C-MAS, is prepared and awaiting a drive gear prior to test initiation. The progress of these test cores will be reported as the testing evolves.

III.C. PROBLEM AREAS

The materials screening tests at the laboratory and matrix insert level are progressing well. A delay in the delivery of ring gears has slowed, somewhat, the progress of the accelerated testing of full size cores. New gears will be available early in the second quarter.

III.D. FUTURE PLANS

Three new MAS materials have been procured and are being prepared for introduction into the hot face and cold face testing programs next reporting period. A leached LAS host core has been fitted with 5 new material matrix inserts (3-MAS, 1-LAS, 1-leached LAS) and will begin testing next period. Two MAS cores are about to begin full size core accelerated corrosion testing.

III.E. TASK SUMMARY

A majority of the materials scheduled for laboratory testing under hot face and cold face conditions have progressed to completion, and the resulting data have been reported. The final chemical analyses for the first set of four matrix inserts exposed to accelerated corrosion testing have been completed and reported. The laboratory and accelerated corrosion engine tests have generated supportive data, although the laboratory test appears to be more severe than the engine accelerated chemical attack test. Finally, two cores are being prepared for accelerated corrosive testing in the salt ingestion gas turbine engine.

TASK IV. AEROTHERMODYNAMIC PERFORMANCE

IV.A. INTRODUCTION

The matrix fin configuration selected for a given heat exchanger, under specific engine conditions, has a significant influence on the level of thermal stress and aerothermodynamic performance. In order to evaluate aerothermodynamic performance of prospective fin configurations, a shuttle rig was designed and fabricated (Section Q in Reference 1).

The essential parameters required for accurate heat exchanger performance prediction are the basic heat transfer (J = Stanton-Prandtl No. = Colburn No. = C_2RE^{X2}) and pressure drop (F = Fanning Friction Factor = C_1/RE) characteristics of the matrix fin geometry being evaluated as a function of a nondimensional flow parameter (RE = Reynold's No.). In order to obtain the basic heat transfer and pressure drop data, a transient technique similar to the "sliding drawer" technique described in Reference 5 was used. By determining the maximum slope of the fluid temperature difference curve during the cooling transient, the Colburn No. of the test matrix can be determined for each flow condition (Reynold's No.). The theoretical basis for this measurement technique is described in Reference 5.

In addition to the dependence on the maximum slope of the fluid temperature difference curve during the cooling transient, the level of the heat transfer characteristics (Colburn No.) is dependent on the fin parameter values utilized for data reduction. This was previously discussed in Section Q in Reference 1. Utilizing the present technique, the pertinent fin parameters required for data reduction are highly dependent on the accuracy of the wall density (ρ_W) value of the matrix material.

Since erroneous estimates of the fin parameters can introduce significant discrepancies in the F and J curves, an alternate set of heat transfer and pressure drop characteristics that eliminates the necessity of estimating fin parameters was derived (Section Q.6 of Reference 1). In addition, the alternate characteristics allow a direct comparison of test data from different sources, since a universal method of determining pertinent fin parameters is non-existent at this time. The alternate pressure drop and heat transfer characteristics can be presented in the following forms:

$$\frac{\Delta P \cdot P}{L} = C \frac{\dot{W}T}{A_F}^{1.673}$$

$$\frac{NTU}{L} = A \left[\frac{A_F T^{.673}}{\dot{W}} \right]^{-X_2}$$

Where:

ΔP = Matrix pressure drop — KPa (psi)

P = Fluid pressure — KPa (psia)

L = Flow length — cm (in)

W = Air Mass flow rate — Kg/sec/(lb/sec)

T = Fluid temperature — ^{o}K (^{o}R)

A_F = Matrix frontal area — m^2 (ft^2)

σ = Open area ratio

C_J = Fanning Friction Factor constant for laminar flow = F·RE

DH = Hydraulic diameter — cm (in)

NTU = By definition, the number of heat transfer units (determined from the maximum slope of the fluid temperature difference curve during the cooling transient as described in Reference 5)

C_2 = Colburn No. constant for laminar flow = J/RE^{X_2}

X_2 = Reynold's No. (RE) exponent from the Colburn No. ($J = C_2 RE^{X_2}$)

$$\mathbf{C} = 3.56\,(10^{-9})\frac{C_1}{\sigma\,DH^2} \qquad \left[3.506(10^{-10})\ \frac{C_1}{\sigma\,DH^2}\right]$$

$$\mathbf{A} = 4.98\left[62.6(10^{-7})\right]^{-X_2}\frac{C_2\sigma^{-X_2}}{DH^{(1-X_2)}} \qquad \left[4.98\left[21.9(10^{-7})\right]^{-X_2}\frac{C_2\sigma^{-X_2}}{DH^{(1-X_2)}}\right]$$

If $X_2 = -1$; then:

$$\mathbf{A} = 3.11(10^{-5})\ \frac{C_2\sigma}{DH^2} \qquad \left[1.09(10^{-5})\ \frac{C_2\sigma}{DH^2}\right]$$

Once the constants (C and A) have been determined from the equation of the line for the alternate performance characteristics, the pertinent constants (C_1 and C_2) for the basic performance characteristics can be determined from estimated values of σ and DH.

IV.B. STATUS

The heat transfer and pressure drop characteristics for the first twenty-seven matrix fin configurations evaluated in the shuttle rig were presented in Reference 3 (Section IV). Two additional matrix fin configurations were evaluated during this report period. The complete tabulation for all of the matrices evaluated is listed on Tables IV.B.1 and IV.B.2.

CODE:

R — RECTANGULAR
I.T. — ISOSCELES TRIANGULAR
S.T. — SINUSOIDAL TRIANGULAR
H — HEXAGONAL

$$F = C_1 RE^{X_1} \qquad J = C_2 RE^{X_2}$$

$$\frac{\Delta P.P}{L} = C \frac{WT^{1.673}}{AF}$$

$$\frac{NTU}{L} = A \left[\frac{AFT^{0.673}}{W} \right] - X_2$$

CORE NO.	SUP-PLIER	TYPE OF FIN	X FINS/CM. (FINS/IN.)	Y ROWS/CM. (ROWS/IN.)	N HOLES/CM.2 (HOLES/IN.2)	S MM. (IN.)	B MM. (IN.)	H MM. (IN.)	PH MM. (IN.)	A.R. PH/H	ρ_w g/CC. (LB./FT.3)	L/DH	σ	DH MM. (IN.)	β M.2/M.3 (FT.2/FT.3)	C x 10^5	A x 10^2	c_1	x_1	c_2	x_2	J/F @ RE = 100	A_{F_2} CM. ($IN.^2$)
1	A	S.T.	11.0 (28)	13.0 (33)	143 (924)	.109 (.0043)	.109 (.0043)	.660 (.0280)	1.813 (.0714)	2.75	2.20 (137.0)	121	.673	.589 (.0232)	424 (1392)	1.30	4.55	13.4	-1	3.34	-1	.249	103 (16)
2	D	R	11.4 (29)	12.2 (31)	140 (900)	.193 (.0076)	.193 (.0076)	.627 (.0247)	.879 (.0346)	1.40	1.55 (97.0)	107	.599	.655 (.0258)	3654 (1114)	1.23	4.11	14.0	-1	4.19	-1	299	103 (16)
3	D	R	8.3 (21)	8.7 (22)	71.6 (462)	.216 (.0085)	.216 (.0085)	.940 (.0370)	1.211 (.0477)	1.29	1.49 (92.8)	72	.669	.968 (.0381)	2765 (843)	.64	2.10	14.9	-1	4.18	1	.281	96 (15.2)
4	I	I.T.	15.8 (40)	9.1 (23)	142.6 (920)	.135 (.0053)	.135 (.0053)	.970 (.0382)	1.270 (.0500)	1.31	1.66 (97.1)	121	.642	.589 (.0232)	4356 (1328)	1.11	5.11	10.9	1	3.93	-1	.361	72 (11.2)
5	C	S.T.	9.9 (25)	15.4 (39)	151 (975)	.135 (.0053)	135 (.0053)	.516 (.0203)	2.032 (.0800)	3.95	1.43 (89.0)	179	.669	401 (.0158)	5688 (1734)	2.25	10.2	9.1	-1	62	.8	171	103 (16)
6	D	R	6.9 (17.5)	7.5 (19)	51.5 (332)	.300 (.0118)	.300 (.0118)	1.036 (.0408)	1.450 (.0571)	1.40	1.47 (91.4)	87	.615	1.092 (.0430)	2253 (687)	.515	1.55	16.7	-1	4.28	1	.256	46 (7.1)
7	C	S.T.	5.1 (13)	6.3 (16)	32.2 (208)	.178 (.0070)	.178 (.0070)	1.410 (.0555)	3.906 (.1538)	2.77	1.51 (94.3)	53	.737	1.316 (.0518)	2240 (683)	.33	17.4	18.6	-1	.324	5	174	103 (16)
8	E	R	4.1 (10.5)	14.4 (36.5)	59.4 (383)	.284 (.0112)	.213 (.0084)	.482 (.019)	2.418 (.0952)	5.0	2.40 (149.5)	89	.611	.787 (.0310)	3103 (946)	1.10	3.85	18.4	1	5.55	-1	.302	60 (9.3)
9	E	R	5.3 (13.5)	15.6 (39.5)	82.6 (533)	.386 (.015)	.228 .009)	.411 (.0162)	1.88 (.074)	4.57	2.34 (146.3)	109	.606	.645 (.0254)	3129 (954)	1.89	4.29	17.5	-1	5.0	1	287	101 (15.6)
10	A	S.T.	14.6 (37)	14.4 (36.6)	209.5 (1351)	.056 (.0026)	066 (.0026)	.630 (.0248)	1.374 (.0541)	2.18	2.09 (130.4)	128	.767	.649 (.0218)	5589 (1707)	1.60	5.9	16.3	1	3.29	1	202	103 (16)
11	A	S.T.	6.3 (16)	10.2 (26)	64.5 (416)	.127 (.0050)	.127 (.0050)	.861 (.0335)	3.175 (.1250)	3.73	2.20 (137.3)	91	.720	775 (.0305)	3716 (1133)	.76	2.35	14.5	1	2.79	1	192	103 (16)
12	A	R	7.0 (17.8)	7.1 (18)	49.6 (320)	.290 (.0114)	.290 (.0114)	1.123 (.0442)	1.427 (.0562)	1.27	1.67 (104.2)	62	.634	1.130 (.0445)	2244 (684)	.46	1.75	16.5	1	5.0	-1	.303	66 (10.2)
13	A	R	5.6 (14.2)	5.6 (14.2)	31.3 (202)	.274 (.0108)	.274 (.0108)	1.514 (.0596)	1.788 (.0704)	1.18	1.63 (101.5)	47	.718	1.487 (.0586)	1896 (578)	.25	4.43	18.2	1	1.44	-.75	.250	66 (10.2)
14	E	R	6.1 (15.5)	8.3 (21)	50.5 (326)	.305 (.012)	.381 (.015)	.837 (.033)	1.64 (.0645)	1.98	2.39 (149.3)	70	.557	1.02 (.0402)	2181 (665)	.62	2.3	15.9	1	6.12	-1	.385	62 (9.6)
15	E	R	6.1 (15.5)	11.0 (28)	67.3 (434)	.190 (.0075)	.330 (.013)	.584 (.023)	1.638 (.0645)	2.85	2.34 (146.8)	85	.558	.822 (.0324	2711 (827)	1.00	4.04	16.7	1	1.86	-.87	.212	64 (9.9)
16	D	R	6.6 (16.8)	6.7 (17.0)	44.2 (286)	.315 (.0124)	.315 (.0124)	1.179 (.0464)	1.511 (.0597)	1.28	1.51 (94.2)	60	.625	1.186 (.0467)	2106 (642)	.44	1.30	17.1	-1	4.16	-1	.243	46 (7.1)
17	E	R	3.2 (8.0)	15.4 (39.0)	49.1 (312)	.360 (.0142)	.241 (.0095)	.409 (.0161)	3.175 (.125)	7.76	2.31 (144.4)	98	.560	.713 (.0281)	3139 (957)	1.45	8.0	18.3	-1	3.09	-.88	.293	64 (9.9)
18	A	I.T.	7.9 (20)	4.7 (12)	37.4 (240)	.257 (.0101)	.257 (.0101)	1.859 (.0732)	2.540 (.1000)	1.37	1.53 (95.5)	60	.653	1.183 (.0458)	2244 (684)	.40	6.20	15.6	-1	1.00	-.72	.233	101 (15.6)
19	A	S.T	15.0 (38)	13.6 (34.5)	203.9 (1311)	.061 (.0024)	.061 (.0024)	.676 (.0266)	1.336 (.0526)	1.98	2.10 (131.0)	122	.787	.579 (.0228)	5422 (1653)	1.38	6.50	16.1	-1	3.94	1	.245	103 (16)
20	A	S.T.	10.8 (27.5)	14.6 (37)	157.4 (1018)	.066 (.0026)	.066 (.0026)	.820 (.0244	1.846 (.0727)	2.98	2.18 (136.3)	107	.780	.592 (.0233)	5264 (1605)	1.36	5.03	16.4	-1	3.19	1	.195	66 (10.2)

Table IV. B. 1 Shuttle Rig Matrices (1-20)

CODE:

R — RECTANGULAR
I.T. — ISOSCELES TRIANGULAR
S.T. — SINUSOIDAL TRIANGULAR
H — HEXAGONAL

$F = C_1 RE^{X_1}$

$J = C_2 RE^{X_2}$

$$\frac{\Delta P.P}{L} = C \frac{WT}{AF}^{1.673} \qquad \frac{NTU}{L} = A \left[\frac{AFT}{W}^{0.673}\right]^{-X_2}$$

CORE NO.	SUP-PLIER	TYPE OF FIN	X FINS/CM (FINS/IN.)	Y ROWS/CM (ROWS/IN.)	N HOLES/CM² (HOLES/IN.²)	S MM (IN.)	B MM (IN.)	H MM (IN.)	PH MM (IN.)	AR PH/H	Pw gM/CC (LB./FT.³)	L/DH	σ	DH MM (IN.)	β M²/M³ (FT.²/FT.³)	C X10⁵	A X10²	C_1	X_1	C_2	X_2	J F @ RE-100	A_F CM² (IN.²)
21	E	R	5.6 (14.3)	10 (25.3)	56.1 (362)	.223 (.0088)	.279 (.011)	.724 (.0285)	1.78 (.070)	2.45	2.02 (126.2)	71	.637	.991 (.0390)	2572 (784)	.62	4.70	17.1	−1	1.80	−.83	.222	103 (16)
22	E	R	3.9 (10)	15.4 (39)	60.5 (390)	.277 (.0109)	.208 (.0082)	.442 (.0174)	2.54 (.100)	5.75	2.29 (143.2)	94	.608	.739 (.0291)	3290 (1003)	1.28	4.20	18.8	−1	5.37	−1	.286	103 (16)
23	E	R	2.4 (6.2)	16.7 (42.3)	40.6 (262)	.381 (.015)	.191 (.0075)	.406 (.016)	4.09 (.161)	10.0	2.39 (149.1)	95	.618	.737 (.0290)	3355 (1023)	1.43	8.64	21.2	−1	1.62	−.81	.184	103 (16)
24	E	R	4.7 (12)	12.6 (32)	59.5 (384)	.417 (.0164)	.279 (.0110)	.516 (.0203)	2.12 (.0833)	4.10	1.94 (121.0)	89	.521	.790 (.0311)	2637 (804)	1.18	2.45	16.9	−1	4.17	−1	.247	103 (16)
25	C	S.T.	9.8 (25)	12.8 (32.5)	126 (813)	.183 (.0072)	.183 (.0072)	.599 (.0236)	2.03 (.0800)	3.39	2.33 (145.7)	153	.512	.417 (.0164)	4907 (1496)	2.4	4.3	9.4	−1	2.07	−1	.220	103 (16)
26	I	H	6.8 (17.3)	5.9 (15)	40.3 (260)	.323 (.0127)	.323 (.0127)	1.37 (.054)	1.47 (.058)	1.07	1.62 (101.3)	51	.656	1.37 (.054)	1912 (583)	.32	1.1	17.4	−1	4.48	−1	.257	46 (7.1)
27	B	H	15 (38.1)	13 (33)	195 (1260)	.058 (.0023)	.058 (.0023)	.711 (.028)	.665 (.0262)	.94	2.40 (150)	99	.852	.711 (.028)	4801 (1464)	.81	4.75	15.4	−1	4.0	−1	.260	46 (7.1)
28	A	R	7.9 (20)	7.9 (20)	62 (400)	.173 (.0068)	.173 (.0068)	1.10 (.0432)	1.27 (.050)	1.16	1.60 (100)	65	.745	1.10 (.0432)	2715 (828)	.35	1.85	13.9	−1	4.25	−1	.306	103 (16)
29	A	R	6.9 (17.5)	6.9 (17.5)	47.5 (306)	.279 (.011)	.279 (.011)	1.17 (.046)	1.45 (.057)	1.24	1.67 (104.2)	61	.649	1.17 (.0461)	2217 (676)	.38	1.75	14.9	−1	5.26	−1	.353	103 (16)

Table IV. B. 2 Shuttle Rig Matrices (21-29)

The present matrix sample size contains seventeen rectangular (core no. 2, 3, 6, 8, 9, 12 thru 17, 21 thru 24, 28 and 29), two hexagonal (core no. 26 & 27), eight sinusoidal (core no. 1, 5, 7, 10, 11, 19, 20 and 25) and two isosceles triangular (core no. 4 and 18) fin configurations. In addition, the present sample size represents a good cross-section of the different manufacturing processes, which are currently being evaluated as follows:

1. Supplier A — Corrugating or extrusion
2. Supplier C — Corrugating
3. Suppliers D and E — Calendering
4. Supplier I — Extrusion
5. Supplier B — Stacked tube

Matrix samples 28 (Figure IV.B.1) and 29 (Figure IV.B.2) evaluated during this report period were extruded by Supplier A. The alternate heat transfer and pressure drop characteristics, which are based on measured test data, for matrices 28 and 29 are shown on Figures IV.B.3 and IV.B.4 respectively.

The wall densities of matrix specimens are determined using mercury intrusion porosimetry data generated using a motor driven digital readout porosimeter. This unit has a hypobaric response from 35 Kpa (5.1 psia) and a hyperbaric capability of 103350 Kpa (15000 psia). The porosimeter has been inoperable for the previous two quarters; however replacement parts have recently been received so additional wall density data will be generated during the next reporting period. Consequently, the pertinent fin parameters (σ and DH) required for the standard performance characteristics for matrices 28 and 29 are based on an estimated value for the wall density (ρ_ω) of the material. Figures IV.B.5 and IV.B.6 illustrate the standard heat transfer (J) and pressure drop (F) characteristics for matrices 28 and 29, respectively. Once the wall density of the material is measured these characteristics may require adjustment.

In order to compare matrix fin geometries on an equivalent basis, the hydraulic diameter, material wall thickness and flow length should be approximately the same. From the existing matrix sample size (Table IV.B.1 and IV.B.2), the embossed square matrix no. 6 and extruded matrices 12 (square) and 18 (isosceles triangular) appear to have hydraulic diameters and flow lengths equivalent to the approximated values for matrices 28 and 29. The standard and alternate heat transfer and pressure drop characteristics for these matrices are repeated on Figures IV.B.7 and IV.B.8, respectively.

From the alternate performance characteristics (Figure IV.B.8) matrix 29 exhibits the same heat transfer characteristics with slightly lower pressure drop characteristics when compared to matrix 12, which was fabricated from the same basic tooling. As previously discussed in reference 3, the importance of the fin material thickness is again illustrated by matrix 28. Due to the significantly thinner wall (.173 mm), matrix 28 exhibits the highest heat transfer potential and the lowest pressure drop.

Based on the standard performance characteristics (Figure IV.B.7), which are based on the actual geometric opening with the wall thickness factored out, matrices 28 and 29 appear to be comparable to the similar matrices (6 and 12) previously evaluated.

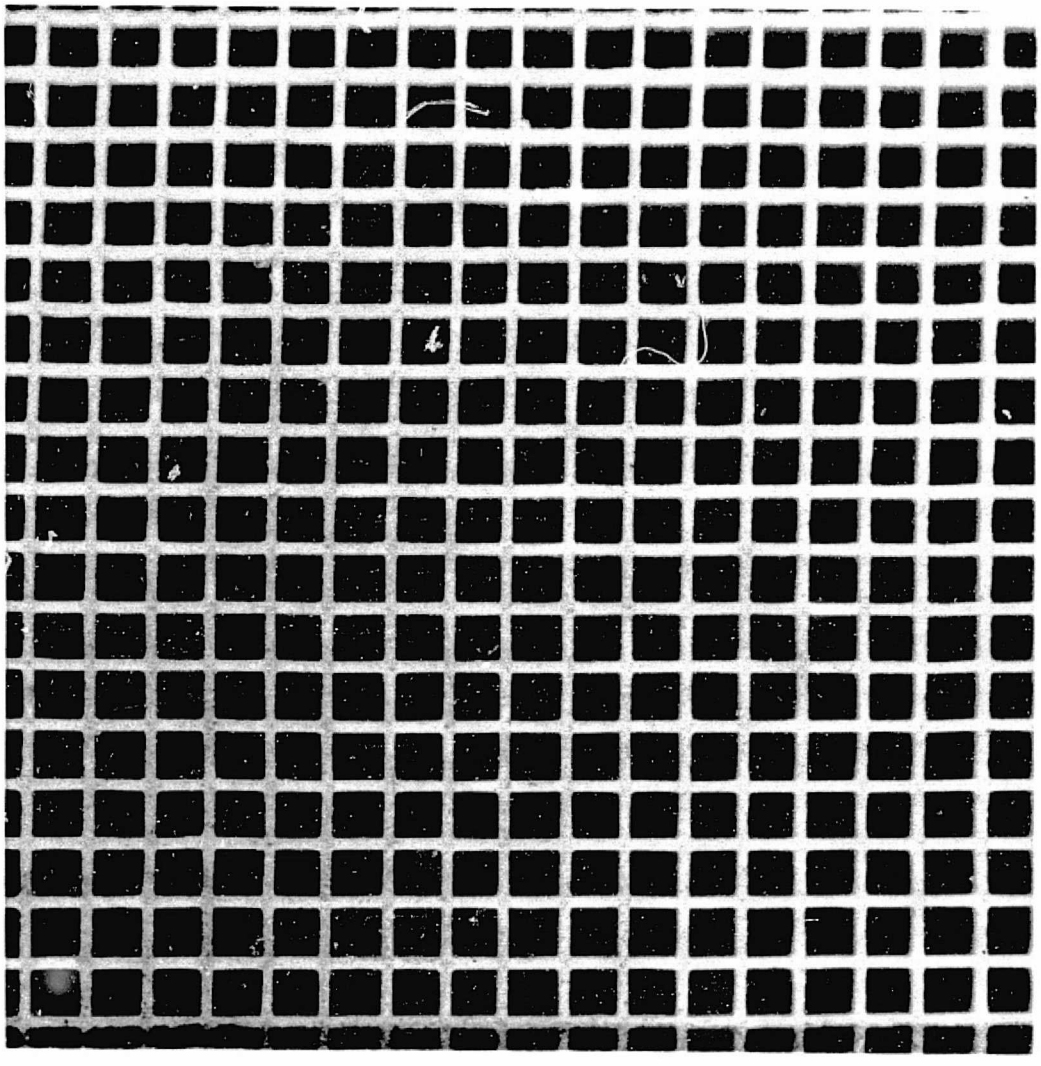

Figure IV. B. 1 Photograph of Matrix 28.

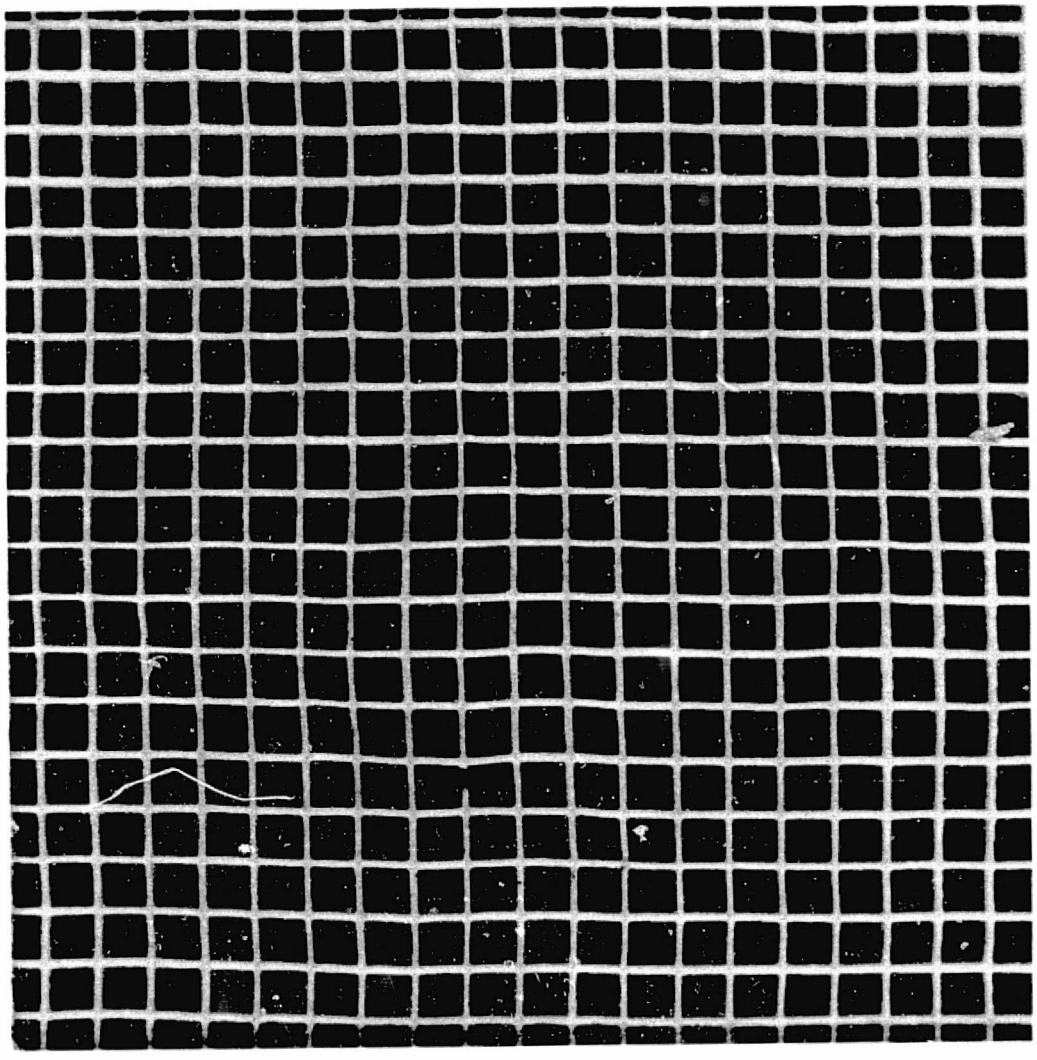

Figure IV. B. 2 Photograph of Matrix 29.

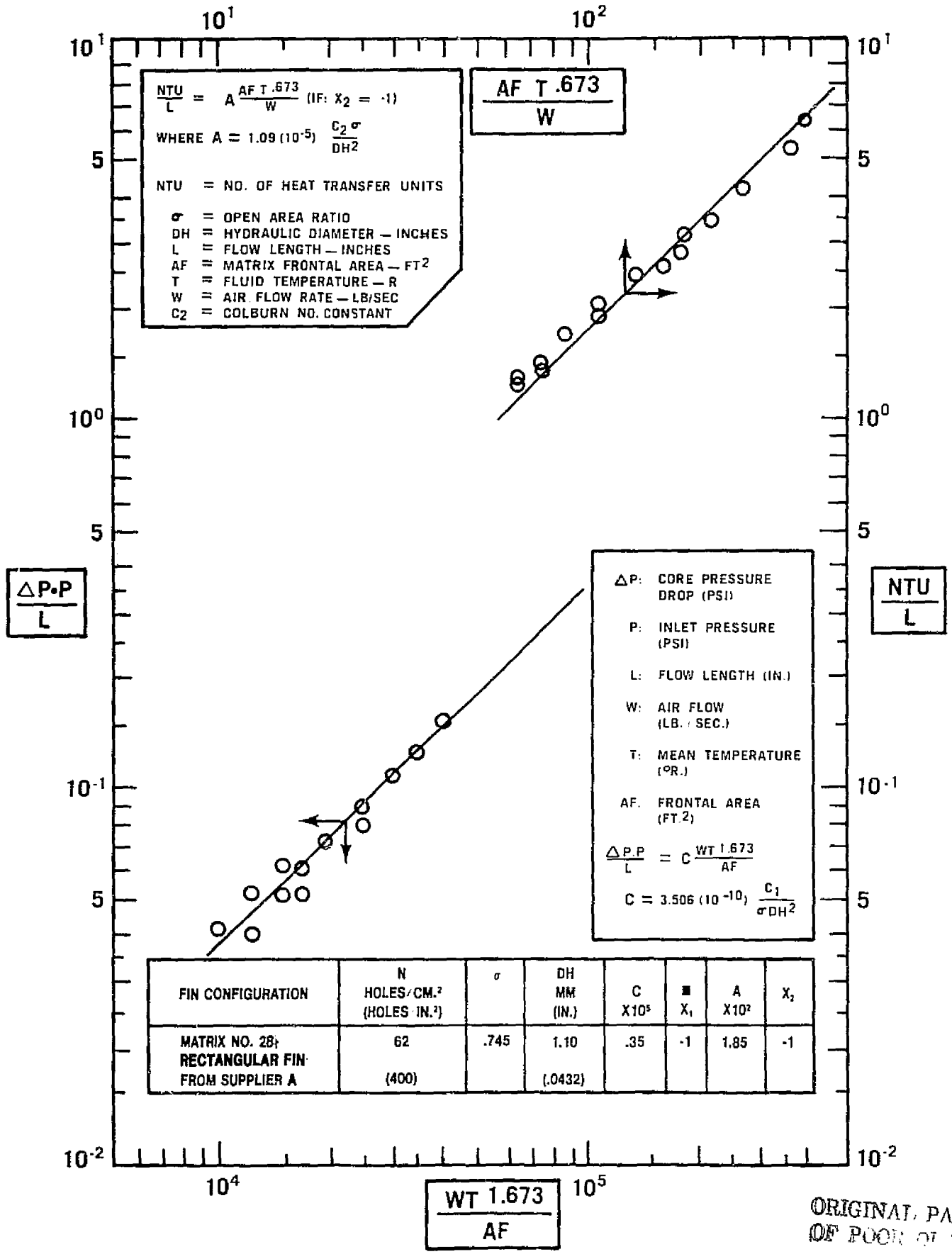

FIN CONFIGURATION	N HOLES/CM.² (HOLES/IN.²)	σ	DH MM (IN.)	C X10⁵	■ X_1	A X10²	X_2
MATRIX NO. 28; RECTANGULAR FIN FROM SUPPLIER A	62 (400)	.745	1.10 (.0432)	.35	-1	1.85	-1

Figure IV. B. 3 Alternate Thermodynamic Performance Characteristics of Matrix 28.

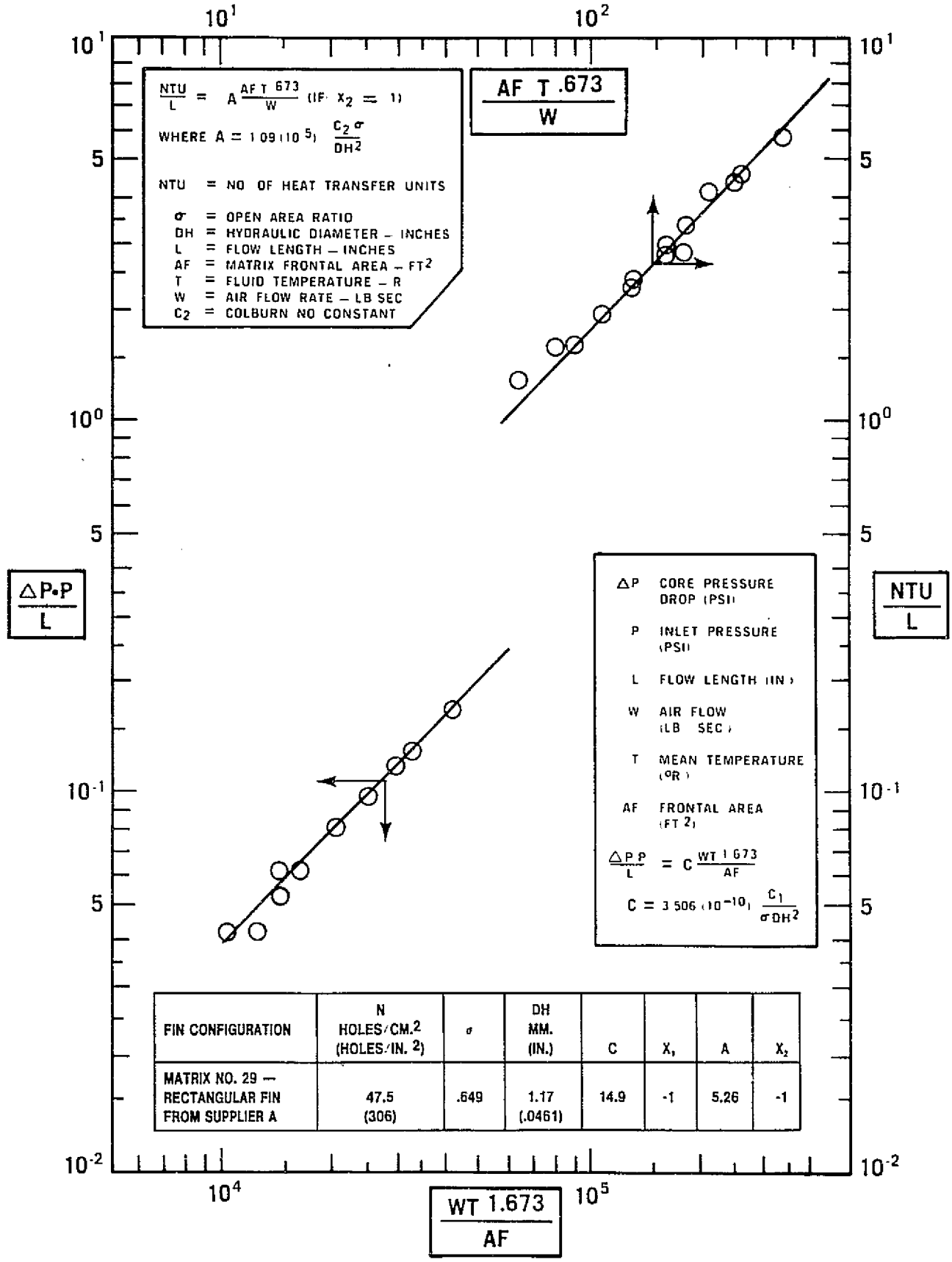

FIN CONFIGURATION	N HOLES/CM.² (HOLES/IN.²)	σ	DH MM. (IN.)	C	X_1	A	X_2
MATRIX NO. 29 — RECTANGULAR FIN FROM SUPPLIER A	47.5 (306)	.649	1.17 (.0461)	14.9	-1	5.26	-1

Figure IV. B. 4 Alternate Thermodynamic Performance Characteristics of Matrix 29.

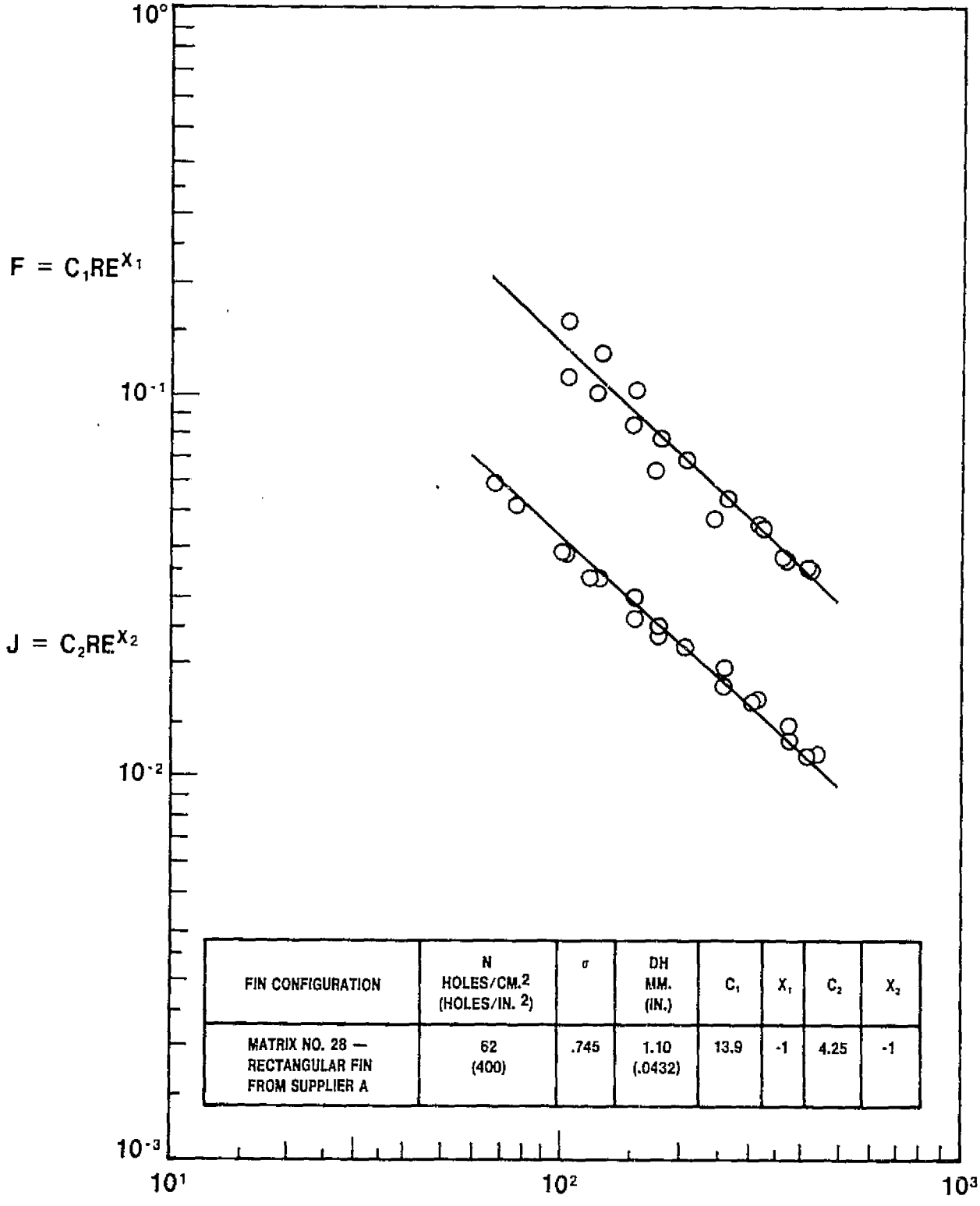

FIN CONFIGURATION	N HOLES/CM.^{2} (HOLES/IN. ^{2})	σ	DH MM. (IN.)	C_1	X_1	C_2	X_2
MATRIX NO. 28 — RECTANGULAR FIN FROM SUPPLIER A	62 (400)	.745	1.10 (.0432)	13.9	-1	4.25	-1

Figure IV. B. 5 Standard Thermodynamic Performance Characteristics of Matrix 28.

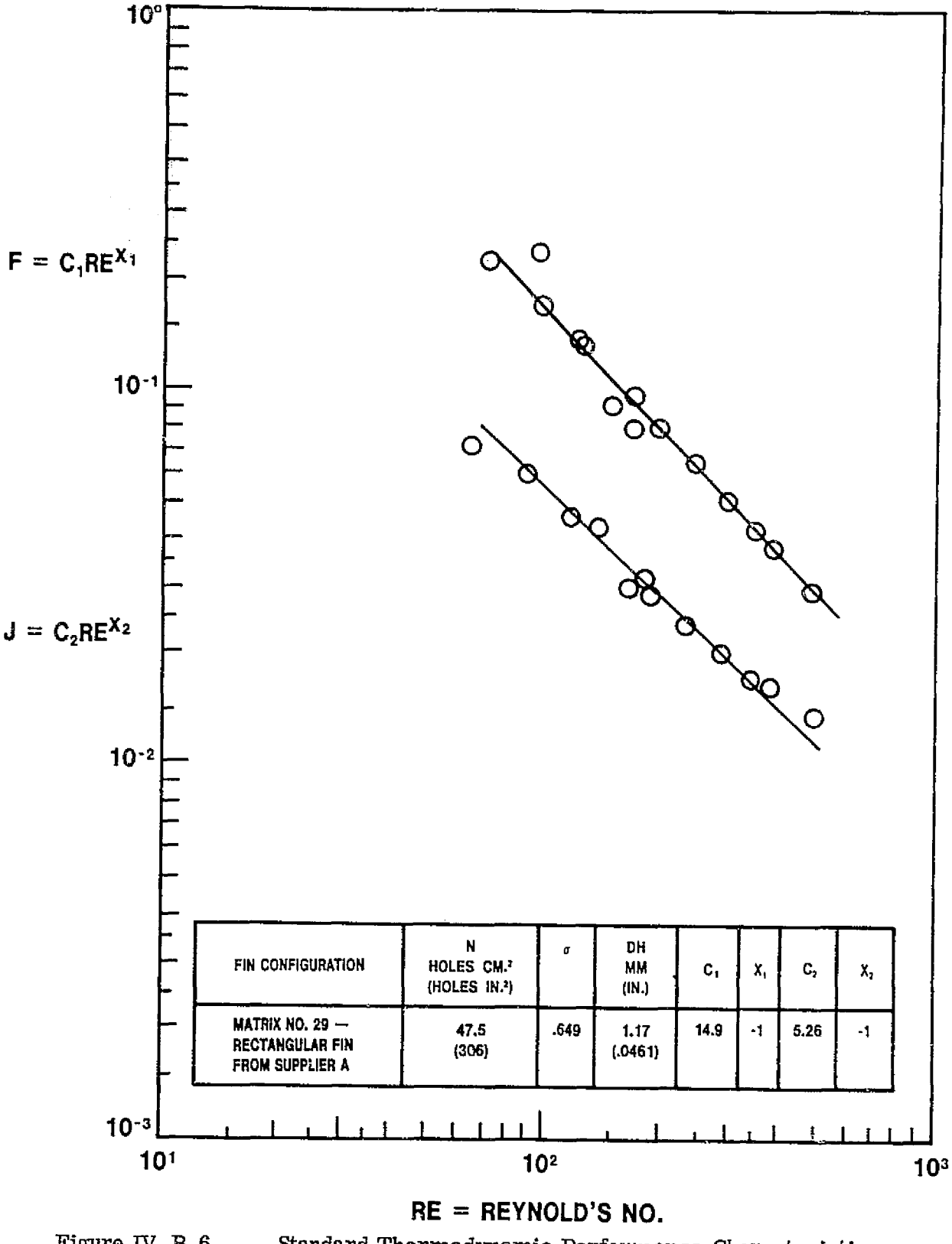

FIN CONFIGURATION	N HOLES CM.² (HOLES IN.²)	σ	DH MM (IN.)	C_1	X_1	C_2	X_2
MATRIX NO. 29 — RECTANGULAR FIN FROM SUPPLIER A	47.5 (306)	.649	1.17 (.0461)	14.9	-1	5.26	-1

Figure IV. B. 6 Standard Thermodynamic Performance Characteristics of Matrix 29.

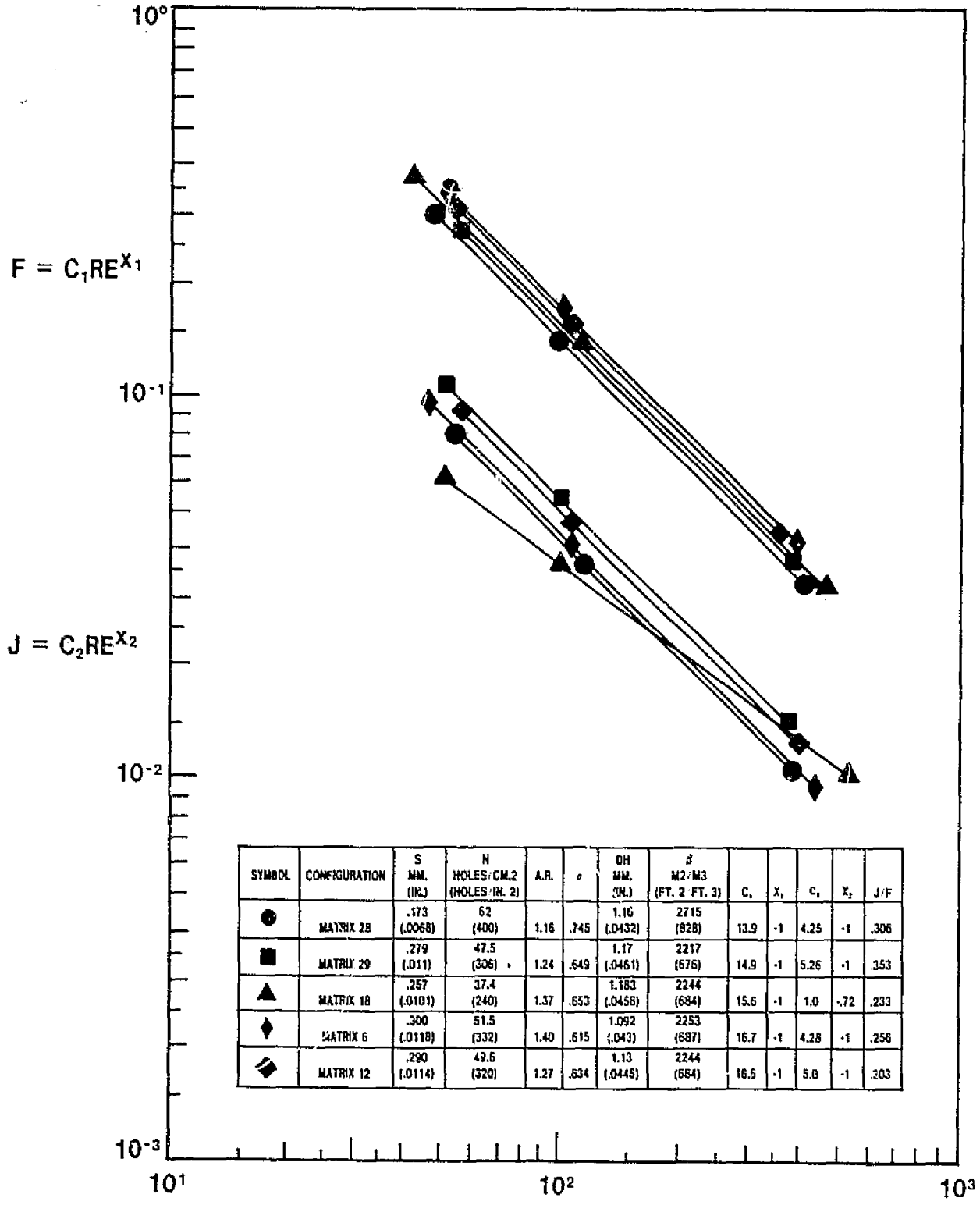

SYMBOL	CONFIGURATION	S MM. (IN.)	N HOLES/CM.2 (HOLES/IN. 2)	A.R.	σ	DH MM. (IN.)	β M2/M3 (FT. 2/FT. 3)	C_1	X_1	C_2	X_2	J/F
●	MATRIX 28	.173 (.0068)	62 (400)	1.16	.745	1.16 (.0432)	2715 (828)	13.9	-1	4.25	-1	.306
■	MATRIX 29	.279 (.011)	47.5 (306)	1.24	.649	1.17 (.0461)	2217 (676)	14.9	-1	5.26	-1	.353
▲	MATRIX 18	.257 (.0101)	37.4 (240)	1.37	.653	1.183 (.0458)	2244 (684)	15.6	-1	1.0	-.72	.233
♦	MATRIX 6	.300 (.0118)	51.5 (332)	1.40	.615	1.092 (.043)	2253 (687)	16.7	-1	4.28	-1	.256
◆	MATRIX 12	.290 (.0114)	49.6 (320)	1.27	.634	1.13 (.0445)	2244 (684)	16.5	-1	5.0	-1	.303

Figure IV.B.7 Standard Thermodynamic Performance Characteristics of Matrices 6, 12, 18, 28 and 29.

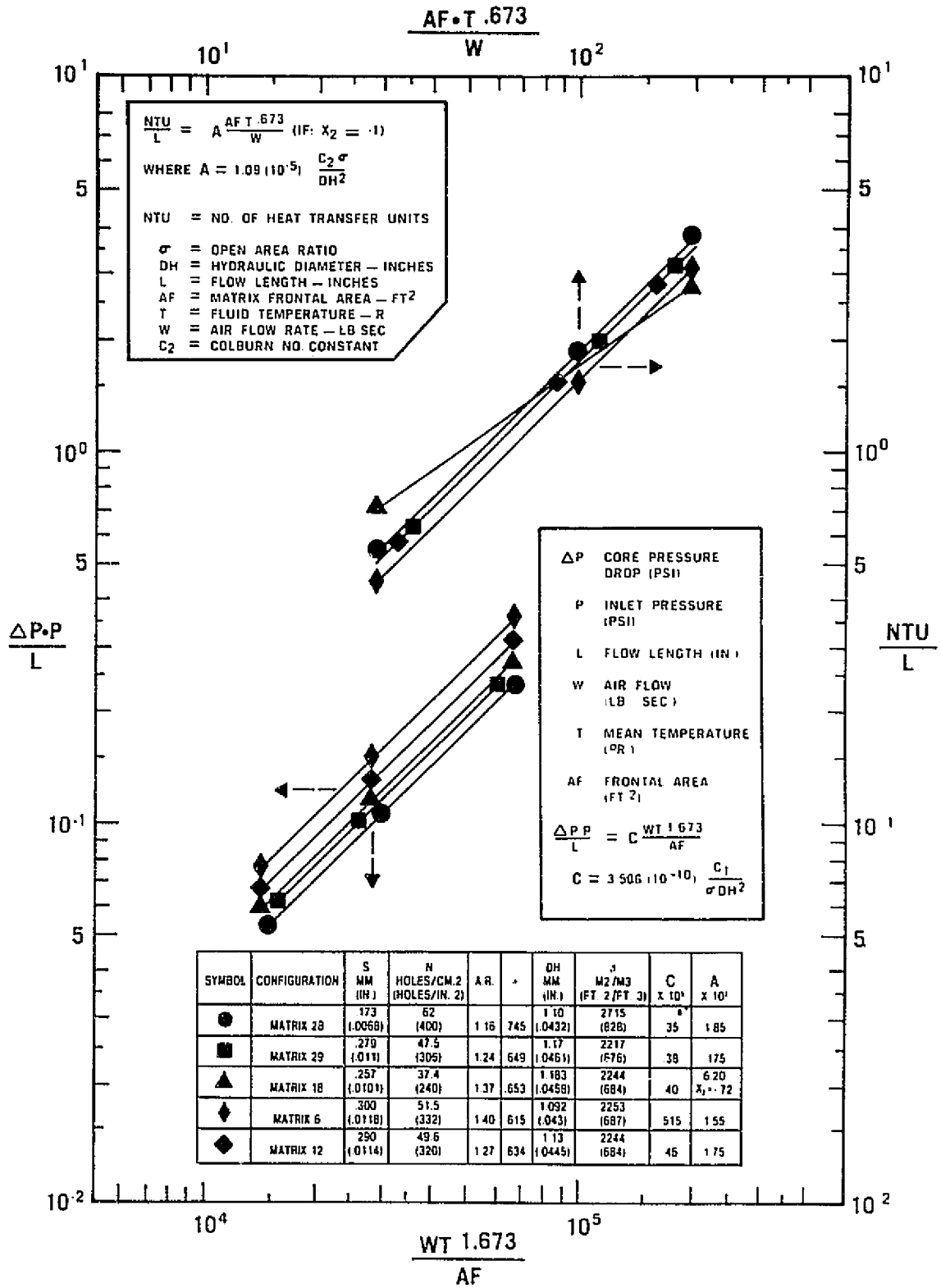

SYMBOL	CONFIGURATION	S MM (IN.)	N HOLES/CM.2 (HOLES/IN. 2)	A.R.	σ	DH MM (IN.)	J M2/M3 (FT 2/FT 3)	C X 10^4	A X 10^1
●	MATRIX 28	.173 (.0068)	62 (400)	1.16	.745	1.10 (.0432)	2715 (826)	35	1.85
■	MATRIX 29	.279 (.011)	47.5 (305)	1.24	.649	1.17 (.0461)	2217 (676)	38	1.75
▲	MATRIX 18	.257 (.0101)	37.4 (240)	1.37	.653	1.183 (.0459)	2244 (684)	40	6.20 $X_1 = .72$
♦	MATRIX 6	.300 (.0118)	51.5 (332)	1.40	.615	1.092 (.043)	2253 (687)	515	1.55
◆	MATRIX 12	.290 (.0114)	49.6 (320)	1.27	.634	1.13 (.0445)	2244 (684)	45	1.75

Figure IV.B.8 Alternate Thermodynamic Performance Characteristics of Matrices 6, 12, 18, 28 and 29.

IV.C. PROBLEM AREAS

No major problems exist at this time. A minor problem at this time is the in-house porosimeter, which is temporarily inoperable. This condition should be rectified during the next report period, since the replacement part has been ordered.

IV.D. FUTURE PLANS

Four additional matrix samples are scheduled for evaluation during the next report period.

IV.E. TASK SUMMARY

With the two additional extruded square matrices tested during this report period, a total of twenty-nine matrix fin configurations have been evaluated at the present time. Seventeen rectangular, eight sinusoidal, two isosceles triangular, and two hexagonal configurations comprise the present matrix sample size.

Due to the significant reduction of the wall material thickness (.173 mm) for the extruded square matrix 28, it exhibits superior heat transfer and pressure drop characteristics compared to equivalent matrices previously evaluated.

V. DESIGN STUDIES OF ADVANCED REGENERATOR SYSTEMS

V.A. INTRODUCTION

Since 1973, design studies of ceramic heat exchanger systems have been carried out in order to analytically evaluate the structural performance of the various suppliers' matrices and to compare different drive, mounting, seal and stress relief schemes. Two types of rotary heat exchangers have been studied: a regenerator sized for the Ford 707 gas turbine engine and a preheater sized for the Ford Stirling engine. The regenerator has a 716 mm (28.2 in) outside diameter and is 73 mm (2.86 in) thick. The preheater has a 458 mm (18.04 in) outside diameter, a 190 mm (7.50 in) inside diameter, and is 41 mm (1.6 in) thick. These ceramic heat exchanger systems have been analyzed for temperature inlet conditions of 800°C (1472°F) and 1000°C (1832°F) (Reference 1, 2). Task V of the NASA/Ford ceramic Regenerator Program deals with design studies emphasizing regenerator system materials and configurations intended to improve aerothermodynamic performance, reduce thermal stress, and provide for higher temperature operation.

V.B. STATUS

V.B.1 Material Properties

In the previous quarterly progress report, the results of statistical analyses of the radial and tangential modulii of rupture (MOR) and the radial compressive strength of specimens cut from several Supplier A thin-wall aluminum silicate regenerator cores incorporating a sinusoidal triangular fin with a wall thickness of .061 mm (.0024 in) were reported. In order to more completely characterize the mechanical properties of this matrix, the radial and tangential modulii of elasticity (MOE) have been measured and are reported here.

As were the modulii of rupture, the elastic modulii were measured using a four-point bend test. Specimen dimensions were 152 mm x 25 mm x 13 mm (6.0 in x 1.0 in x 0.5 in). The loading spans were 102 mm and 51 mm (4.0 in and 2.0 in). The specimen faces were ground flat and parallel to $\pm$ .025 mm (.001 in). The MOE was determined by strain-gaging the tensile surface of the specimen and recording load vs. strain. The specimens were cut from a 716 mm (28.2 in) diameter regenerator core at a radial location of about 343 mm (13.5 in). Weibull plots of the strength data are repeated in Figures V.B.1.1 through V.B.1.3 for reference. The MOE data are plotted in Figures V.B.1.4 and V.B.1.5.

A statistical evaluation of the radial and tangential flexure strength and modulus has been carried out for the Supplier I extruded MAS matrix incorporating an isosceles triangular fin with a wall thickness of .135 mm (.0053 in). A full-size extruded regenerator has not been produced, so test specimens were cut from 51 mm (2 in) square sample extrusions. For these samples, the radial direction was considered to be perpendicular to the matrix separator sheets. Specimen dimensions were 51 mm x 13 mm x 13 mm (2.0 in x 0.5 in x 0.5 in) and the loading spans were 38 mm and 13 mm (1.5 in and 0.5 in). As always, the specimen faces were ground flat and parallel to $\pm$ .025 mm (.001 in). Weibull plots of the strength and modulus data are presented in Figures V.B.1.6 through V.B.1.9.

Flexure strength and elastic modulus data, as well as radial compressive strength data, have been generated for the Supplier D embossed rectangular fin MAS-2 matrix incorporating a wall thickness of approximately .193 mm (.0076 in). As discussed in Task I, a Supplier D MAS-2 regenerator has been placed on engine test at 800°C (1472°F). A finite element thermal stress analysis, based on preliminary mechanical property data, was described in the previous quarterly report and indicated that this

regenerator, properly stress relieved, has the potential for operation at an inlet temperature of 1000°C (1832°F). Flexure test specimens with dimensions of 114 mm x 25 mm x 13 mm (4.5 in x 1.0 in x 0.5 in) were cut from a 716 mm (28.2 in) diameter regenerator core at a radius of 343 mm (13.5 in) and prepared in the usual manner. Radial compressive strength specimens with dimensions of 51 mm x 51 mm x 51 mm (2.0 in x 2.0 in x 2.0) were taken from approximately the same radial location on the core. Compressive strength was measured by loading the specimens to failure in a testing machine at a cross-head speed of 5 mm/min (0.2 in/min). Upper and lower specimen surfaces were ground flat and parallel to ± .025 mm (.001 in). In order to provide uniform loading, thin elastomer sheets were incorporated on the specimen loaded surfaces.

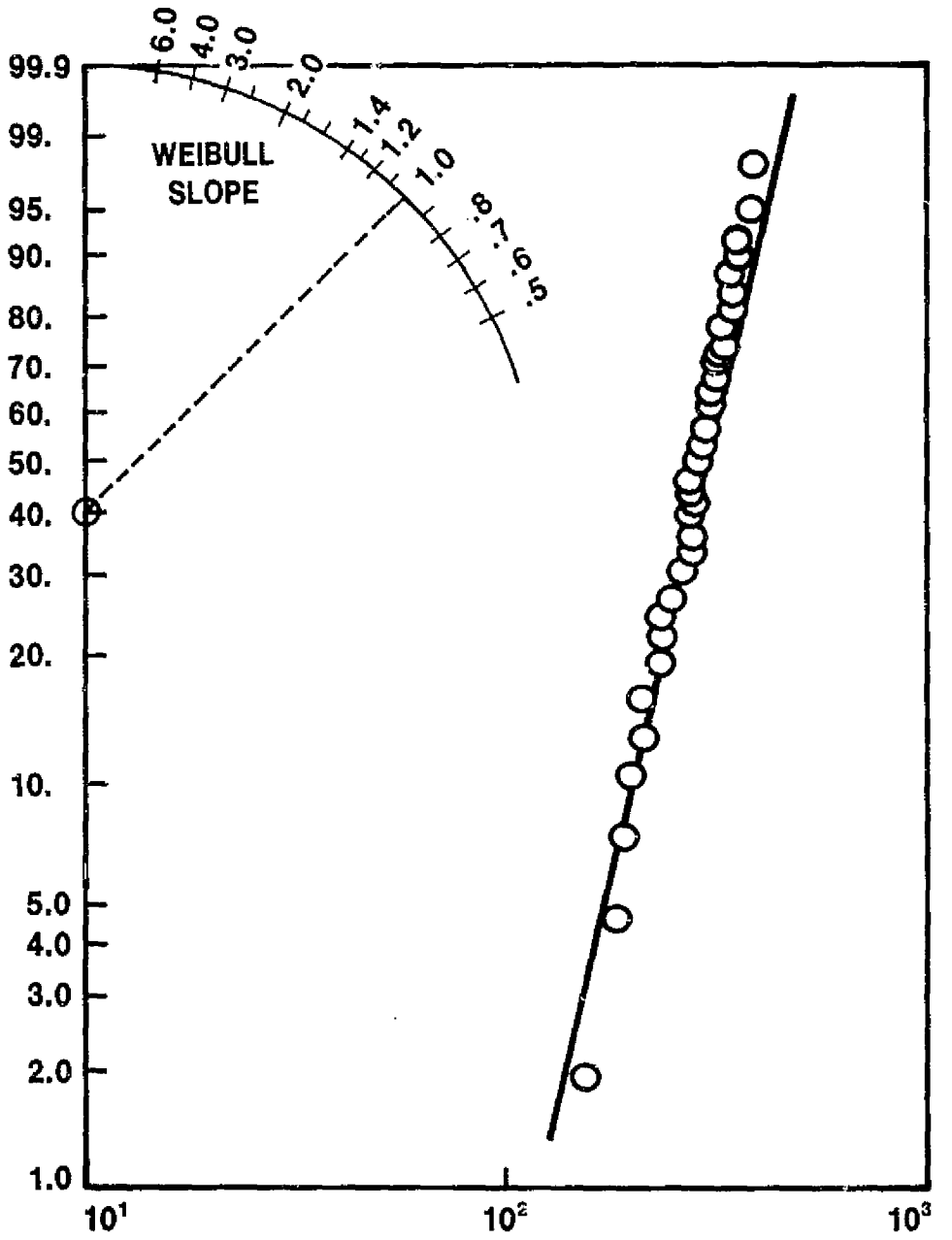

Figure V. B. 1. 1 Supplier A Thin-Wall AS Tangential MOR.

The radial and tangential MOR, MOE and the radial compression data are plotted in Figures V.B.1.10 through V.B.1.14.

Table V.B.1.1 summarizes the pertinent geometry and strength characteristics of the AS and MAS materials including B_{10} and B_{50} strength and modulus, and the strain tolerance which is the ratio of average MOR to MOE.

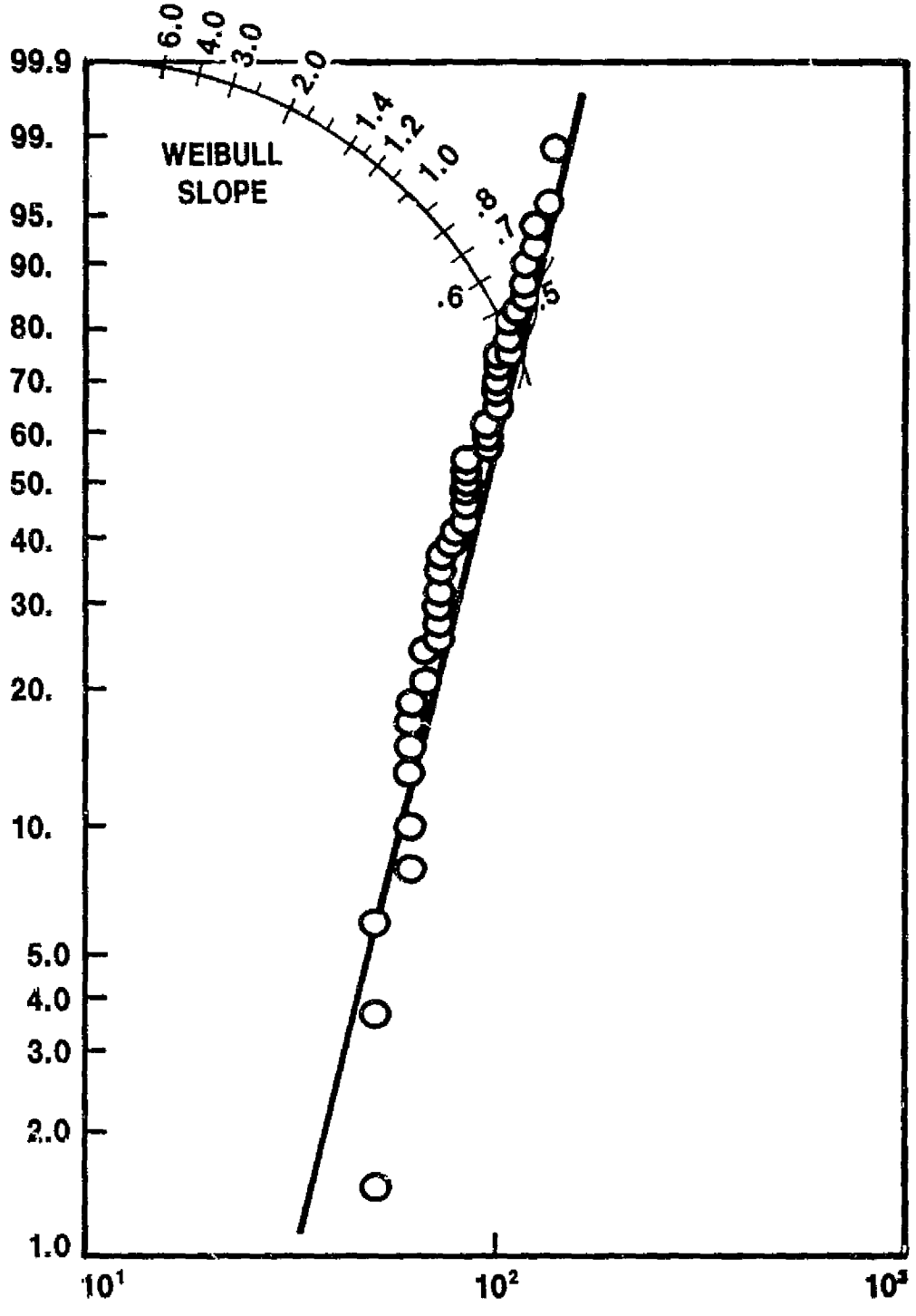

Figure V. B. 1. 2 Supplier A Thin-Wall AS Radial MOR.

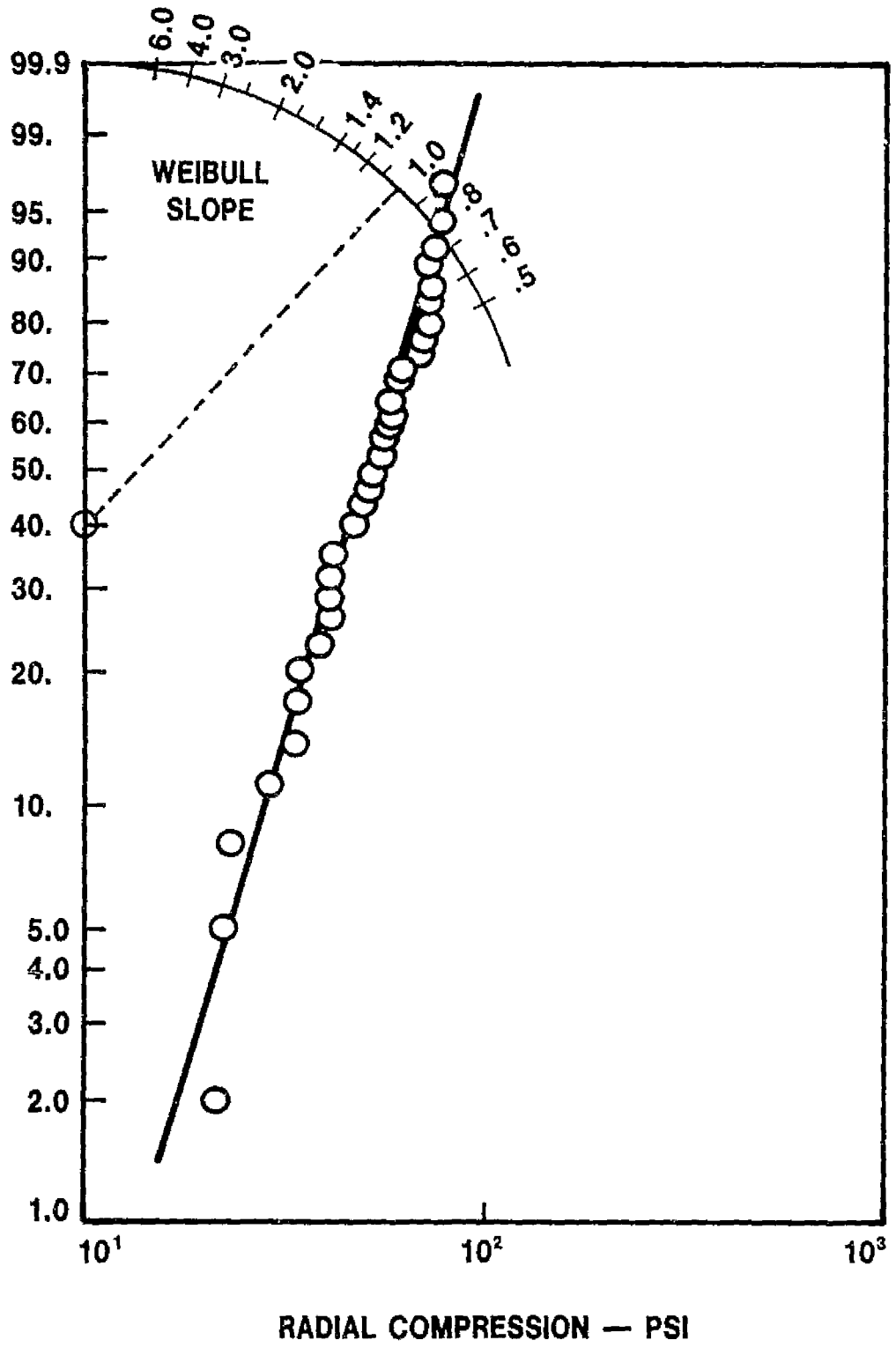

Figure V. B. 1. 3 Supplier A Thin-Wall AS Radial Compression Strength.

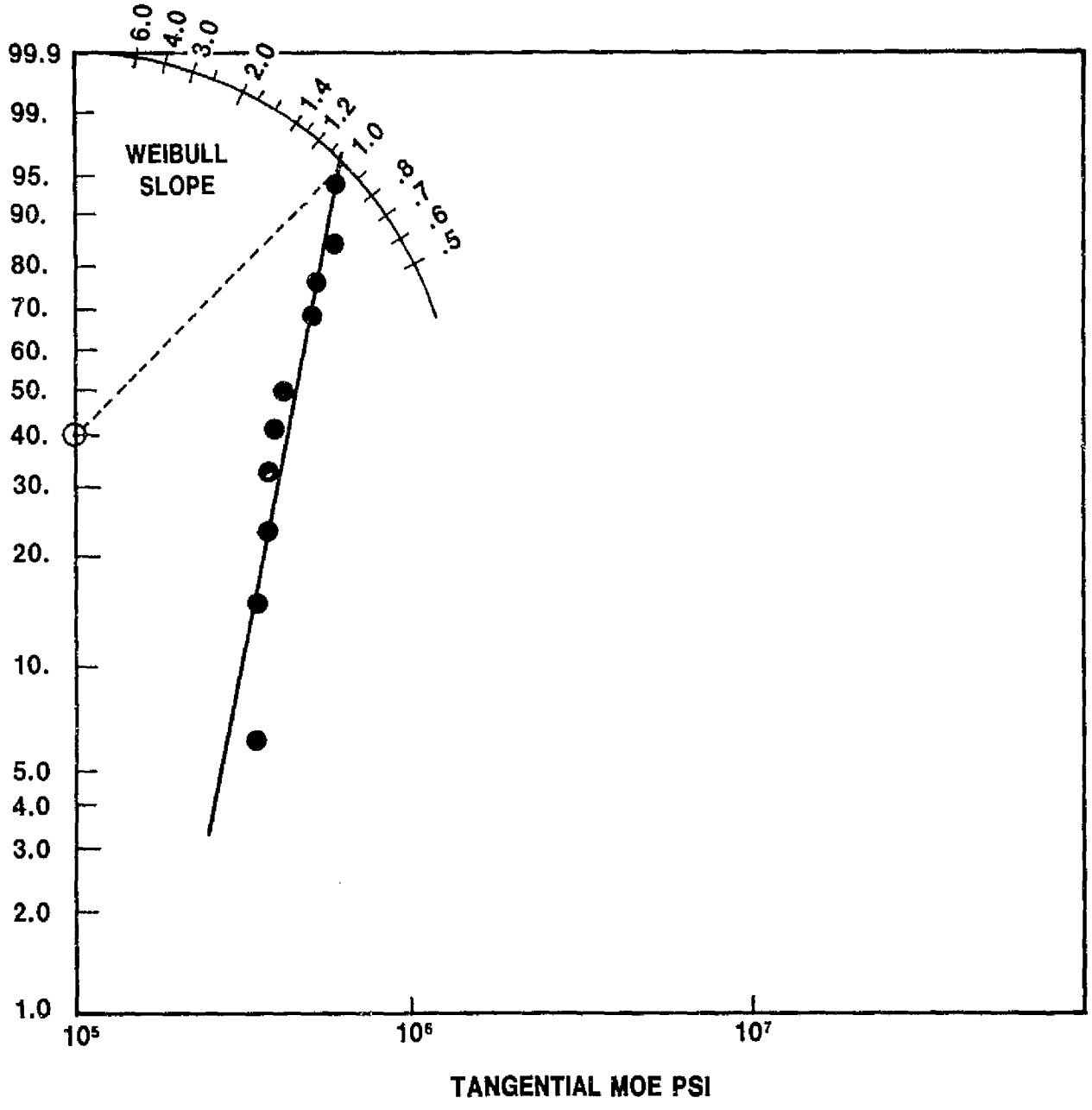

Figure V. B. 1. 4 Supplier A Thin-Wall AS Tangential MOE.

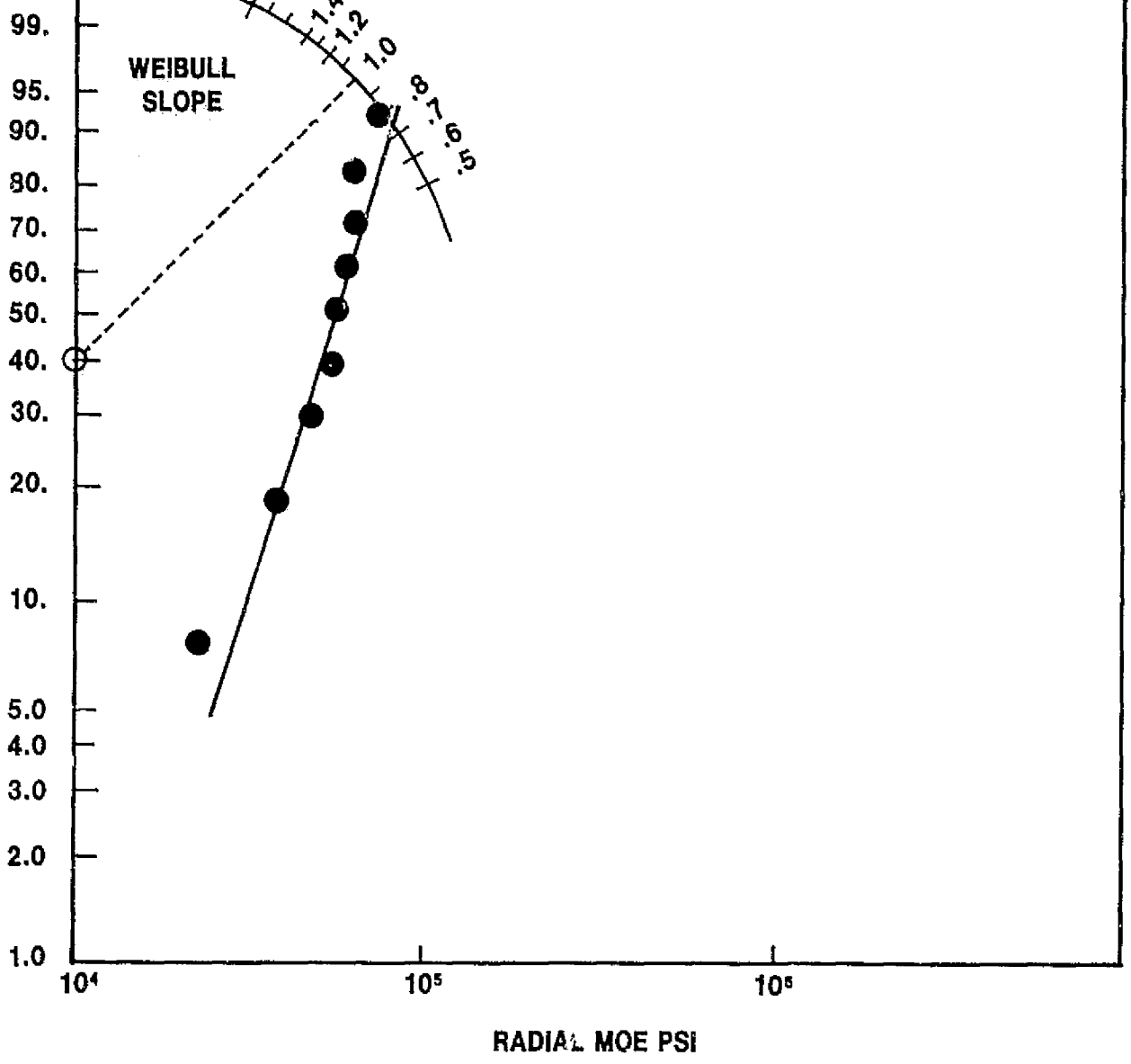

Figure V. B. 1. 5 Supplier A Thin-Wall AS Radial MOE.

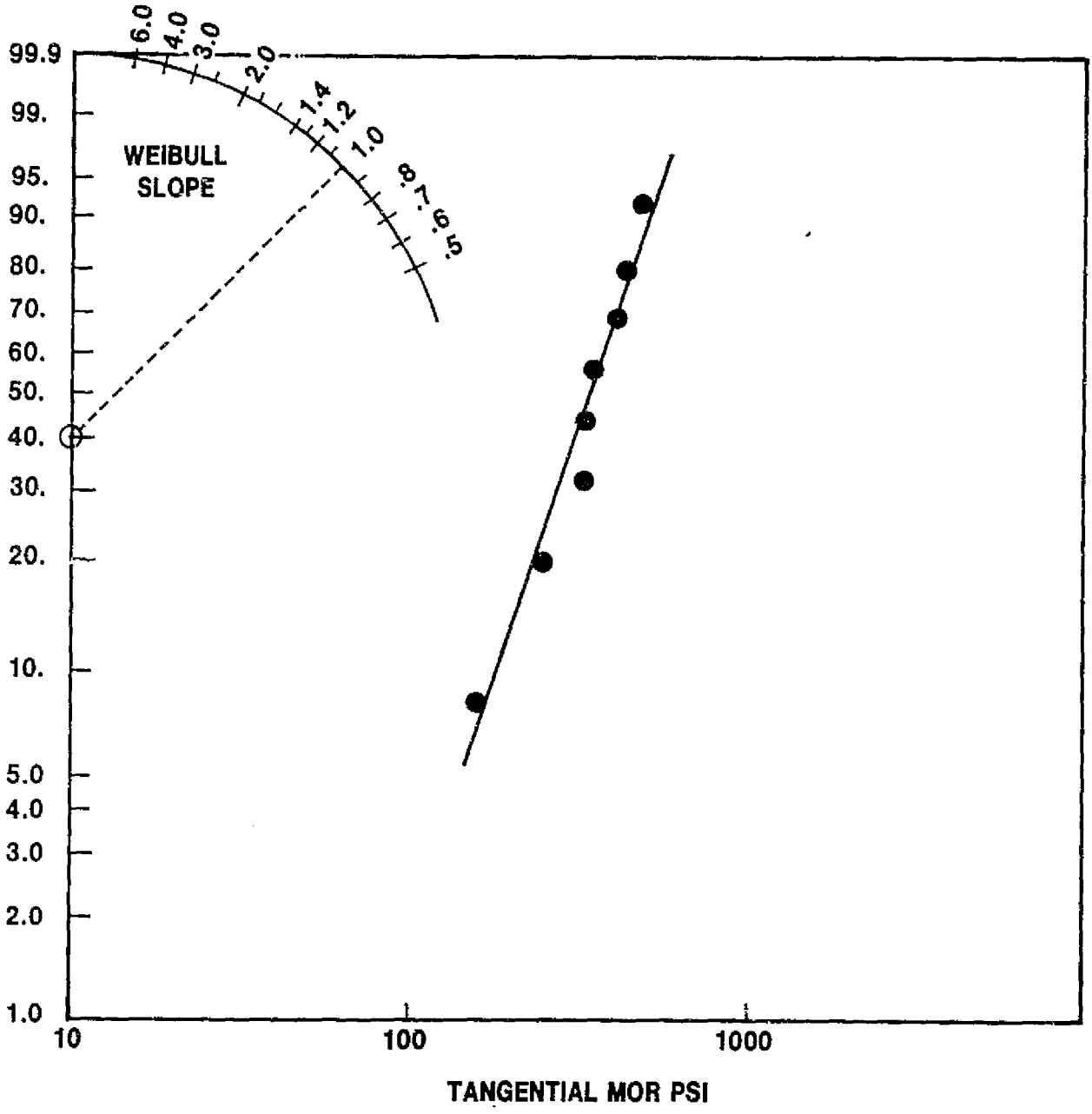

Figure V. B. 1. 6 Supplier I MAS Tangential MOR.

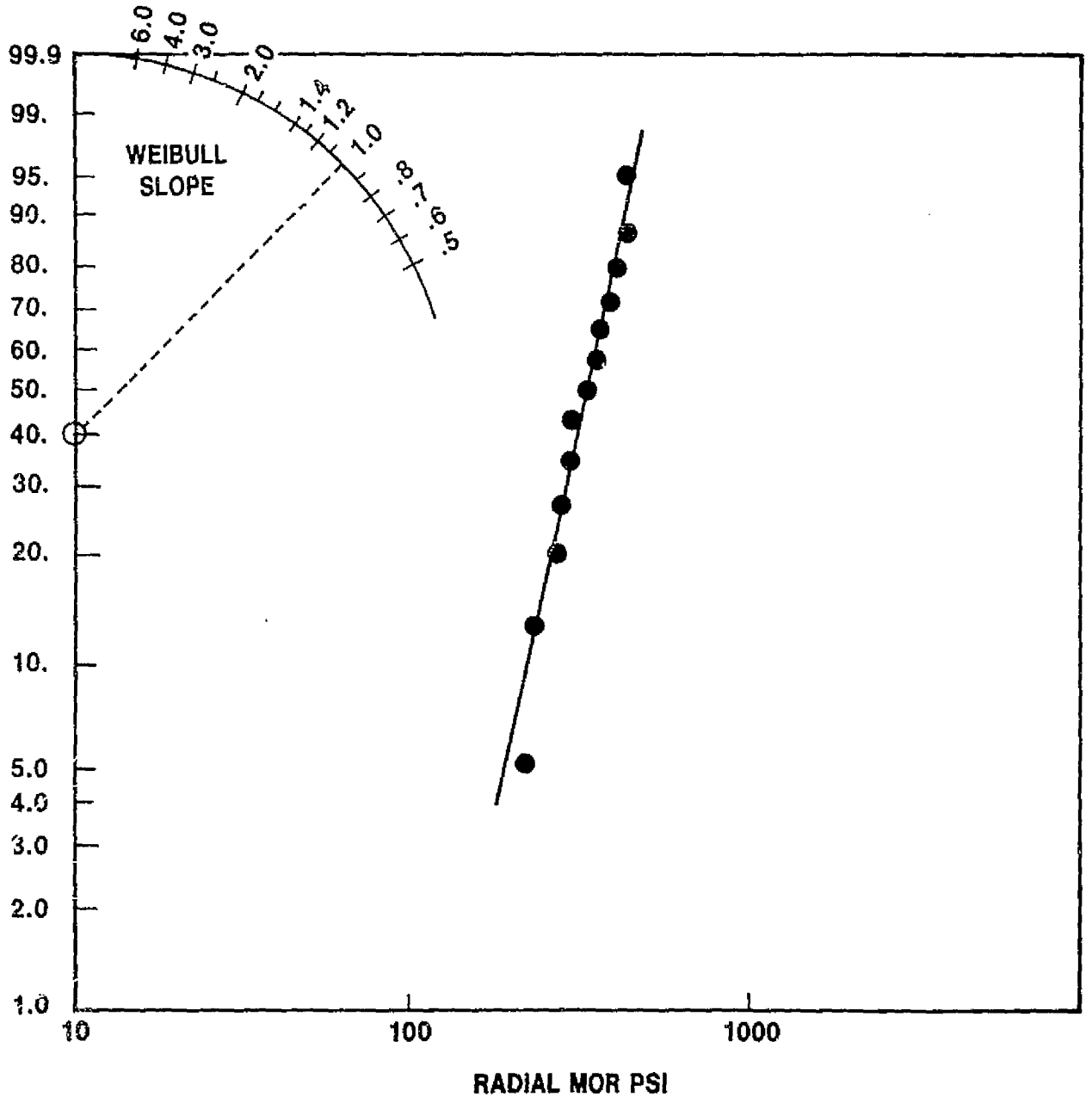

Figure V. B. 1. 7 Supplier I MAS Radial MOR.

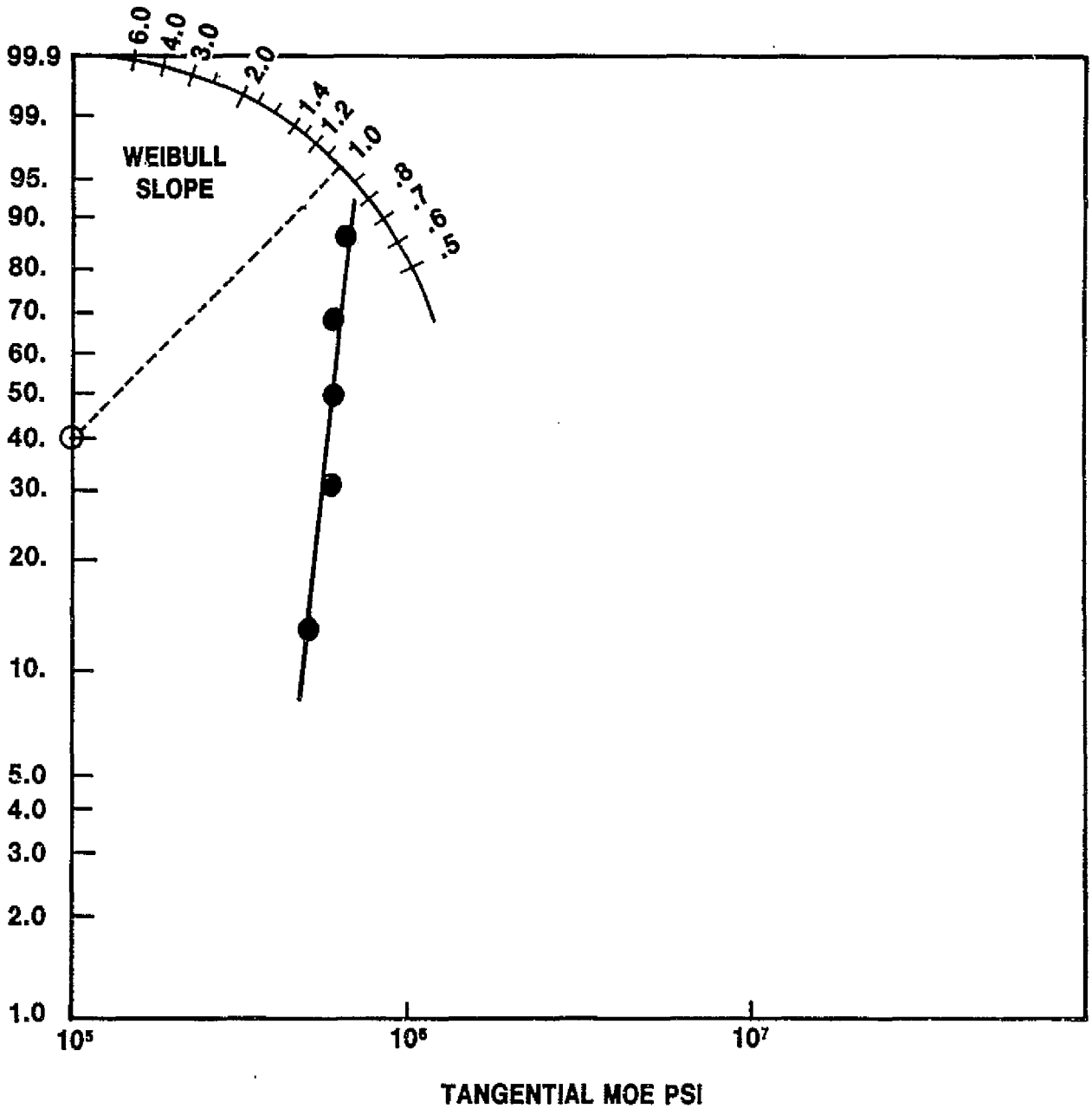

Figure V. B. 1. 8 Supplier I MAS Tangential MOE.

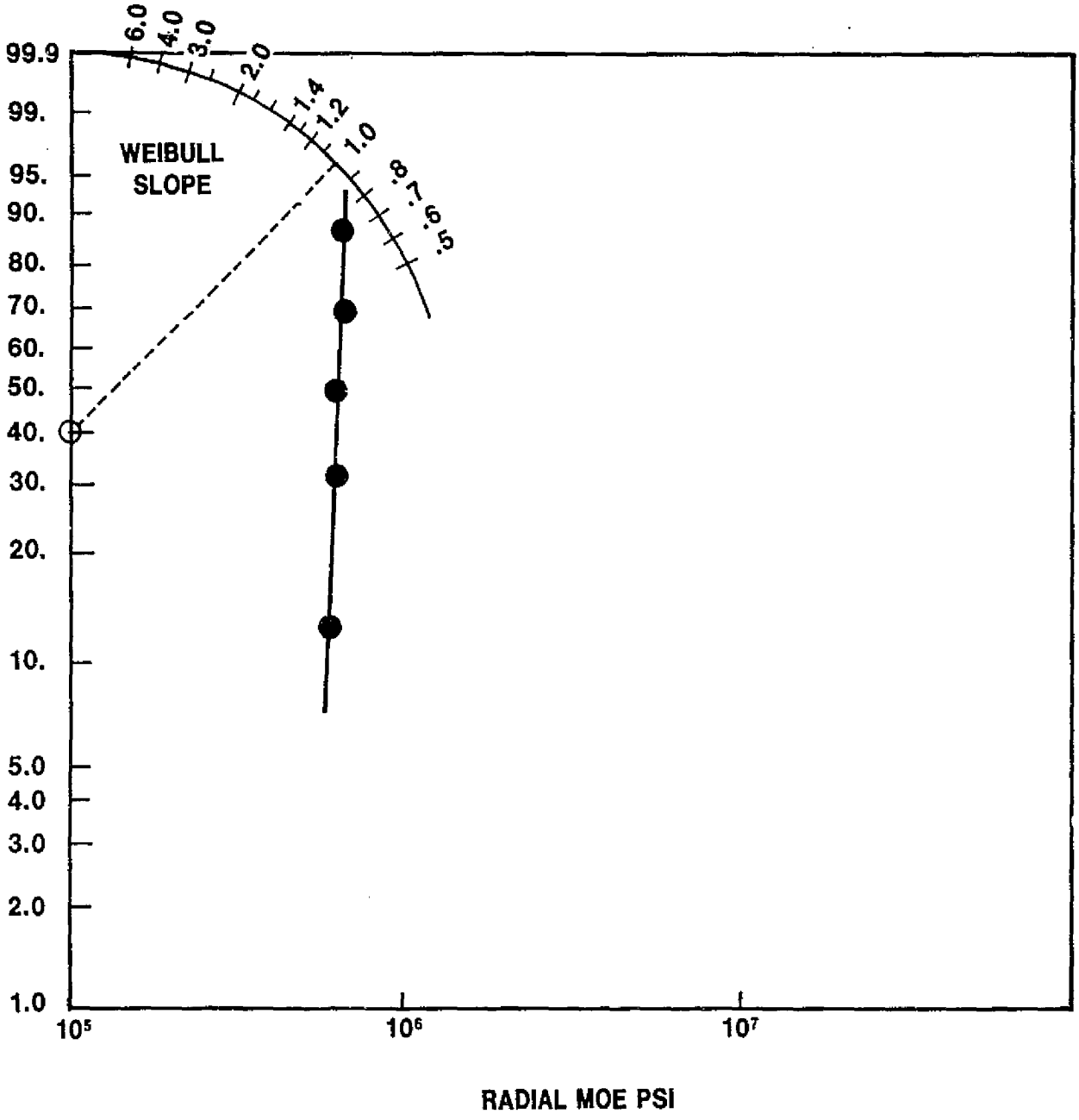

Figure V. B. 1. 9 Supplier I MAS Radial MOE.

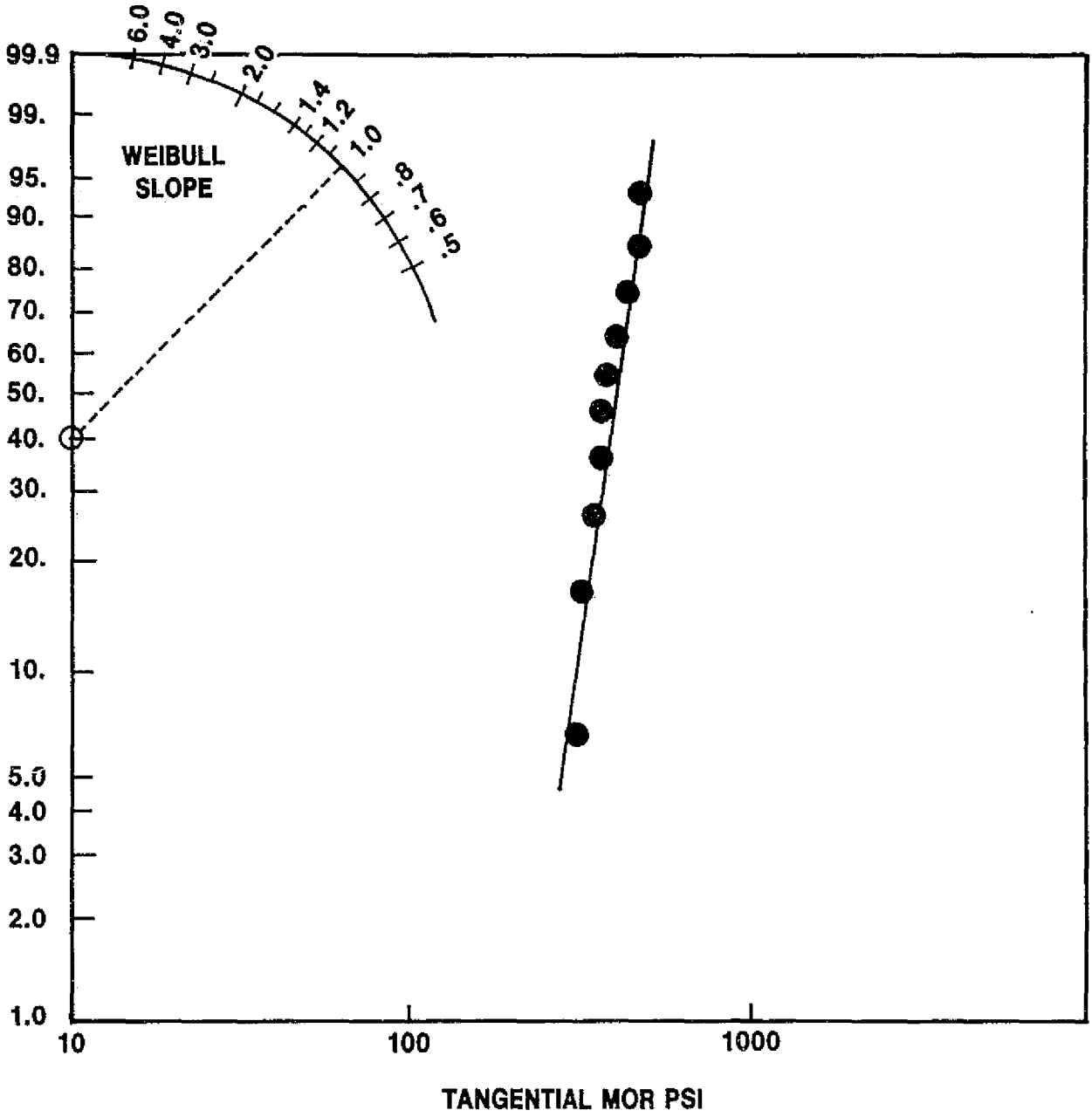

Figure V. B. 1. 10 Supplier D MAS-2 Tangential MOR.

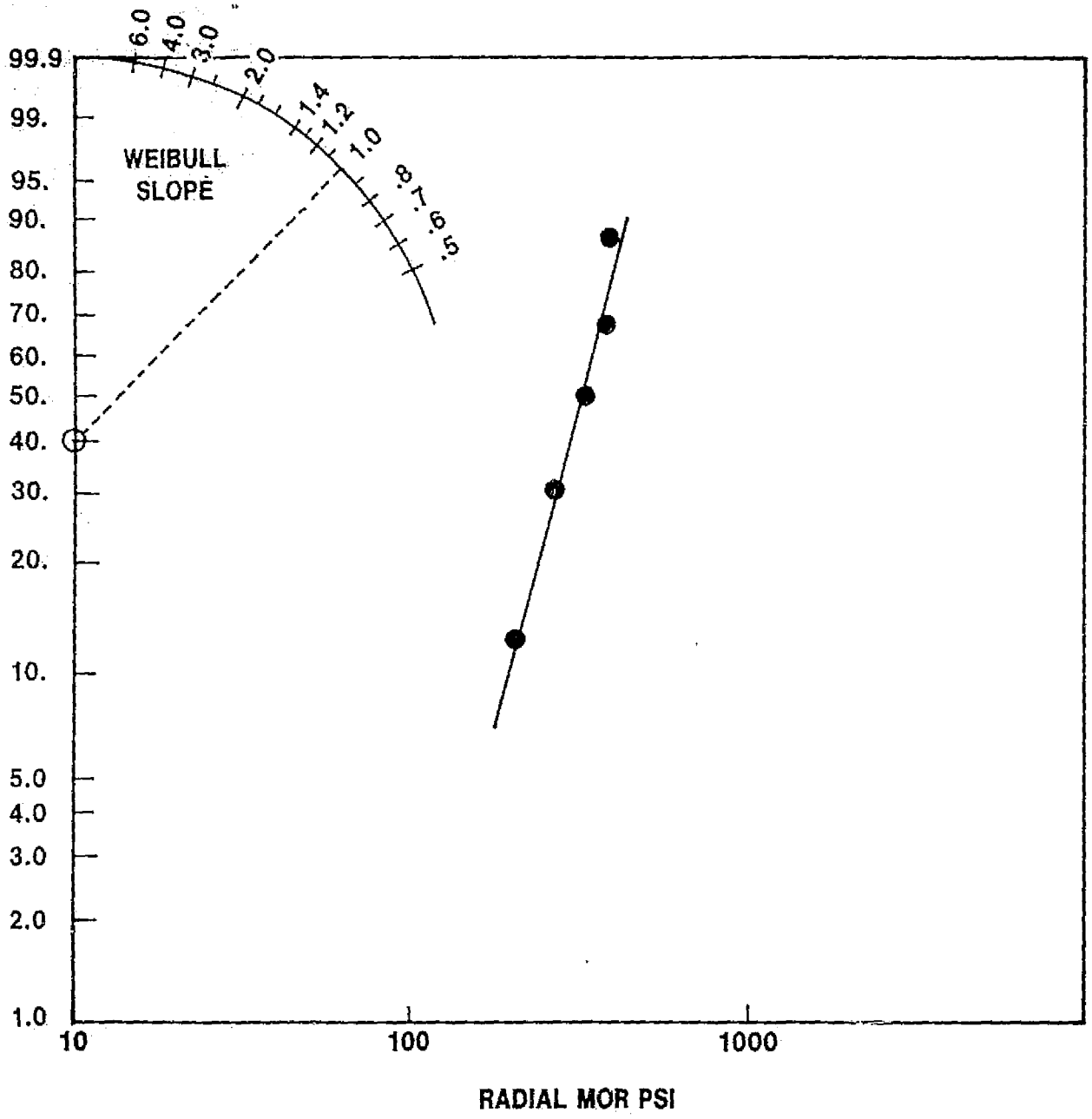

Figure V.B.1.11 Supplier D MAS-2 Radial MOR.

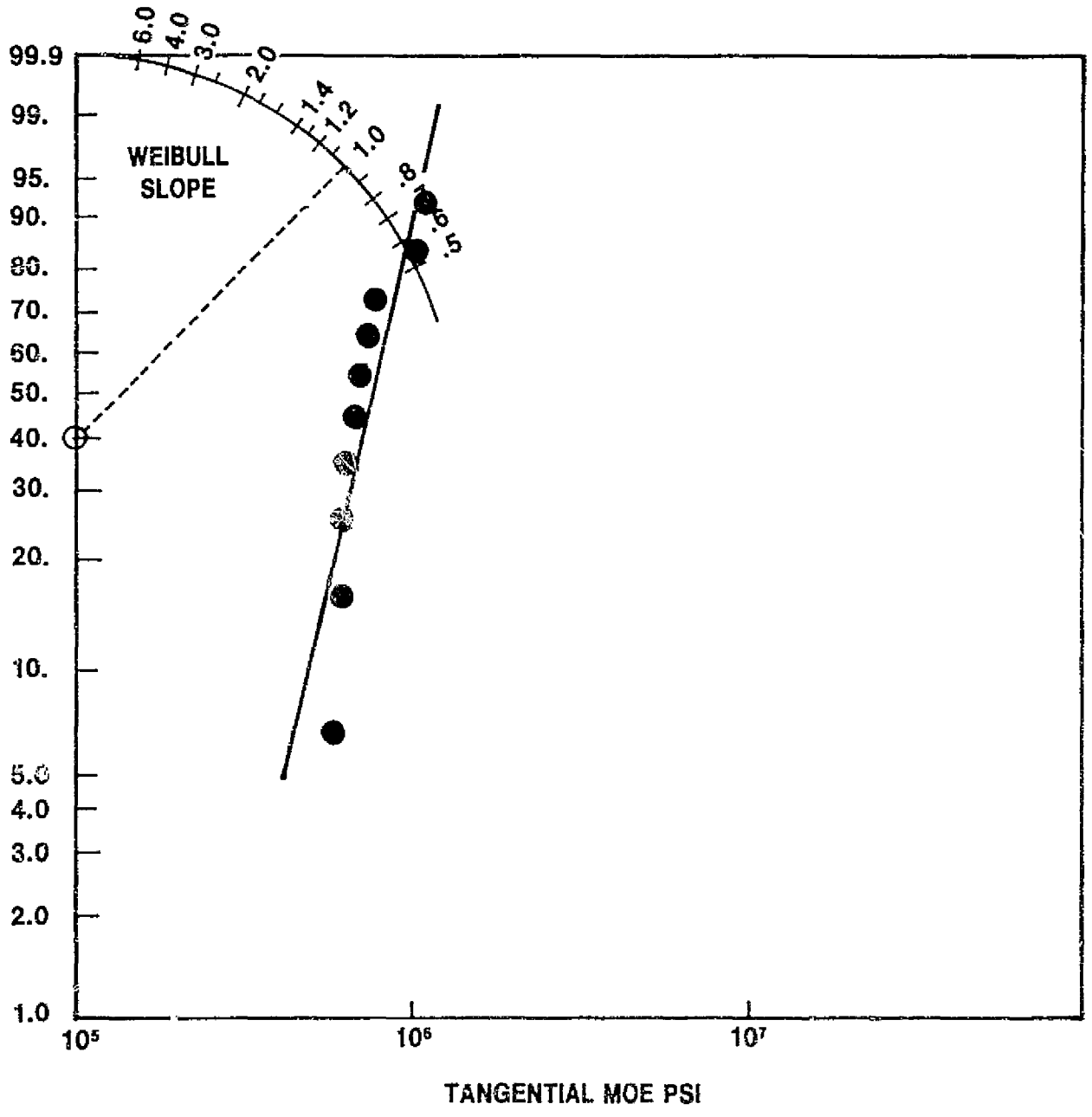

Figure V. B. 1. 12 Supplier D MAS-2 Tangential MOE.

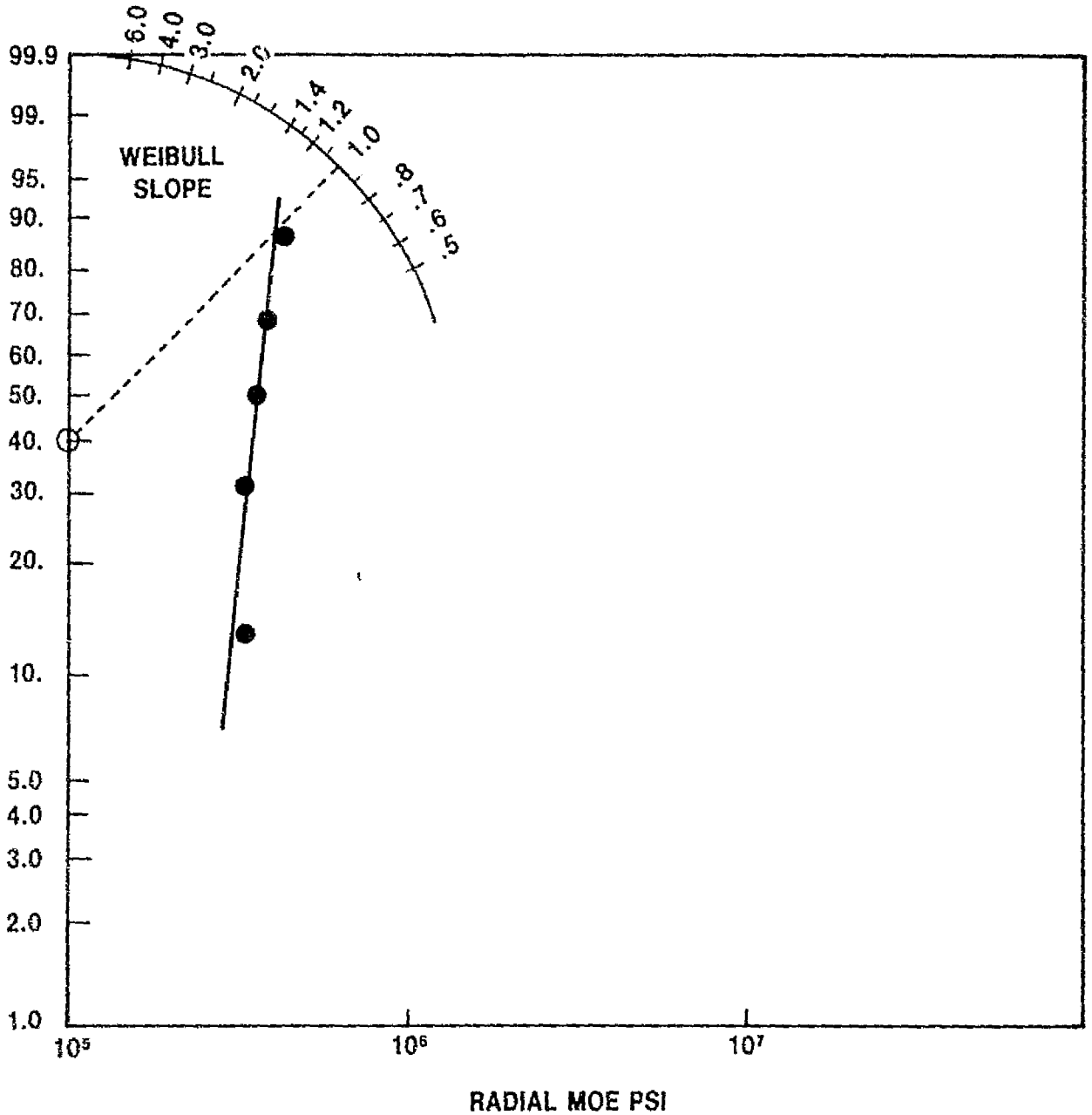

Figure V. B. 1. 13 Supplier D MAS-2 Radial MOE.

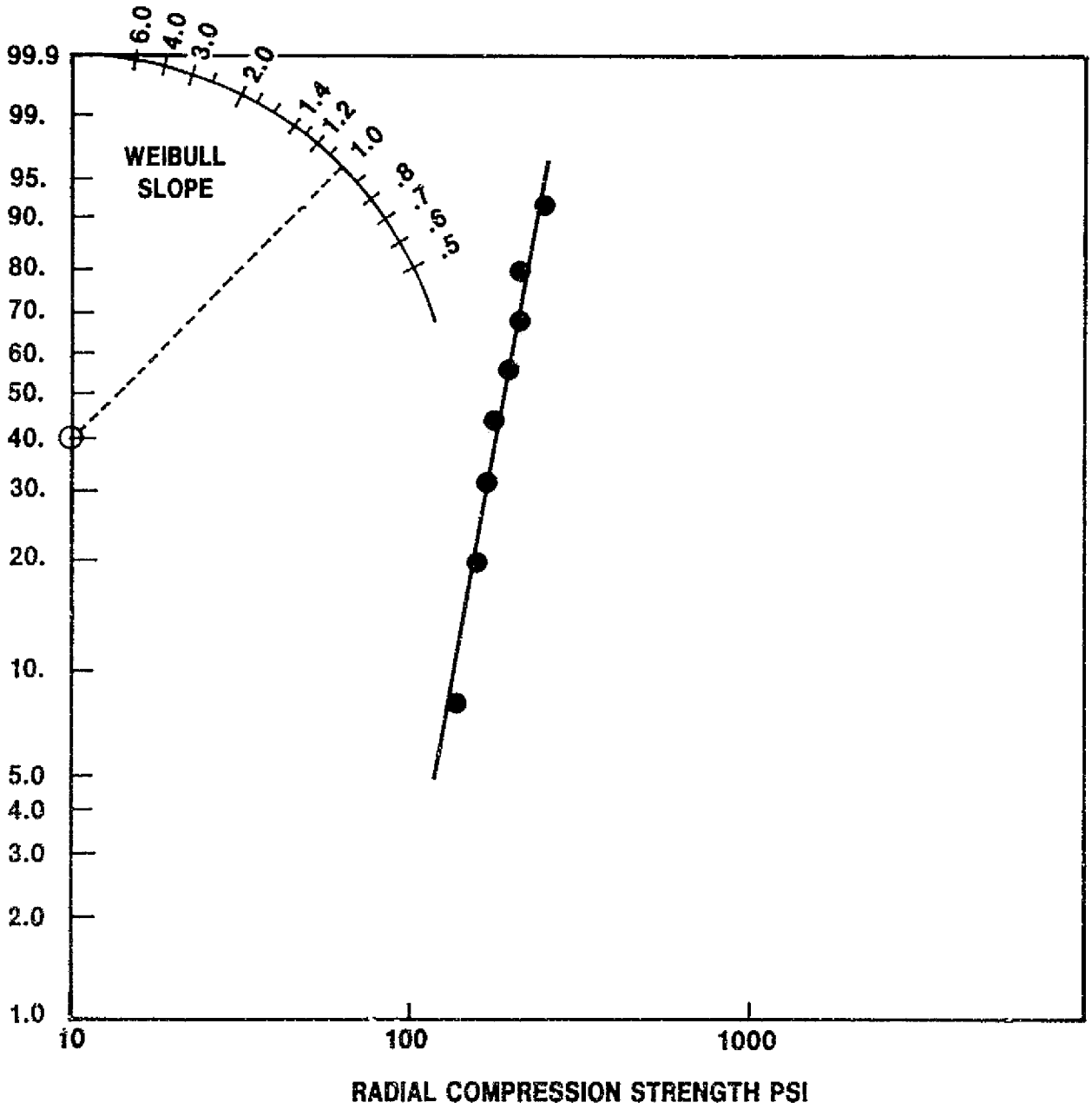

Figure V. B. 1. 14 Supplier D MAS-2 Radial Compression Strength.

CODE:

R — RECTANGULAR	W — WRAPPED
I.T. — ISOSCELES TRIANGULAR	C — CORRUGATED
S.T. — SINUSOIDAL TRIANGULAR	EX — EXTRUDED
H — HEXAGONAL	EM — EMBOSSED

SUP-PLIER	TYPE OF FIN	X FINS / CM. (FINS / IN.)	Y ROWS / CM. (ROWS / IN.)	N HOLES / CM.² (HOLES / IN.²)	S MM. (IN.)	B MM. (IN.)	H MM. (IN.)	B_{50} MOR_T Kpa (PSI)	B_{10} MOR_T Kpa (PSI)	B_{50} MOE_T Kpa (PSI) (X10⁻⁶)	B_{10} MOE_T Kpa (PSI) (X10⁻⁶)	B_{50} MOR_R Kpa (PSI)	B_{10} MOR_R Kpa (PSI)	B_{50} MOE_R Kpa (PSI) (X10⁻⁶)	B_{10} MOE_R Kpa (PSI) (X10⁻⁶)	B_{50} $COMP_R$ Kpa (PSI)	B_{10} $COMP_R$ Kpa (PSI)	STRAIN TOL. (PPM)	MAT'L	MFG. PROCESS
A	S.T.	15.0 (38)	13.6 (34.5)	203.9 (1311)	.061 (.0024)	.061 (.0024)	.676 (.0266)	1998 (290)	1399 (203)	3.1 (.45)	2.14 (.31)	620 (90)	386 (56)	.379 (.055)	.193 (.028)	345 (50)	200 (29)	450	AS	W, C
I	I.T.	15.8 (40)	9.1 (23)	142.6 (920)	.135 (.0053)	.135 (.0053)	.970 (.0382)	2274 (330)	1240 (180)	4.13 (.60)	3.38 (.49)	2274 (330)	1516 (220)	4.31 (.625)	4.07 (.59)			578	MAS	EX
D	R	11.4 (29)	12.2 (31)	140 (900)	.193 (.0076)	.193 (.0076)	.627 (.0247)	2756 (400)	2067 (300)	5.34 (.775)	3.38 (.49)	2343 (340)	1378 (200)	2.49 (.362)	2.05 (.298)	1309 (190)	944 (137)	516	MAS	W, EM

Table V. B. 1. 1 Matrix Mechanical Properties

V.B.2 Drive and Mount Analysis

As described in Task I, there have been repeated instances of Supplier A thin-wall AS regenerator core compressive stress failures during the process of elastomerically bonding the ring gear to the ceramic matrix. Cohesive failures of the matrix at the elastomer/core interface during engine operation have also been prevalent in this type of regenerator, and have happened occasionally with thick-wall Supplier A AS cores. Recently, elastomer configurations providing a more compliant bond between the core and the gear have been incorporated, with some success, to inhibit such failures.

The operating experience of regenerators incorporating compliant elastomer schemes is described in Task I. These schemes are intended to preclude compressive stress failure in the bonding fixture and to isolate the core from stress imposed during operation by the drive support system. One such scheme, which provided mixed durability results, provided compliance by introducing 300+ equally spaced axial holes in the elastomer. As described in Task I, a more successful scheme incorporates thin elastomer pads bonded alternately to the ring gear and the core and connected by thin elastomer beams such that no where around the rim is the gear bonded directly to the core. This interrupted configuration is produced by molding the elastomer around foam rubber pads attached alternately to the gear and the core around the rim.

In the previous quarterly report, the apparent compressive modulus of the 300+ hole compliant system was evaluated and compared to that of the standard elastomer system. It was determined that a reduction in modulus of about half was realized by this scheme. Recently, compressive stress-strain data were generated for the interrupted scheme, and this information is plotted in Figure V.B.2.1 along with stress-strain data for the standard and 300+ hole schemes for comparison.

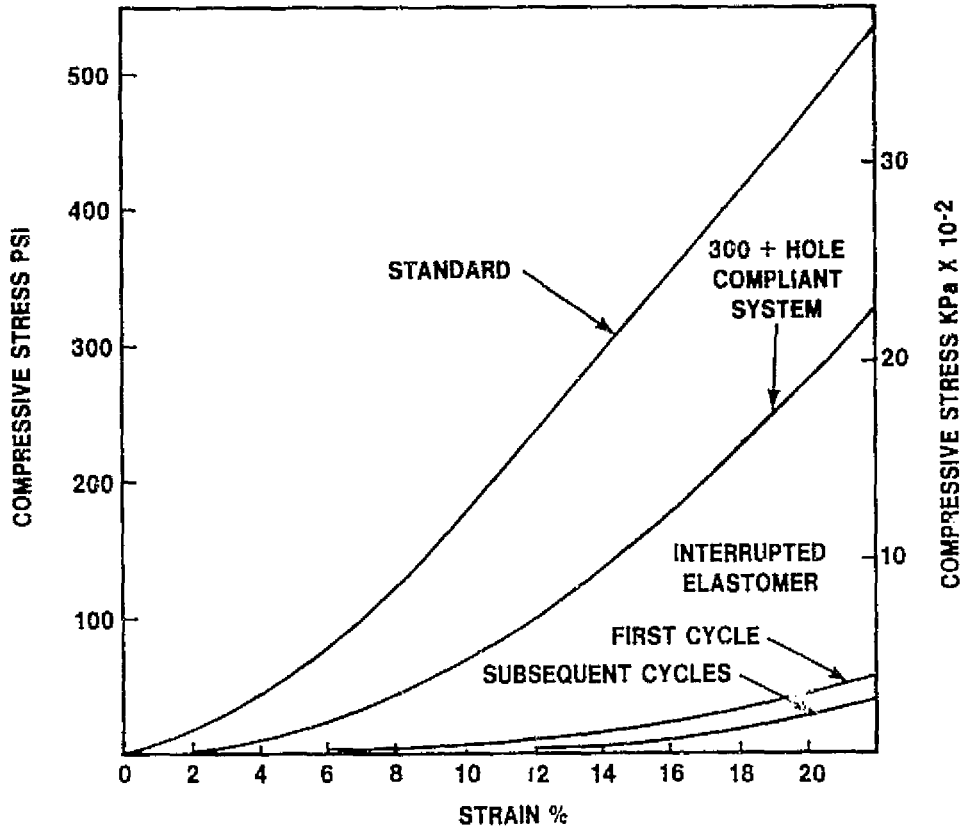

Figure V.B.2.1 Compressive Stress vs. Strain for Compliant Elastomer Systems.

To determine the reduction in apparent modulus realized by this compliant system, a 94 mm x 44 mm x 5 mm (3.75 in x 1.77 in x .190 in) specimen of the elastomer configuration was tested at room temperature using a testing machine at a cross-head speed of .5 mm/min (.02 in/min).

It can be seen from this graph that the interrupted configuration provides a decrease in apparent modulus of about 90% compared to the standard scheme. As described in Task I, no thin-wall AS cores incorporating this elastomer configuration have failed during the bonding operation or have suffered ring gear separations during engine operation.

In addition to the compression testing of the three elastomer configurations, three 707 engine regenerators, each incorporating a different elastomer scheme, have been subjected to a static torque of about twice that encountered during engine operation, and the ring gear radial deflection for each case was measured. The following core/elastomer combinations were tested to a static torque of 1356 Nm (1000 ft-lbs):

1. A thick-wall AS core incorporating the standard elastomer configuration.

2. A thick-wall AS core incorporating a compliant elastomer scheme consisting of 180 equally-spaced axial holes through the elastomer.

3. A thin-wall AS regenerator incorporating the interrupted elastomer scheme.

None of the cores tested sustained any damage due to the torsion load.

The static torque test consisted of clamping the regenerator to a back-plate on which were mounted the fixed and spring support rollers located in their respective engine positions. Torque was applied through a pinion attached to a lever arm. The ring gear deflection was measured using dial indicators located strategically around the regenerator periphery. The test results are shown in Figure V.B.2.2. The maximum deflection of the ring gear occurs between the fixed roller and the pinion. For the standard elastomer scheme at a torsion load of 1356 Nm (1000 ft-lbs), this deflection is .813 mm (0.032 in). For the 180 hole scheme and for the interrupted scheme, the maximum ring gear deflections at this load are .33 mm (0.013 in) and .419 mm (0.0165 in) respectively.

V.C. PROBLEM AREAS

There are no current problems.

V.D. FUTURE PLANS

As promising materials are identified through characterization of their thermal expansion and chemical stability (Task III), mechanical properties will be evaluated and regenerator systems incorporating these materials will be analyzed for structural integrity at the 1000°C (1832°F) through 1200°C (2192°F) operating conditions.

V.E. TASK SUMMARY

The radial and tangential modulii of elasticity of the Supplier A thin-wall sinusoidal fin AS matrix, and the radial and tangential flexure strength and modulii of the Supplier I extruded isosceles triangular fin matrix and the Supplier D embossed rectangular fin MAS-2 matrix have been evaluated using Weibull statistics.

Two compliant elastomer schemes have been evaluated. The interrupted elastomer scheme which has operated successfully in the engine has been shown to provide a 90% increase in compliance compared to the standard configuration.

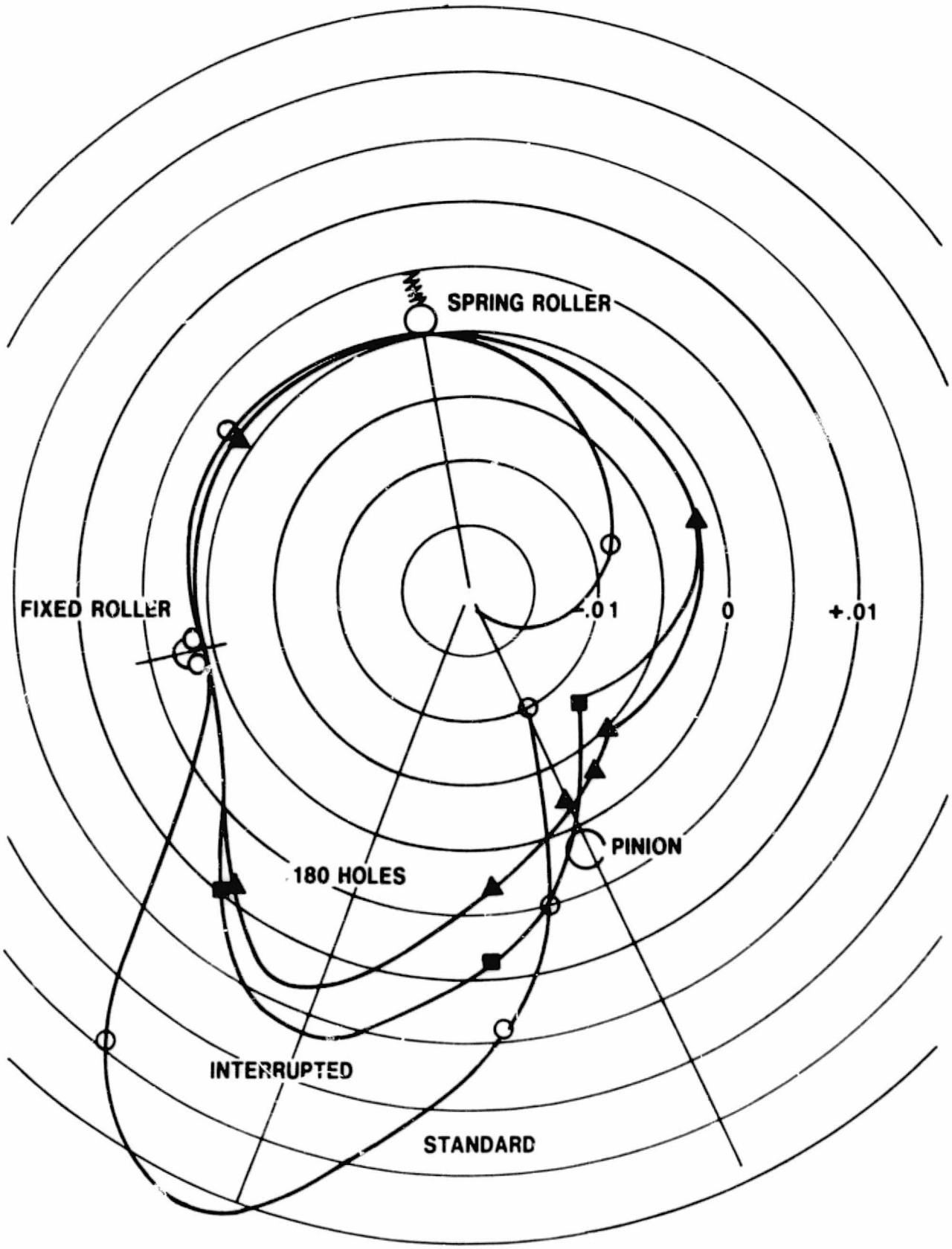

Figure V. B. 2. 2 Regenerator Ring Gear Deflection.

VI. THERMAL STABILITY TESTS OF CERAMICS

VI.A. INTRODUCTION

To increase efficiency, designers propose higher operating temperatures for the alternate heat engines of the future. This, in turn, places greater thermal demands on the regenerator core. In anticipation of these elevated temperature requirements, the thermal stability testing program is designed to systematically test materials, with and without corrosive agents present, over the temperature range of 1000°C (1832°F) to 1200°C (2192°F).

VI.B. STATUS

VI.B.1 1000°C (1832°F) Test Temperature

Three additional material sample sets were acquired to bring the test total to 13 experimental materials (1-LAS/MAS, 8 MAS, 2-leached LAS, 1-LAS, 1-S_iC) plus the 9455 LAS standard. The three new MAS materials, two in a wrapped configuration and one formed by extrusion, are in the sample preparation stage (grinding, cleaning, and initial measuring), so they do not appear in the data presented in this report.

Figure VI.B.1.1 illustrates the behavior of various candidate regenerator materials when held at 1000°C (1832°F) for long periods of time in an air atmosphere. The central area of this graph at low test times is quite congested, with many data points laterally displaced. These represent superimposed data; and the reader should note that all data points reside at the test hour notations on the abscissa. A majority of the materials exhibit good stability. The previously observed instability of the LAS/MAS material persists, and the expansion rate appears constant. The leached LAS material of Supplier A has undergone additional contraction and appears to have restabilized. As this test nears completion, the differences in material behavior become apparent.

Figure VI.B.1.2 contrasts a similar group of specimens, tested in like thermal manner but, in this case, sodium is available for interaction with the materials' structures. Please note the differences in ordinate scales among different figures. Many of the test materials (several MAS specimens, the silicon carbide, and an experimental LAS material from Supplier B) exhibit good stability. The 9455 LAS standard and the LAS/MAS material of Supplier K suffer from the test conditions, while the contractive behavior of the leached LAS from Supplier A is presumably thermally induced.

VI.B.2 1100°C (2012°F) Test Temperature

Test efforts to date have involved seven experimental materials and the 9455 LAS standard. With the recent introduction of three new materials, this portion of the thermal stability testing program will compare, when completed, data from ten experimental materials (7-MAS, 2-leached LAS, 1-LAS) plus the 9455 LAS standard.

Figure VI.B.2.1 displays comparative data among eight materials. Good thermal stability is evidenced by the MAS materials. The MAS composition, if processed to an equilibrium state, should evidence good thermal stability at this temperature. The two leached LAS materials are clearly not meant for service at this temperature, as sufficient thermal motivation towards further reconstitution is obviously present. Of some surprise is the steady growth of the experimental LAS material of Supplier B, especially when compared to the 9455 LAS standard which typifies the inherent thermal stability of LAS.

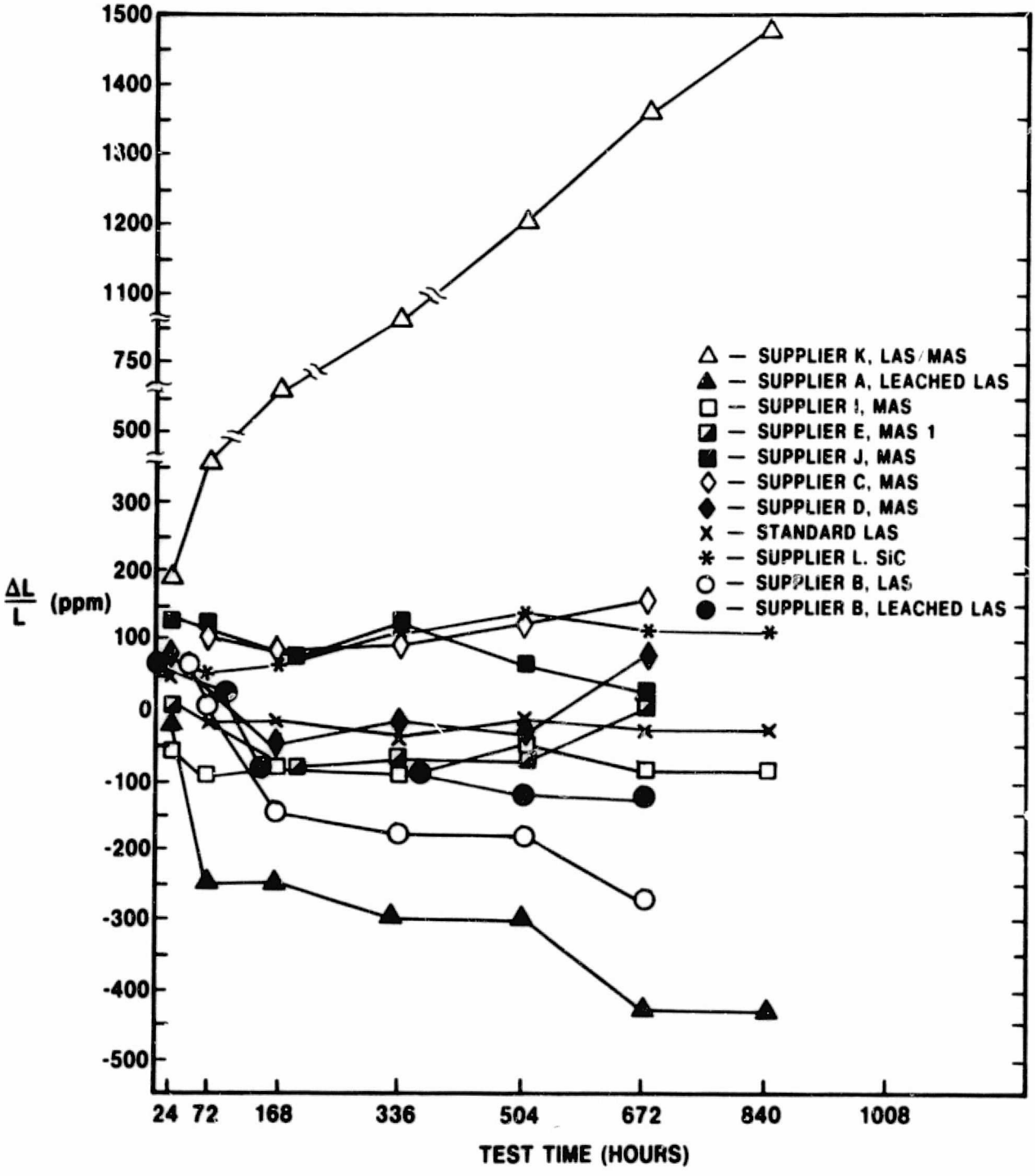

Figure VI. B. 1. 1 Physical Stability of Various Materials at 1000°C (1832°F).

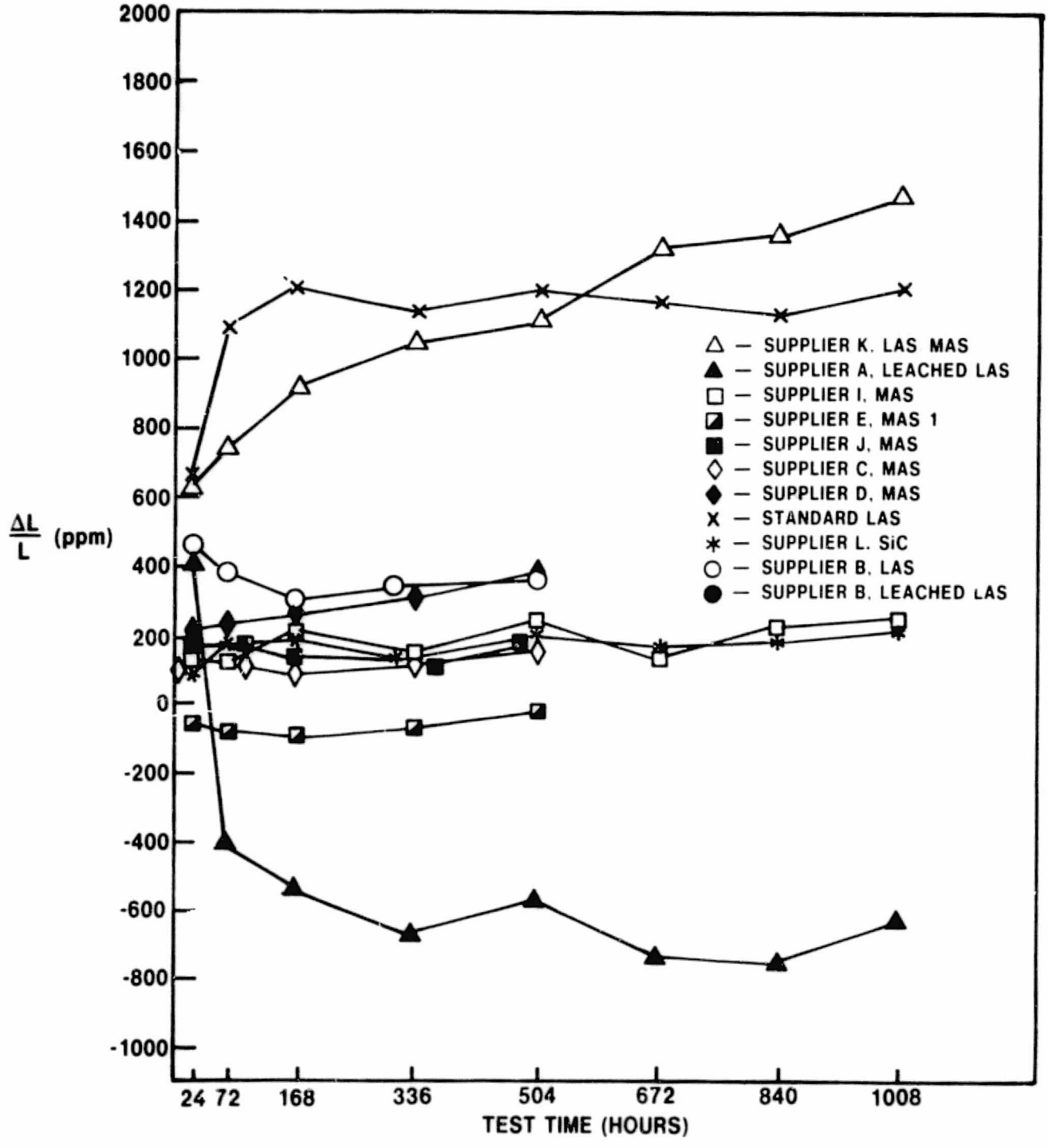

Figure VI. B. 1.2 Physical Stability of Various Materials at 1000°C (1832°F) with Sodium Present.

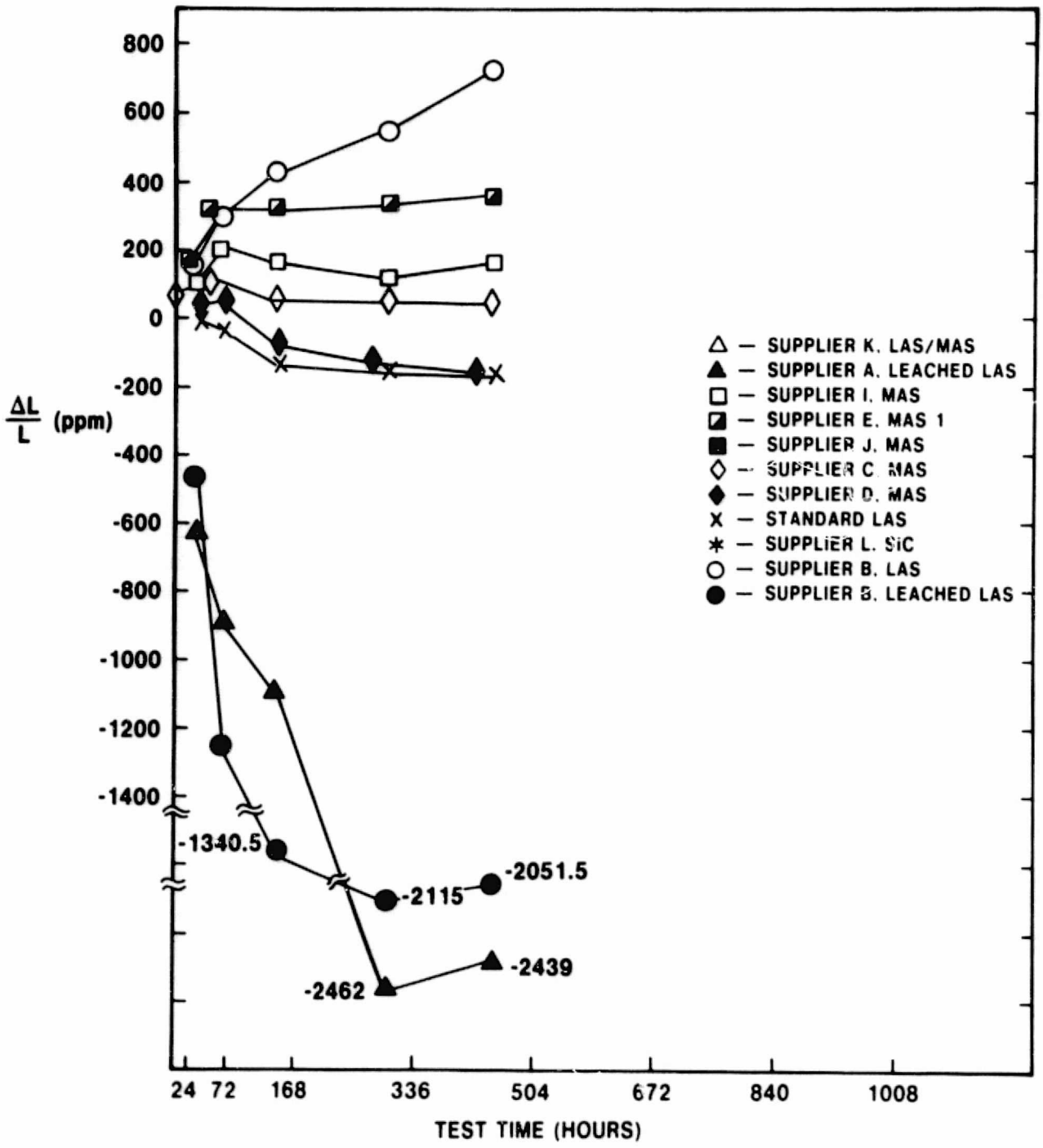

Figure VI. B. 2. 1 Physical Stability of Various Materials at 1100°C (2012°F).

Figure VI.B.2.2 presents data for similar sets of test specimens; however, these samples had received a salt treatment before thermal testing. Note the expanded ordinate scale compared to the previous figure. The MAS materials appear relatively unaffected by sodium, while the experimental LAS material has undergone an expected large growth. The two leached LAS materials have suffered a loss in physical integrity which makes meaningful measurements impossible. Please note the measurement magnitudes printed by each data point. On the basis of these results, the leached LAS materials will be terminated from further testing at this temperature.

VI.B.3 1200°C (2192°F) Test Temperature

Samples originally selected for testing at this temperature included a leached LAS material, four MAS materials, and the 9455 LAS standard. The leached LAS material was terminated based on early severe contraction at this test temperature. Subsequently, these results were supported by the 1100°C (2012°F) data reported above. It should be emphasized that this material was not intended for service at these elevated temperatures. With the addition of three new MAS materials, the total test population for this portion of the thermal stability testing program will be seven experimental materials (all of MAS composition) plus the 9455 LAS standard.

Figure VI.B.3.1 displays data gathered from the original set of four MAS materials and the 9455 LAS standard. The heavy vertical line between 504 and 672 hours represents a temperature overrun experienced with the test furnace. This resulted in a visible physical deterioration of many of the samples, and these indications suggest that the ultimate temperature attained may have exceeded 1400°C (2552°F). Prior to this perturbance, the MAS materials exhibited good thermal stability, as the ordinate scale is quite fine. A problem, experienced at elevated test temperatures which causes measurement problems, is the tapering or crowning of the finished ends of the test specimens. This is presumably due to the enhanced freedom, at these temperatures, for processing stress redistribution. The data after the temperature overrun only serve to point out the type and extent of reaction incurred by the different materials. New specimens are presently being prepared and new data will be taken.

Figure VI.B.3.2 graphically illustrates the reaction to sodium, at these temperatures, of a similar specimen set. Considering the magnitude of the test temperature and the corrosive nature of the test environment, the small dimensional changes exhibited by these MAS materials are encouraging. Individual material trends should emerge as the test progresses; however, it would appear that some MAS configurations may hold the potential for service in regenerators at elevated temperatures.

VI.C. PROBLEM AREAS

A temperature overrun experienced by the 1200°C (2192°F) thermal stability (without sodium) sample set has rendered those test specimens useless for further study. A new test series is in preparation, and the test sequence will be re-run.

VI.C. FUTURE PLANS

Testing will continue at all three test temperatures. The original sample sets begun at 1000°C (1832°F) should be completed during the next reporting period. Three new MAS materials will be introduced at all three test temperatures.

VI.E. TASK SUMMARY

As the thermal stability testing of ceramic materials progresses, several trends are becoming evident. The MAS materials are more stable than the AS and LAS materials, at elevated temperatures under corrosive conditions. The leached LAS

material iterations tested as of this writing are not serviceable at 1100°C (2012°F) and 1200°C (2192°F). Although a furnace malfunction has necessitated starting a new specimen set for 1200°C (2192°F) thermal stability testing without sodium present, the remainder of the program is progressing well, and the acquisition of additional MAS materials has expanded the scope of this testing program well beyond the original contractural goals.

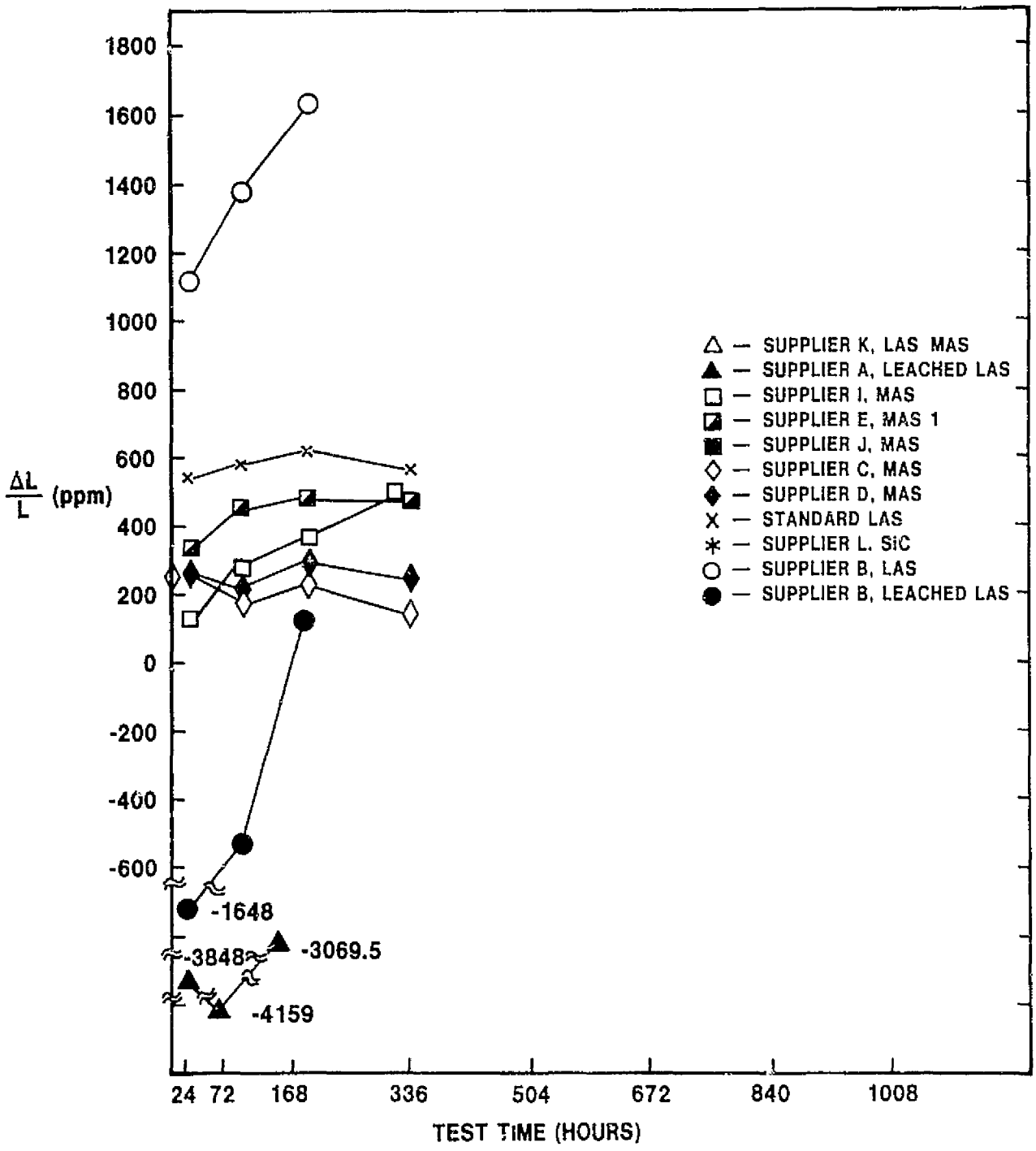

Figure VI. B. 2. 2 Physical Stability of Various Materials at 1100°C (2012°F) with Sodium Present.

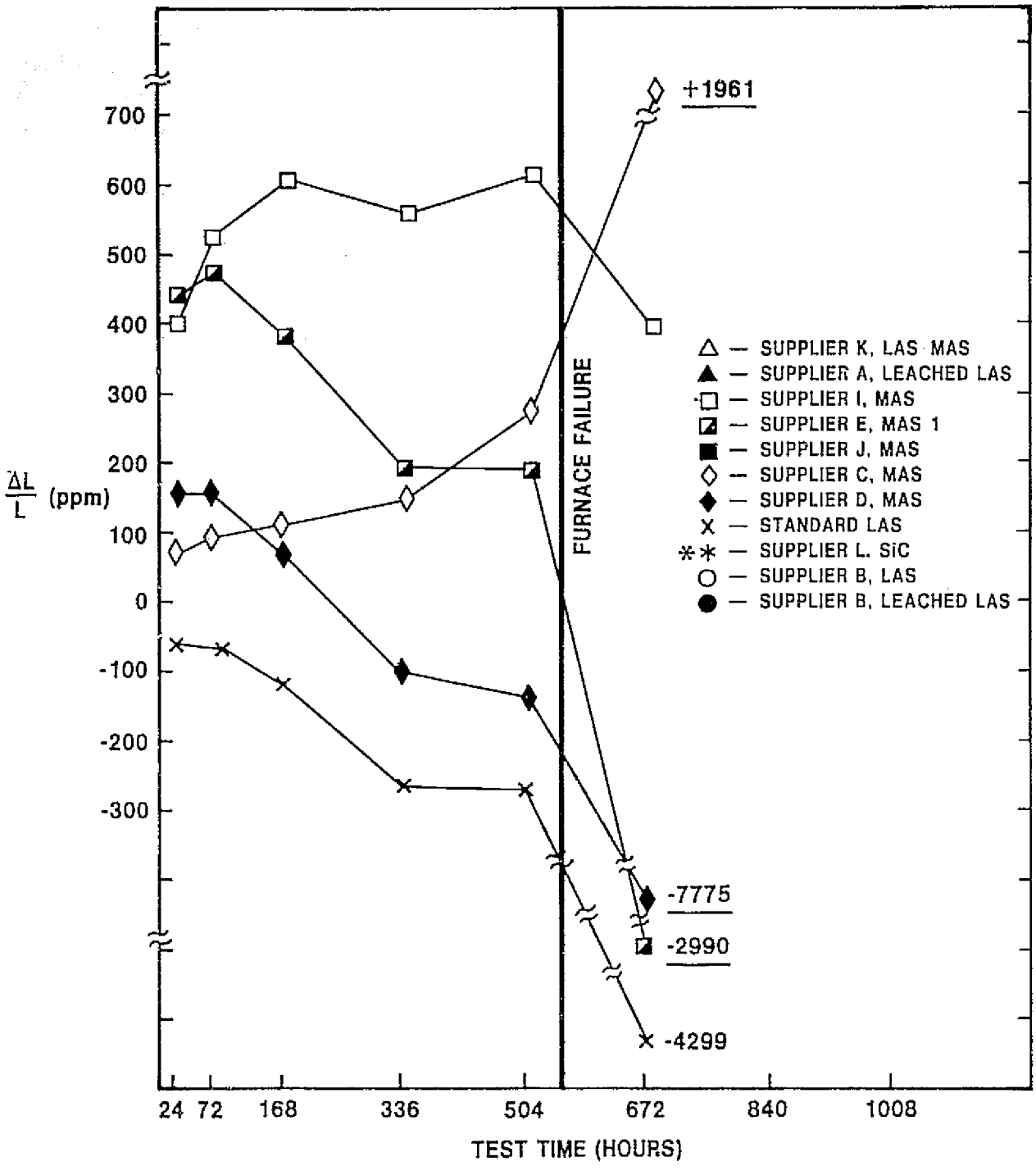

Figure VI. B. 3. 1 Physical Stability of Various Materials at 1200°C (2192°F).

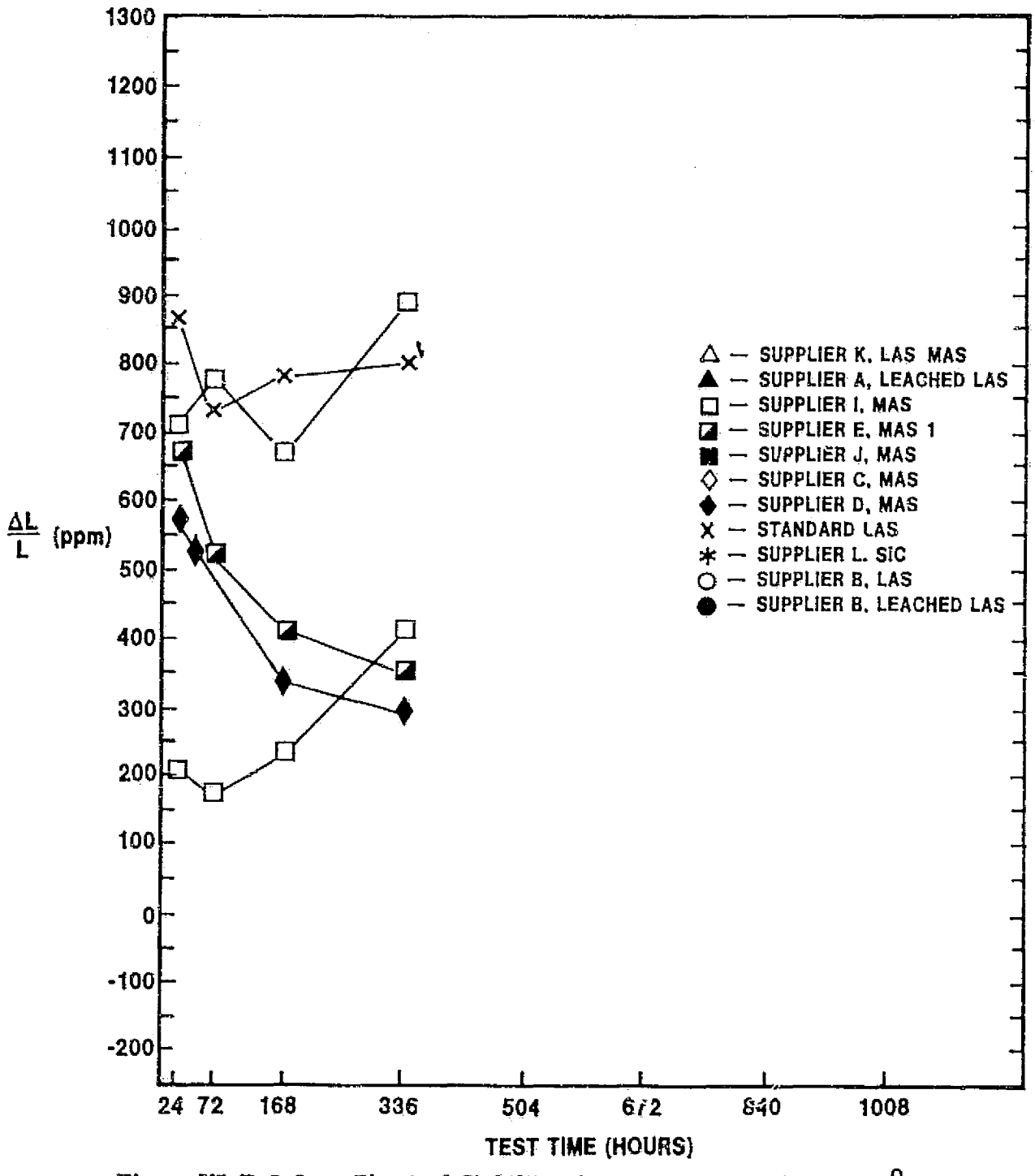

Figure VI. B. 3. 2 Physical Stability of Various Materials at 1200°C (2192°F) with Sodium Present.

VII. MANUFACTURING COST STUDIES

VII.A. INTRODUCTION

A manufacturing cost study, based on a 170 horsepower Stirling engine pre-heater operating at 1000° (1832°F), yielded a core cost of $25-30 (1975 dollars) figured on an annual production base of 500,000 units. The preheater, in a core configuration, has an outer diameter of 457.2 mm (18 inches), an inner diameter of 190.5 mm (7.5 inches), and a thickness of 39.88 mm (1.57 inches).

The purpose of this task is to update this existing cost study.

VII.B. STATUS

An overall objective of this task is to express manufacturing costs in terms of 1978 dollars, reflecting both inflation and the higher cost of processing. Last reporting period was spent in the evolution of heat exchanger models of current interest on which to base a series of comparative cost studies. The Manufacturing Development Department of Ford's Engineering and Research Staff was contacted pursuant to the evaluation of an automotive regenerator configuration with a diameter of 368 mm (14.5 inches) and a thickness of 89 mm (3.5 inches). Due to their departmental priorities, this evaluation was not completed during the last reporting period.

Additional meetings between Turbine Engineering and Manufacturing Development personnel during this reporting period has resulted in the completion of the cost study tasks. The prioritized listing is as follows:

1. 368 mm (14.5 inch) diameter, 89 mm (3.5 inch) thick automotive gas turbine regenerator,

2. 267 mm (10 inch) diameter, 38 mm (1.5 inch) thick automotive Stirling regenerator,

3. Cost comparison of hub versus rim mount for configuration 1.

All analyses will be based on the 1975 cost study, but each will include updated cost information including any technological changes in processing. Work is underway.

VII.C. PROBLEM AREAS

There are no current problems.

VII.D. FUTURE PLANS

Manufacturing Development cost analysis personnel are currently working on the analysis of the first configuration. Their present level of time commitment should result in a completed analysis during the next reporting period. The results of this study, if complete, will be included in the reporting of next period's progress. Efforts will then be directed towards the analysis of configuration 2. Turbine Engineering personnel will closely interact with Manufacturing Development personnel in the execution of this task.

VII.E. TASK SUMMARY

A list of analysis models has been completed and a task prioritization agreed upon by Manufacturing Development Department cost analysts. Work is underway on configuration 1:a regenerator core for an automotive gas turbine engine.

VIII. CORE MATERIAL AND DESIGN SPECIFICATION

VIII.A. INTRODUCTION

Quality control of vendor-supplied hardware is a crucial step in the fabrication of an automotive gas turbine regenerator. Therefore, it is important that the proposed heat exchanger system for alternate engines be well-defined prior to large production efforts. It is the charter of this task to create and periodically update this definition, set down in the form of a regenerator core material and design specification.

A thorough updating of an existing specification representative of regenerator cores intended for service at 800°C (1472°F) was completed and reported last period. The remaining effort in this two-part task is to assemble as much input as possible towards the goal of a knowledgeable iteration of the existing specification, so it would apply to regenerator cores suitable for 1000°C (1832°F) temperature service. The pursuit of additional test information will continue as the primary effort of this contractural task.

VIII.B. STATUS

VIII.B.1 800°C (1472°F) Specification

A thorough review and extensive modification of the existing specification, reflecting progress in material, design, and fabrication technology, was completed and reported last period. No additional effort was directed toward this task during this reporting period.

VIII.B.2. 1000°C (1832°F) Specification

A rather preliminary effort to define what properties a regenerator core must possess to successfully operate at 1000°C (1832°F) is ongoing. This effort is defined as preliminary, because limited test data exist at this elevated temperature on which to base material and design parameters. High temperature laboratory and engine testing are in progress. It is proposed that the high temperature engine testing done as part of this NASA/Ford development program be expanded in response to the data disparity which exists between the two operating temperatures. As test experience accumulates, the 1000°C (1832°F) core material and design specification will evolve.

VIII.C. PROBLEM AREAS

There are no current problems.

VIII.D. FUTURE PLANS

VIII.D.1 800°C (1472°F) Specification

No additional effort will be directed toward the updated specification.

VIII.D.2 1000°C (1832°F) Specification

The ongoing effort to gather, collate, and analyze the high temperature test data towards an enlarged information base pursuant to the iteration of the low temperature specification will continue.

VIII.E. TASK SUMMARY

A regenerator core material and design specification for 800°C (1472°F) has been completed as part of this contract task. The iteration of this document for 1000°C (1832°F) regenerator operation is dependent upon an ongoing test program which features both laboratory and engine evaluation of proposed regenerator materials and configurations.

TASK IX. PROJECT MANAGEMENT

IX.A. INTRODUCTION

It appears desirable to test more cores at 1000°C (1832°F) regenerator inlet temperatures, rather than 800°C (1472°F), since automotive turbine and Stirling engines will have to operate nearer the higher temperature if they are to be competitive with other power plants. It is also desirable to place more lower cost materials, like MAS, on durability test; again to allow the turbine and Stirling to be more competitive with other power plants. To meet these two new objectives, which would result in a major change in program direction, a study was initiated in January 1978. Three different plans or "cases," which would place more emphasis on higher temperature testing, were studied. Their individual impact on the overall Regenerator Program was evaluated in the following Section.

IX.B. STATUS

IX.B.1 Weibull Analysis of Program Changes

A Weibull Analysis was used to study the effect of redirecting the program to increase the amount of engine testing conducted at 1000°C (1832°F). The three different approaches or cases studied were:

Case I: The present program remains unchanged, with 4 engines operating at 800°C (1472°F), 1 at 1000°C (1832°F), and 1 engine used for accelerated chemical attack testing.

Case II: The 4 engines operating at 800°C (1472°F) converted as quickly as possible (about 4 months) to 1000°C (1832°F) engines and all 800°C (1472°F) cores are retired. Six new, thin-wall AS and 2 new MAS cores are started on 1000°C (1832°F) test in these 4 engines.

Case III: Two of the 4 engines at 800°C (1472°F) are converted to 1000°C (1832°F) tests as quickly as possible (about 1-1/2 months), and two new thin-wall AS cores and two new MAS cores are tested at 1000°C (1843°F) in these engines. The two highest-hour thick-wall AS cores and the two highest-hour, thin-wall AS cores are continued on test at 800°C, (1472°F). In both case II and III the two cores that were on test at 1000°C (1832°F) are continued on test.

The hours of operation at the end of 1978 on all of the cores tested for each one of these cases has been estimated. In the Case I program, three cores are expected to reach 10,000 hours at 800°C (1472°F) and a second MAS core at 800°C (1472°F) will attain about 3000 hours. Both cores at 1000°C (1832°F) will exceed 3500 hours of test, with the high hour one attaining about 6300 hours.

In the Case II Program, the highest hour 800°C (1472°F) core will attain about 8000 hours and 6 new AS thin-wall cores will accumulate up to 2000 hours each at 1000°C (1832°F).

In the Case III Program, two old 800°C (1472°F) cores will reach 10,000 hours, and two new AS thin wall and MAS cores will accumulate up to 2000 hours each at 1000°C (1832°F).

In the next three figures, the results of a Weibull analysis are presented, and it shows the relative merits of these programs in projecting usable reliability data. The 800°C (1472°F) results will be discussed first, and it is apparent that the 800°C thick-

wall AS test results obtained from Case I will allow the greatest confidence to be made in projecting a B_{10} life for this material (Figure IX.B.1.1). Case II results in a significant reduction of the confidence in projecting a B_{10} life, while Case III is almost as good as Case I. The lower confidence in the Case II projections are due to the complete termination of the 800°C (1472°F) tests in early 1978.

The same trend is apparent in the 800°C (1472°F) thin-wall AS test results in Figure IX.B.1.2. For all three cases, confidence in a high-hour B_{10} projection is low, because very few thin-wall cores exist with high hours. Case I and III programs use the same high-hour, thin-wall cores so both have the same confidence levels. This level is significantly higher than that of Case II.

The 1000°C (1832°F) results are shown in Figure IX.B.1.3, and the thick and thin-wall AS cores must be considered together, because of the small sample available. The results must be considered as a projection of the life of AS material at 1000°C (1832°F), rather than a projection of a thick or thin-wall configuration of this material.

Since all three cases use the same two cores as their sample, and the new AS cores on test will accumulate 2000 hours or less in 1978, all three cases have the same confidence levels. The confidence is projecting a B_{10} life of 3500 hours at 1000°C (1832°F) at the end of 1978 would be only 50%. This is a very low value, and the only way to improve it is by extending the testing one more year. At the end of 1979, if there were no failures, the confidence in projecting a B_{10} life of 3500 hours at 1000°C (1832°F) would be about 99%.

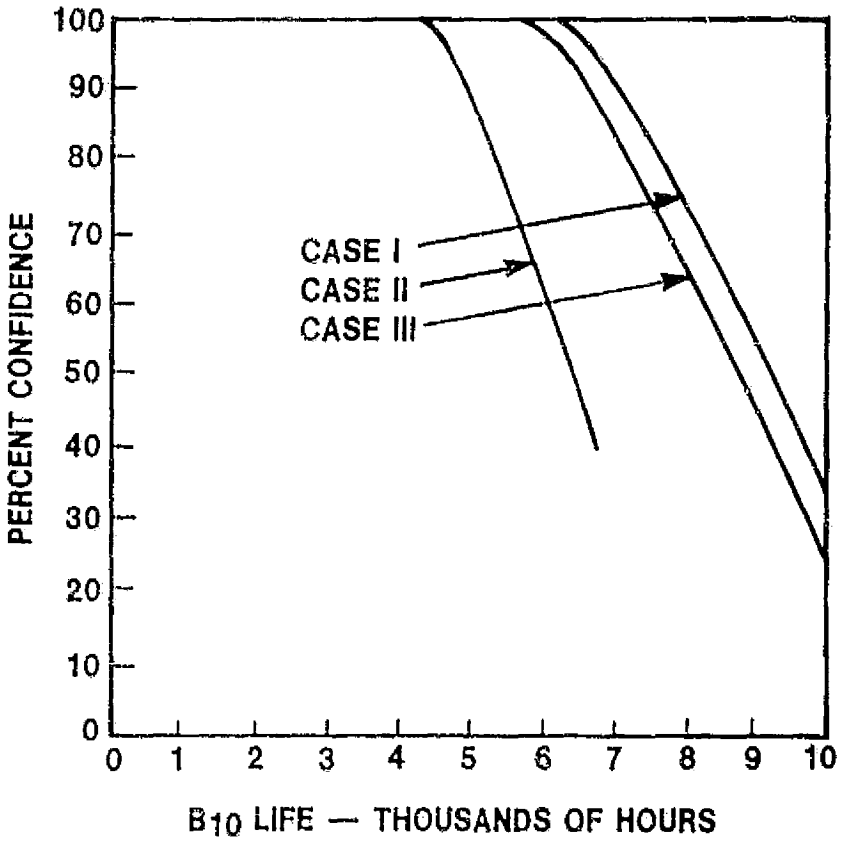

Figure IX. B. 1. 1 Reliability of Thick-Wall AS Regenerators at 800°C (1472°F).

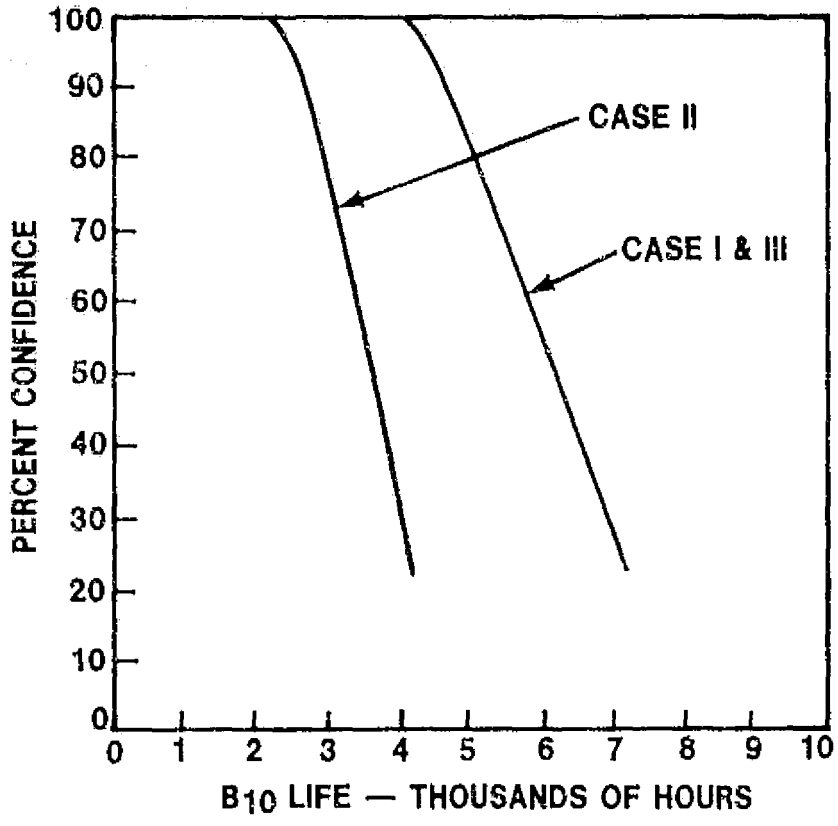

Figure IX. B. 1. 2 Reliability of Thin-Wall AS Regenerators at 800°C (1472°F).

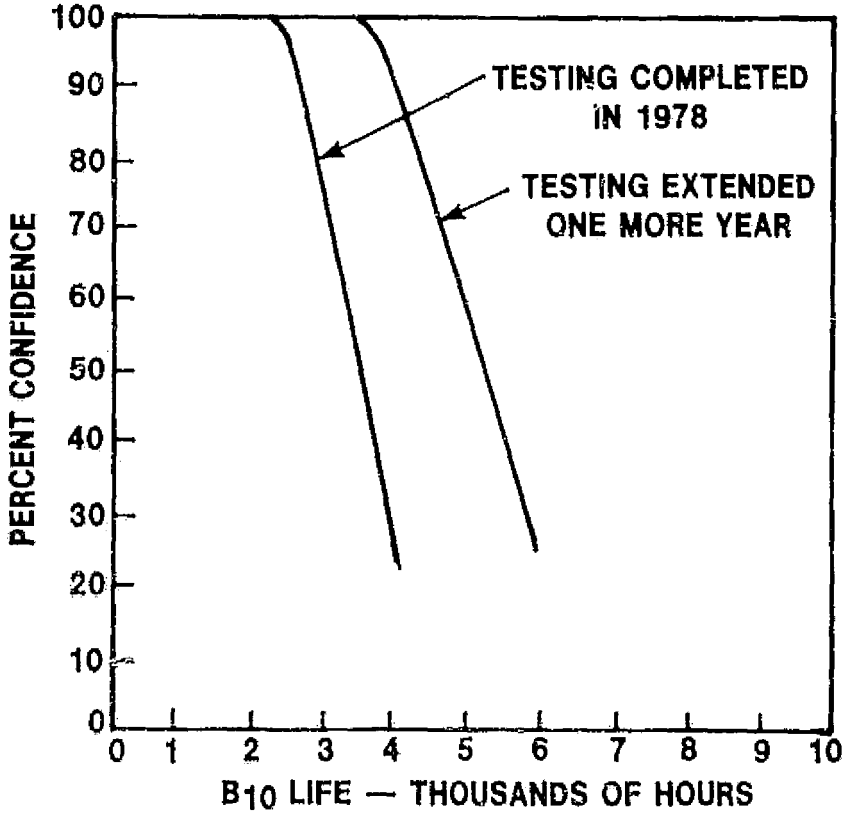

Figure IX. B. 1. 3 Reliability of AS Regenerators at 1000°C (1832°F).

In all of the preceding analyses, it was necessary to use the slope, m, of the Weibull failure distribution curve. Since there have been no failures of AS or MAS regenerators, it has been necessary to assume a value of m. A value of 5, which was obtained on rim mounted LAS and CPD6 cores, was assumed. Figure IX.B.1.4 shows the effect of m on the confidence-reliability curves. A higher value results in more importance being attached to cores which have accumulated high hours. For example, three cores, each of which accumulated 10,000 hours, could be used to project a B_{10} life of 7000 hours with 92% confidence using an m equal to 5. If testing were limited to 7000 hours, it would require the testing of 23 cores at 7000 hours to project a B_{10} life of 7000 hours with 92% confidence.

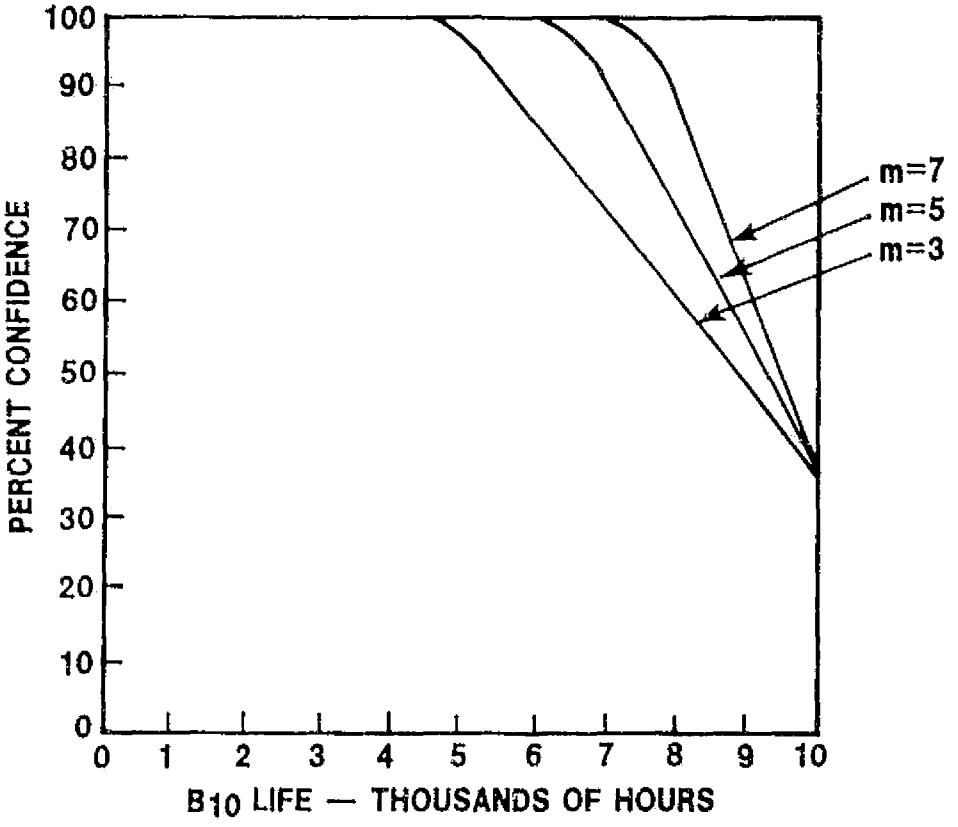

Figure IX.B.1.4 Effect of Slope, m, on Confidence - Reliability Curves.

IX.B.2 Increased Engine Testing at 1000°C (1832°F)

The above analyses of the 800°C (1472°F) and 1000°C (1832°F) testing as well as the future needs of the program suggest that it is highly desirable to convert two 800°C (1472°F) durability engines to 1000°C (1832°F) durability engines as soon as possible in 1978. This would allow a high confidence to be made in B_{10} life projections at 800°C, as well as allowing more AS and MAS cores to be placed on test at 1000°C. It would also allow the two high-hour, 1000°C (1832°F) cores to be tested in separate engines, as protection in case of a disastrous engine failure. A failure in the 1000°C (1832°F) engine today could wipe out both high-hour, 1000°C (1832°F) cores.

The same analysis shows that a low confidence must be placed on any B_{10} life projections at 1000°C (1832°F), even those made at the end of 1978. Continuation of the 1000°C (1832°F) tests for another year would increase the confidence in the B_{10} projections to a reasonable level.

Ford and NASA Project Management have agreed, therefore, to convert two 800°C (1472°F) engines as quickly as possible in the second quarter of 1978 to 1000°C (1832°F) test engines. The regenerator cores that will be continued on test are described in Case III in Section IX.B.1 above.

IX.B.3 Extension of the Program Completion Date

NASA Project Management has agreed to a Ford request that the program be extended for an additional six months. Both the program extension and the change in program direction, described in Section IX.B.2, to place more emphasis on 1000°C (1832°F) testing, will be done at no additional cost to NASA.

The impact on the engine test hour accumulation of both the extension and the increased 1000°C (1832°F) testing is shown in Figure IX.B.3.1. This figure compares the core hour accumulation objective for 1978 with the original program to the total core hour accumulation objective in the revised program. The revised program results in a reduction in the test hours at 800°C (1472°F) and a fourfold increase in the test hours at 1000°C (1832°F).

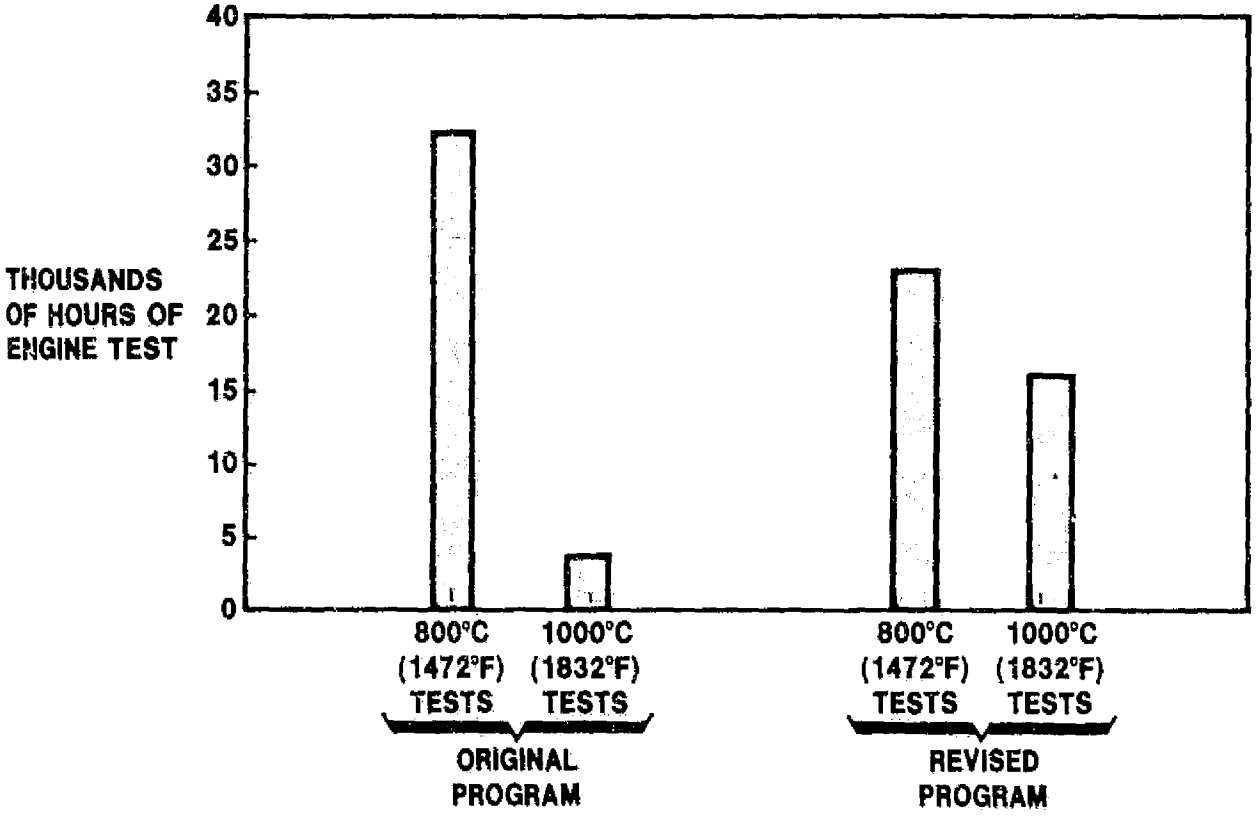

Figure IX.B.3.1 Effect on Test Hour Accumulation of Program Extension.

IX.C. PROBLEM AREAS

There are no problems associated with this task.

IX.D. FUTURE PLANS

The conversion of two 800°C (1472°F) test engines to two 1000°C (1832°F) engines will be implemented as quickly as possible in the second quarter of 1978.

IX.E. TASK SUMMARY

As early as possible in the second quarter of 1978, two 800°C (1472°F) engines will be converted to 1000°C (1832°F) engines, and the program completion date will be extended 6 months. Both of these changes, which will be done at no additional cost to NASA, will result in four times more hours being accumulated at 1000°C (1832°F) under the revised program.

TASK X. REPORTING REQUIREMENTS

X.A. INTRODUCTION

In addition to Quarterly Progress Reports, Ford will also publish three "Topical" reports as part of the NASA/Ford Ceramic Regenerator Program. The subjects of these three reports are to be determined by mutual agreement of Ford and NASA Project Management.

X.B. STATUS

During this report period the subjects of the three Topical Reports were agreed upon by Ford and NASA personnel. The title and a brief abstract of these reports follows:

1. Evaluation of Regenerator System Performance. This study will tie together the major factors affecting the selection of the regenerators in a future, high-temperature, passenger-car turbine engine. Cost and size (for equal performance) will be the ultimate criteria used in this selection. The best obtainable wall thickness, open area, fin efficiency, and leakage will be estimated for each combination of ceramic material, manufacturing process and fin shape. The estimation will be based on an assumption of continued development and evolution of today's technology for a ten-year period. The Report will be published in the second quarter of 1978.

2. Feasibility Study of Silicon Nitride Heat Exchangers. If regenerator inlet temperatures exceed 1100 or 1200°C (2012 or 2192°F), something other than an oxide ceramic may be required. Silicon Nitride will be examined from a stress, performance and manufacturing feasibility viewpoint. Its advantages and limitations will be reviewed in detail. This report will be published in the third quarter of 1978.

3. Regenerator Matrix Physical Property Data. The key physical property data, including F and J factors, compressive strength, coefficient of expansion, modulus of elasticity, MOR, and chemical attack results will be compiled for a limited number of key matrix configurations. The key matrix configurations will be decided jointly by Ford and NASA. This report will be published in the fourth quarter of 1978.

Detailed outlines of each report have been submitted to and approved by the NASA Project Manager.

X.C. PROBLEM AREAS

There are no problem areas associated with this task.

X.D. FUTURE PLANS

It is planned to publish the first report, "Evaluation of Regenerator System Performance," in the next quarter.

X.E. TASK SUMMARY

The subjects and timing of the three "Topical Reports" have been determined by NASA and Ford personnel. The first report "Evaluation of Regenerator System Performance" will be published in the next quarter.

REFERENCES

1. Anderson, D. H., Fucinari, C. A., Rahnke, C. J., and Rossi, L. R., Annual Summary Report, No. 2630-1, Automotive Gas Turbine Ceramic Regenerator Design and Reliability Program, ERDA Contract No. E (11-1) 2630, Sept. 15, 1975.

2. Cook, J. A., Fucinari, C. A., Lingscheit, J. N., and Rahnke, C. J., Annual Summary Report, No. 2630-18, Automotive Gas Turbine Ceramic Regenerator Design and Reliability Program, ERDA Contract No. E (11-1) 2630, Oct. 15, 1976.

3. Cook, J. A., Fucinari, C. A., Lingscheit, J. N., and Rahnke, C. J., Annual Summary Report, No. NASA CR-135330, Ceramic Regenerator Systems Development Program, NASA Contract No. DEN3-8, Dec. 1977.

4. Cook, J. A., Fucinari, C. A., Lingscheit, J. N. Rahnke, C. J. RAO, V.D., Quarterly Progress Report for Oct.-Dec. 1977, No. NASA CR-135380, Ceramic Regenerator Systems Development Program, NASA Contract No. DEN3-8, Feb. 1978.

5. C. P. Howard, "Heat Transfer and Flow Friction Characteristics of Skewed Passage and Glass-Ceramic Heat Transfer Surfaces," T. R. No. 59, Department of Mechanical Engineering, Stanford University, Oct. 1963.